

From the: Dr. von Hauner children's hospital, Ludwig-Maximilians-University Munich



Dissertation
zum Erwerb des Doctor of Philosophy (Ph.D.)
an der Medizinischen Fakultät der
Ludwig-Maximilians-Universität München

***Modulation of liver inflammation and fibrosis by the
interleukin-1 homologue IL-37***

vorgelegt von:

Steffeni Alexandra Mountford

aus

Ebersberg, Germany

Jahr:

2020

First supervisor: Prof. Dr. Philip Bufler
Second supervisor: Prof. Dr. Roland Kappler
Third supervisor: Dr. Daniel Kotlarz, PhD

Dean: **Prof. Dr. med. dent. Reinhard Hickel**

Datum der Verteidigung: 17.12.2020

TABLE OF CONTENTS

TABLE OF FIGURES.....	V
1. INTRODUCTION	1
1.1 Liver inflammation and fibrosis	1
1.1.1 The liver in disease	1
1.1.2 Key players and molecular mechanisms of liver fibrogenesis.....	2
1.2 IL-37	4
1.2.1 IL-37 discovery and expression	4
1.2.2 The IL-37tg mouse model	5
1.2.3 IL-37 – a dual functioning cytokine	5
1.2.4 IL-37 and liver disease	6
1.3 Objectives and working model	7
1.4 Models of study	8
1.4.1 Cell lines.....	8
1.4.2 Liver fibrosis animal models.....	8
1.4.2.1 Bile duct ligation (BDL)- induced liver fibrosis	9
1.4.2.2 Carbontetrachloride (CCl ₄)-induced liver fibrosis	9
1.4.2.3 Colitis associated liver disease in IL-10KO/IL-37tg mice.....	9
1.4.2.4 MDR2 Knock out (KO) mouse model	9
2. MATERIALS AND METHODS	11
2.1 Materials	11
2.1.1 Equipment	11
2.1.2 Consumables	11
2.1.3 Chemicals and reagents	12
2.1.4 Buffers and solutions.....	15
2.1.4.1 General	15
2.1.4.2 Immunostaining.....	15
2.1.4.3 Hydroxyproline assay.....	15
2.1.4.4 Isolation of murine hepatic stellate cells and Kupffer cells	16
2.1.4.5 SDS gel chromatography and western blotting.....	18
2.1.5 Cell lines and media	18
2.1.6 Commercially available kits.....	19
2.1.7 Primary antibodies for western blotting.....	20
2.1.8 Primary antibodies for immunohistochemistry/immunofluorescence	20
2.1.9 Secondary antibodies.....	20
2.1.10 siRNAs	20
2.1.11 cmRNAs	21
2.1.12 Proteins/Cytokines	21
2.1.13 Primer qRT-PCR	21
2.1.13.1 Mouse primer.....	21
2.1.13.2 Human primer.....	23
2.1.13.3 House keeping genes	24

2.1.14	Primer genotyping	24
2.1.14.1	IL-37tg	24
2.1.14.2	MDR2KO.....	24
2.1.15	Animals.....	25
2.1.16	Medication and sedation.....	25
2.1.17	Software.....	25
2.2	Methods.....	26
2.2.1	Tissue culture.....	26
2.2.1.1	General maintenance	26
2.2.1.2	cmRNA transfection	27
2.2.1.3	siRNA mediated knock down of IL-37	27
2.2.1.4	Recombinant human IL-37 treatment.....	27
2.2.1.5	Cell harvest	27
2.2.2	Protein analysis.....	27
2.2.2.1	Whole cell lysis and organ lysis	27
2.2.2.2	Protein quantification.....	28
2.2.2.3	Western blot.....	28
2.2.2.4	Secondary probing.....	28
2.2.3	Nucleic acid analysis	28
2.2.3.1	RNA extraction and quality control.....	28
2.2.3.2	cDNA.....	29
2.2.3.3	qRT-PCR	29
2.2.4	Histology.....	29
2.2.4.1	Preservation, embedding and sectioning of samples	29
2.2.4.2	Hematoxylin/Eosine staining.....	30
2.2.4.3	Pikro Sirius Red Staining.....	31
2.2.4.4	Immunohistochemistry	31
2.2.4.5	Immunofluorescence.....	32
2.2.4.6	Quantification	33
2.2.5	Biochemical analysis	33
2.2.5.1	Liver serum values.....	33
2.2.5.2	Hydroxyproline measurement	34
2.2.5.3	Cytokine measurement	34
2.2.6	Isolation of human PBMCs	34
2.2.7	Primary cell culture.....	35
2.2.7.1	Isolation and cultivation of murine hepatic stellate cells.....	35
2.2.7.2	Isolation of murine Kupffer cells.....	35
2.2.7.3	Cell staining.....	35
2.2.7.4	Migration assay.....	36
2.2.8	<i>In-vivo</i> studies.....	37
2.2.8.1	Animals.....	37
2.2.8.2	Genotyping of animals.....	37
2.2.8.3	Animal models.....	39
2.2.9	Statistical analysis.....	40

3. RESULTS.....	41
3.1 IL-37 modulates liver inflammation and fibrosis in liver fibrosis mouse models....	41
3.1.1 Bile duct ligation-induced liver fibrosis.....	41
3.1.1.1 Pro-fibrogenic gene expression increases after bile duct ligation.....	41
3.1.1.2 Transgene IL-37 expression improves survival and serum biochemistry in bile duct ligated mice	42
3.1.1.3 Transgene IL-37 expression reduces fibrosis in bile duct ligated mice	43
3.1.1.4 Transgene IL-37 expression shows trend towards reduced pro-inflammatory and pro-fibrotic gene expression 3 days after bile duct ligation	45
3.1.1.5 Low dose, short term rhIL-37 (1 µg) treatment shows no effect on fibrosis associated gene expression in bile duct ligated mice	45
3.1.1.6 High dose, short term rhIL-37 (2x5 µg) treatment shows no effect on fibrosis associated gene expression in bile duct ligated mice	46
3.1.2 CCl ₄ -induced liver fibrosis.....	47
3.1.2.1 CCl ₄ injected mice develop fibrosis after 6 weeks.....	47
3.1.2.2 Transgene IL-37 expression reduces inflammatory markers in CCl ₄ -treated mice	50
3.1.2.3 Transgene IL-37 expression reduces fibrosis in CCl ₄ -treated mice.....	51
3.1.3 Transgene IL-37 expression reduced colitis associated liver inflammation and fibrosis	51
3.1.4 Role of IL-37 in the MDR2KO model of liver fibrosis	53
3.1.4.1 IL-37 overexpression by chemically modified RNAs (cmRNA) in cell lines	53
3.1.4.2 MDR2KO-mice develop bridging fibrosis at the age of 5 weeks.....	59
3.1.4.3 Male mice develop more fibrosis than age-matched female mice	59
3.1.4.4 Low dose chemically-modified (cm) RNA injections show now effect on reducing fibrosis factors in MDR2KO mice	60
3.1.4.5 High dose cmRNA injections show now effect on reducing fibrosis factors in MDR2KO mice	61
3.1.4.6 IL-37 cmRNA-injected mice produce antibodies against IL-37.....	62
3.2 Impact of IL-37 on human hepatic stellate cell function.....	63
3.2.1 Overexpression of IL-37 in human stellate cell line LX2.....	63
3.2.2 Recombinant human IL-37 reduces gene expression of pro-fibrotic <i>ACTA2</i>	63
3.2.3 siRNA-mediated knockdown of endogenous IL-37 in LX2 cells.....	64
3.3 The functional role of IL-37 in mouse hepatic stellate cells	66
3.3.1 Spontaneous activation of wt murine hepatic stellate cell in culture	66
3.3.2 Transgene IL-37 expression reduces pro-inflammatory response in mHSC	67
3.3.3 Recombinant IL-37 does not modulate the pro-inflammatory response of mHSC..	69
3.4 The functional role of IL-37 in murine Kupffer cells.....	69
3.4.1 Transgene IL-37 expression reduces pro-inflammatory response in KC.....	69
3.4.2 The impact of transgene IL-37 on KC migration	70
4. DISCUSSION.....	72
5. ABSTRACT	78
6. ZUSAMMENFASSUNG	79

7. REFERENCES.....	80
8. APPENDIX.....	87
8.1 List of abbreviations.....	87
8.2 Affidavit.....	89
8.3 Confirmation of congruency between printed and electronic version of the doctoral thesis.....	90
8.4 Acknowledgements.....	91
8.5 List of all scientific publications to date.....	92

TABLE OF FIGURES

Figure 1: Natural course of hepatic fibrosis.	2
Figure 2: IL-37 is a dual functioning cytokine	6
Figure 3: Working hypothesis	8
Figure 4: Pro-fibrogenic gene expression increases after bile duct ligation.	42
Figure 5: Transgene IL-37 expression improves survival and serum biochemistry in bile duct ligated mice.	43
Figure 6: Transgene IL-37 expression reduces fibrosis in bile duct ligated mice.	44
Figure 7: Transgene IL-37 expression shows trend towards reduced pro-inflammatory and pro-fibrotic gene expression 3 days after bile duct ligation.	45
Figure 8: Low dose, short term rhIL-37 (1 µg) treatment shows no effect on fibrosis associated gene expression in bile duct ligated mice.	46
Figure 9: High dose, short term rhIL-37 (2x5 µg) treatment shows no effect on fibrosis associated gene expression in bile duct ligated mice.	47
Figure 10: CCl ₄ -injected mice develop fibrosis after 6 weeks.	49
Figure 11: Transgene IL-37 expression reduces inflammatory markers in CCl ₄ -treated mice. ..	50
Figure 12: Transgene IL-37 expression reduces fibrosis in CCl ₄ -treated mice.	51
Figure 13: Transgene IL37 expression reduces colitis associated liver inflammation.	53
Figure 14: IL-37 overexpression reduces pro-inflammatory markers in RAW264.7 cells after LPS stimulation.	55
Figure 15: IL-37 overexpression reduces inflammation markers in A549 cells after IL-1β stimulation.	57
Figure 16: IL-37 overexpression reduces inflammation markers in LX2 cells after IL-1β stimulation.	59
Figure 17: MDR2KO mice develop bridging fibrosis at the age of 5 weeks	60
Figure 18: Male MDR2KO mice develop more fibrosis than age-matched female mice.	61
Figure 19: Low dose cmRNA injections show now effect on reducing fibrosis factors in MDR2KO mice.	61
Figure 20: High dose cmRNA injections show now effect on reducing fibrosis factors in MDR2KO mice	63
Figure 21: IL-37 cmRNA injected mice develop IL-37 antibodies and produce IL-37.	64
Figure 22: Recombinant human IL-37 reduces pro-fibrogenic gene expression.	65
Figure 23: 10nM IL-37 siRNA downregulates <i>IL-37</i> after IL-1β stimulation	66
Figure 24: IL-37 knockdown in LX2 cells	67
Figure 25: Wt murine hepatic stellate cell activate spontaneously	67
Figure 26: Transgene IL-37 expression reduces pro-inflammatory response in mHSC	69
Figure 27: Recombinant IL-37 does not influence pro-inflammatory response in mHSC	70
Figure 28: Transgene IL-37 expression reduces pro-inflammatory response in KC	71
Figure 29: Transgene IL-37 expression does not affect Kupffer cell migration	72

1. INTRODUCTION

1.1 Liver inflammation and fibrosis

1.1.1 The liver in disease

The liver, more than any other solid organ has the remarkable capability of regenerating damaged tissue through wound healing processes. The healing process termed fibrosis is regulated by various interactions of immune cell subsets and can in many parts be considered as part of the innate immune response in tissue damage (1). Constantly changing metabolic and tissue remodelling processes, combined with exposure to dangerous stimuli lead to tightly regulated inflammation processes in the healthy liver. Only when the liver is exposed to harming stimuli are the tightly regulated inflammatory processes stimulated additionally to rid the liver of dangerous signals. Failure to eliminate these stimuli results in chronic pathological inflammation and disturbed tissue homeostasis, which then can progress to fibrosis, cirrhosis and liver failure (2). Inflammation seems to be the key promoter that drives the dysfunctional wound-healing response through the various stages of liver disease (3).

Regardless of the underlying cause in chronic liver disease (alcohol, viral infection, non-alcoholic fatty liver disease (NASH), cholestatic disorder or autoimmune disease) development of fibrosis represents the first step towards the progression of cirrhosis and its following complications such as organ failure, esophageal variceal bleeding and hepatocellular carcinoma (1, 4). Liver fibrosis and end stage cirrhosis represent the final common pathway of virtually all chronic liver diseases and still lack a specific therapeutic approach (5) (Fig. 1).

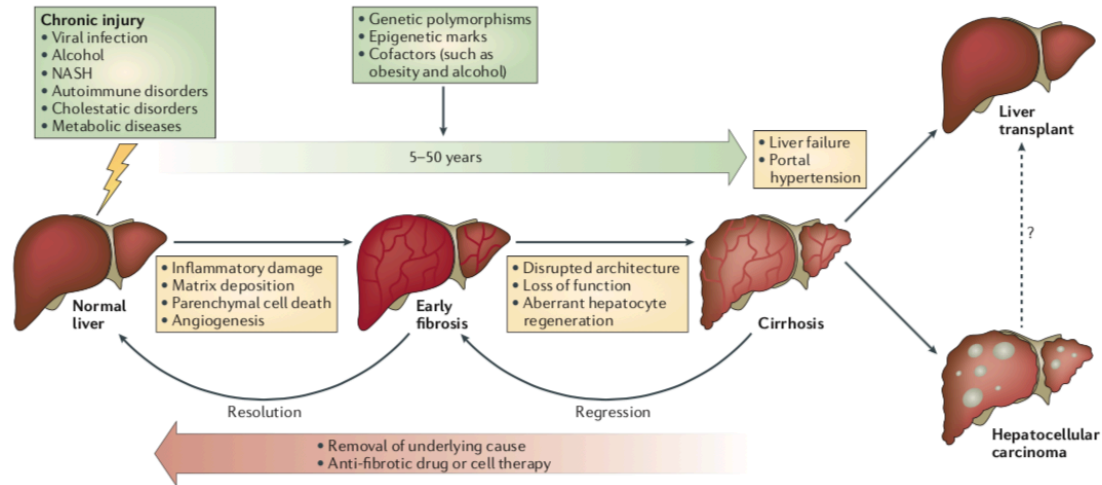


Figure 1: Natural course of hepatic fibrosis. Fibrosis is the wound-healing response of the liver. Independent of the underlying cause (Alcohol, Nash) iterative damage causes matrix deposition, parenchymal cell death, angiogenesis and inflammatory damage resulting in early stage fibrosis. Failure to remove damaging stimuli causes disrupted architecture, loss of function and aberrant hepatocyte regeneration resulting in liver cirrhosis and finally liver failure. Currently liver transplantation is the only available treatment option for patients with endstage liver disease (1).

Progressed fibrosis is characterized by the accumulation of extra-cellular-matrix (ECM), which is rich in fibrillar collagens, mainly collagen I and collagen III. An accumulation of excessive ECM results in liver failure, portal hypertension and is associated with an increased risk of developing liver cancer (6). Since more than 80% of patients with hepatocellular carcinoma (HCC) show signs of hepatic fibrosis it appears that chronic wound healing processes in the liver is an essential contributor to hepatocarcinogenesis (7). Currently the most effective way of combating liver fibrosis is to eliminate the underlying disease (4).

To date, the only effective available treatment for endstage liver disease is liver transplantation. Unfortunately, the shortages of organs, the presence of concurrent disease affecting other tissues in the potential recipient, and recurrence of the primary disease in transplant recipients limit the impact of this treatment option and call for a clear imperative to develop anti-fibrotic therapies (4, 8, 9). Although chronic activation of inflammatory pathways has been shown to promote hepatic carcinogenesis, the molecular link between inflammation and hepatic fibrogenesis has not unravelled thoroughly (10, 11).

1.1.2 Key players and molecular mechanisms of liver fibrogenesis

The liver consists of parenchymal (i.e. hepatocytes) and a variety of non-parenchymal cells, including Kupffer cells (KC), sinusoidal endothelial cells, stellate cells, cholangiocytes, and other types of immune cells (12). The interplay between Kupffer cells and hepatic stellate

cells (HSC) is a key factor in the development of hepatic fibrogenesis. Both cell types are targets of pro-inflammatory mediators (4, 13).

Kupffer cells are the largest group of residential macrophages in the body and represent about 20% of non-parenchymal cells in the liver (14). They derive from circulating monocytes that arise from bone marrow progenitors (15). Due to their high phagocytic capacity, KCs are capable of removing foreign material such as viruses and bacteria, as well as apoptotic cells and cellular debris, which makes them an important gatekeeper in the innate immune response (16). They are located in the sinusoids of the liver and have been shown to migrate along hepatic sinusoidal endothelial cells (17). As a response to lipopolysaccharide (LPS), KCs secrete several mediators including IL-6 that regulate inflammation processes and homeostasis, as well as inflammatory response to injury (18). Kupffer cells are the most prominent inflammatory cells of the liver stimulating HSC activation (10, 19).

The role of hepatic stellate cells in the healthy liver is still being discussed, but they are defined as fat-storing pericytes that constitute 5-8% of all liver cells (20). Once quiescent hepatic stellate cells are exposed to LPS, NF- κ B signalling is initiated via the toll-like receptor (TLR) 4, which leads to the down regulation of TGF- β pseudo receptor Bambi thereby sensitizing quiescent HSCs for TGF- β and providing the direct link between pro-inflammatory and pro-fibrogenic signals (10). LPS stimulation leads to increased expression of several chemokines and adhesion markers thereby activating Kupffer cell chemotaxis (21). Increased TGF- β signalling by recruited Kupffer cells and low levels of Bambi lead to hepatic stellate cell activation resulting in increased deposition of extracellular matrix and subsequent liver fibrosis (4). LPS-induced NF- κ B signalling activates stellate cells and mediators such as IL-1 β and TNF released by activated Kupffer cells enhances their survival and activation (22).

TGF- β has been identified as one of the key regulators of liver physiology and pathology. Its regulation contributes to all stages of liver physiology and pathology, starting from initial liver injury through liver inflammation followed by fibrosis, cirrhosis and finally hepatocellular carcinoma (23). Therefore, targeting the TGF- β signalling pathway has been a possibility in an attempt to inhibit liver disease progression (24). Liver fibrosis and hepatocellular apoptosis is promoted by enhanced TGF- β signalling through activation of Sma- and Mad-related (Smad3) (25, 26).

It was reported that acute and chronic liver injuries are cytokine-driven diseases since several pro-inflammatory cytokines such as IL-1 α , IL-1 β , TNF α and IL-6 are critically involved in inflammation, steatosis, fibrosis and cancer development (27). IL-13, IL-17 and IL-33 have also been shown to promote liver fibrogenesis by activating HSCs (28). Cytokines of the IL-1 family (IL-1F) of ligands and receptors play a pivotal role in the modulation of immune responses (29). Recent data provide evidence for the role of IL-1F cytokine signalling in chronic liver injury and fibrosis (30, 31). For example, IL-1 α and IL-1 β are critically involved in the transformation of steatosis to steatohepatitis and liver fibrosis in hypercholesterolemic mice and ethanol-induced liver damage (32, 33). IL-33 promotes liver fibrosis through the induction of Th2 cells and attraction of innate lymphoid cells in fibrotic livers (34, 35). Understanding the molecular mechanisms leading from initial liver injury to fibrosis and cirrhosis represents a crucial step in developing new anti-fibrotic therapeutic options.

1.2 IL-37

1.2.1 IL-37 discovery and expression

IL-37, formerly known as IL-1 family member 7b (IL-1F7b), is a novel homologue of the IL-1 cytokine family, which broadly suppresses the innate and adaptive immune response (36, 37). IL-37 was first discovered in 2000 by computational cloning and consists of six exons coding for five isoforms, isoform 1 (IL-1F7b, IL-37b) being the largest and most investigated one. IL-37b consists of 5 exons; Exons 1 and 2 hold N-terminal pro-domain containing a putative caspase-1 cleavage site (38). IL-37 protein is expressed in human monocytes and upregulated by LPS (39). Further, IL-37 has been shown to be expressed in tissue macrophages, synovial cells, tonsillar B cells, plasma cells, neoplastic cells as well as epithelial cells of the skin, kidney and intestine (21, 38, 40, 41). IL-37 is expressed in hepatocytes as well as bile duct epithelia and infiltrating lymphocytes (Griessmair et al., Cellular infiltrate and expression of IL-37 in pediatric AIH, PSC and ASC, presented at ESPGHAN 2019). It was shown that overexpression of IL-37 in cells of monocytic or epithelial origin almost completely abolishes the production of pro-inflammatory cytokines as IL-1 α/β , TNF α , IL-6 and IL-8 in response to TLR-ligands or IL-1 β . Vice versa, functional knockdown of IL-37 in primary human tumoural expression of IL-37 by adenoviral transfection was shown to induce a Th1-dependent cells by siRNA increased the production of pro-inflammatory cytokines (36). In addition, intra-tumoural expression of IL-37 by

adenoviral transfection was shown to induce a Th1-dependent regression of established fibrosarcoma tumours in mice (42).

1.2.2 The IL-37tg mouse model

To date the mouse homologue to IL-37 is unknown. Therefore, analysing the role of this cytokine in an IL-37 deficient mouse is not possible. To this end an IL-37 transgene mouse was developed. The expression of the human IL-37 in IL-37tg mice is driven by a constitutively active CMV-promoter, though the protein is almost not detectable in these mice without inflammation (36). It was demonstrated that mRNA instability regions control IL-37 expression in both human primary and transfected cells. Unless stimulation with TLR ligands, pro-inflammatory cytokines or pro-fibrotic TGF- β , IL-37 mRNA is rapidly degraded (36, 43). This explains why IL-37tg mice only show low level of IL-37 protein expression unless any kind of inflammation is established. Accordingly, IL-37tg mice have shown broad anti-inflammatory characteristics in a variety of disease models (36, 37, 44-46).

1.2.3 IL-37 – a dual functioning cytokine

IL-37 is unique in its function since it is a cytokine with a dual functionality (Fig. 2). IL-37 circulating in the extracellular space functions by binding to the alpha chain of the IL-18 receptor (IL-18R α) surface receptor. After binding it forms a complex with anti-inflammatory receptor IL-1R8 (formally Single IgG IL-1 Related Receptor SIGIRR) as the accessory co-receptor thereby inhibiting the transcription of pro-inflammatory genes (37, 47). Several studies have shown that recombinant (rh) IL-37 inhibits inflammation *in vitro* and *in vivo* (47). Wt mice treated with recombinant IL-37 are protected in models of endotoxemia, metabolic syndrome, acute lung injury, spinal cord injury, myocardial infarction, asthma and ischemic liver disease (45, 47-51). Furthermore, IL-37 improves insulin sensitivity and reduces inflammatory cytokine production in adipose tissue (44, 52). It was also shown that recombinant IL-37 reduces joint and systemic inflammation and limits the metabolic costs of chronic inflammation, which promotes exercise tolerance (53). Similar to other IL-1 family members such as IL-1 α and IL-33, IL-37 translocates to the nucleus where it acts as an inhibitor of the innate immune response. Before translocating IL-37 requires caspase-1 mediated cleavage (54, 55). After caspase-1 cleavage, IL-37 binds to the TGF- β -signalling molecule Smad3 thereby inhibiting inflammation at the nuclear level (36). The fact that

inflammation in IL-37tg mice is increased when endogenous Smad3 is depleted shows the relevance of the IL-37/Smad3 interaction (36). To date it has not been evaluated whether the extra- or the intracellular function of IL-37 plays a more significant role in the regulation of anti-inflammatory response. It has been shown in that mouse macrophages stably transfected with human IL-37, only about 20% of IL-37 translocates to the nucleus (55). This finding was associated with decreased cytokine production (36, 55). When the cells were treated with small caspase-1 inhibitor there was no IL-37 translocation to the nucleus, which resulted in no reduction of LPS-induced cytokines (55). Preventing IL-37 translocation in mouse macrophages resulted in the loss of suppression of cytokines production and the anti-inflammatory function of IL-37 (56).

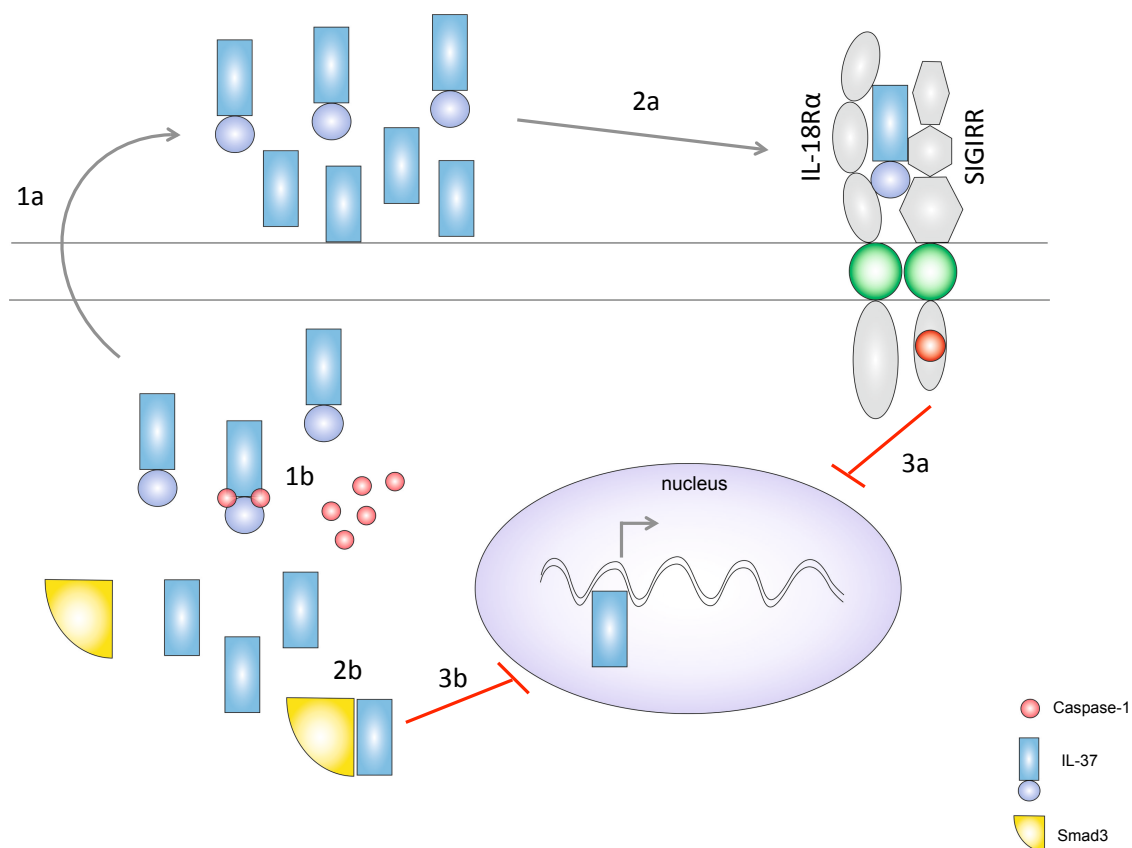


Figure 2: IL-37 is a dual functioning cytokine: (a) Extracellular function of IL37. IL37 is secreted into the extracellular space (1a) where it binds to IL-18R α (2a). After recruiting anti-inflammatory receptor SIGIRR transcription of anti-inflammatory signals is activated. (b) Intracellular function of IL-37: Upon caspase-1 cleavage (1b), IL-37 binds to Smad3 (2b) thereby translocating to the nucleus (3b) and activating anti-inflammatory signalling pathways.

1.2.4 IL-37 and liver disease

Controlled inflammation is an aspect of the healthy homeostatic liver. Failure to resolve the underlying cause results in chronic liver injury and permanent liver damage. In the liver, IL-37 reduced inflammation in a mouse model of hepatic ischaemia (57) and concanavalin A-

induced liver injury (58). In a model of high-fat diet-induced obesity, IL-37 suppressed innate immune responses and inflammation (44). Although transgene IL-37 expression did not protect mice from liver injury in a model of binge drinking, administration of recombinant IL-37 ameliorated expression of hepatic cytokines and moderately improved steatosis (59).

In humans, Moschen and colleagues described a positive correlation of IL-37 mRNA expression in the liver and a negative correlation of IL-37 mRNA expression in subcutaneous adipose tissue with the body mass index of severely obese patients (60). In hepatocellular carcinoma positive IL-37 expression in tumour tissue correlates with a better overall survival in humans (61). Factors suggesting the anti-tumoural effect of IL-37 include the attraction of CD57-positive NK cells, the conversion of JNK/pSmad3L/c-Myc oncogenic signalling to pSmad3C/P21 tumour-suppressive signalling and the induction of autophagy (61-63). Anti-inflammatory IL-37 could therefore play a crucial role in reducing liver inflammation and subsequent liver damage.

1.3 Objectives and working model

Sustained inflammation is the main feature of chronic liver injury and induces liver fibrosis, cirrhosis and potentially hepatocellular carcinoma (5, 64). TGF- β is a core cytokine involved in liver fibrogenesis (4). IL-37 reduces LPS-induced inflammation *in vitro* and *in vivo*. It also interacts with Smad3 – a key molecule of the TGF- β -signalling pathway inhibiting fibrosis in a lung model of aspergillosis (49).

We therefore hypothesize that IL-37 modulates liver inflammation and fibrosis by interacting with the Smad3 signalling pathway thus regulating TGF- β signalling (Fig. 3). In addition, we propose that IL-37 downregulates KC activity thereby modulating KC and HSC cross talk resulting in decreased HSC activation.

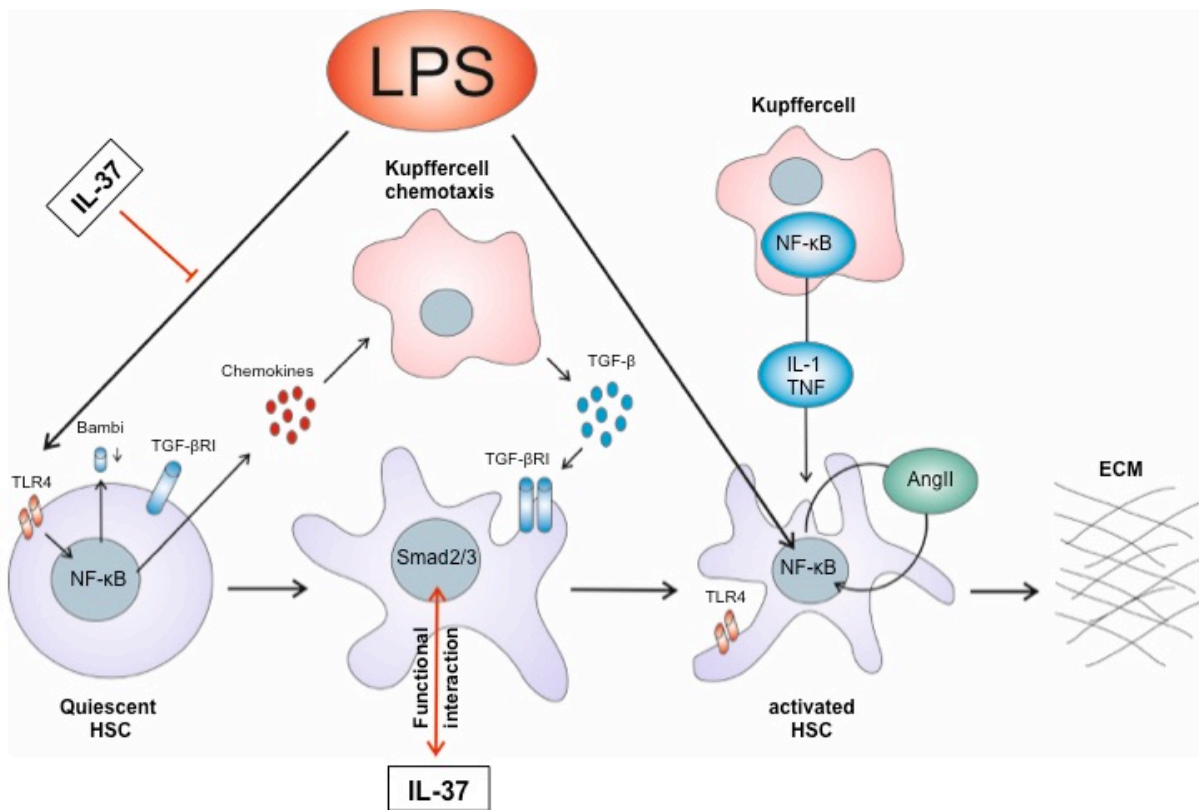


Figure 3: Working hypothesis: LPS activates NF-κB signalling in quiescent hepatic stellate cells, which leads to secretion of chemokines resulting in attraction of Kupffer cells. Additionally, Bambi is down regulated thereby sensitizing stellate cells to TGF-β signalling. Kupffer cells secrete TGF-β leading to an activation of hepatic stellate cells, which in turn produce extracellular matrix leading to fibrosis. IL-1 and TNF secreted by activated Kupffer cells in an NF-κB dependent manner, contribute to survival and sustained activation of hepatic stellate cells. IL-37 reduces LPS-induced inflammation and interacts with Smad3 to reduce liver inflammation and fibrosis.

1.4 Models of study

1.4.1 Cell lines

For *in-vitro* studies we used human hepatic stellate cell line LX-2, which retain key features of hepatic fibrogenesis. Since hepatic stellate cells are the major cell type responsible for liver fibrosis the cells represent a suitable model for human hepatic fibrosis (65).

1.4.2 Liver fibrosis animal models

The development of liver disease can have various underlying causes. Since there is no single model to study liver inflammation and fibrosis, we chose to use four different mouse models mimicking different human liver diseases to study the role of IL-37 in the development of liver injury.

1.4.2.1 Bile duct ligation (BDL)- induced liver fibrosis

Cholestatic liver diseases are characterized by the accumulation of specific bile acids in the liver that lead to inflammation followed by liver injury. Patients suffering this disease show pruritus, fatigue, jaundice and dark urine (66). Liver injury is caused by toxic bile salts, which induce hepatocyte apoptosis *in vitro* (67). Bile-duct ligation is a method in which extra-hepatic biliary obstruction is induced surgically. This prevents bile flow and mimics cholestasis resulting in liver injury. BDL in rodent models leads to altered phagocytic, immune and macrophage functions (68, 69). In obstructive cholestatic liver disease hepatic inflammation plays an important role in both humans and mice. LPS signalling enhances hepatic fibrogenesis caused by bile duct ligation-induced experimental cholestasis in mice (70). On the contrary, gut sterilisation reduces hepatic fibrosis in mice after bile duct ligation (10). The LPS receptor TLR4 is highly expressed on Kupffer cells. Depleting KCs in bile-duct ligation-induced liver injury ameliorates fibrogenesis (71).

1.4.2.2 Carbontetrachloride (CCl₄)-induced liver fibrosis

CCl₄- is a well-established model of toxic liver damage leading to liver fibrosis. A single dose of CCl₄ causes centrilobular necrosis and steatosis, while longer administration leads to liver fibrosis, cirrhosis and HCC (72). Using this mouse model with TLR4-ko mice, liver damage is reduced due to reduced HSC activation (10). Selective inhibition of NF-κB in Kupffer cells reduces CCl₄-induced liver fibrosis by limiting the release of NF-κB-regulated cytokines, such as TNF-α, IL-1β and IL-6 (73).

1.4.2.3 Colitis associated liver disease in IL-10KO/IL-37tg mice

We recently described the protective role of IL-37 against colon inflammation and carcinogenesis during chronic colitis in IL-10KO mice (74). Since inflammatory bowel disease (IBD) may be associated with liver inflammation and fibrosis, we used this model to evaluate whether transgene IL-37 expression reduced inflammation and fibrosis in the model of chronic colitis.

1.4.2.4 MDR2 Knock out (KO) mouse model

MDR2KO mice lack the canalicular phospholipid flippase, which leads to severe cholestasis in the first weeks of life due to missing of phospholipids from the bile. The resulting liver

fibrosis resembles human primary sclerosing cholangitis (PSC) and therefore is a clinically relevant fibrosis model (75).

2. MATERIALS AND METHODS

2.1 Materials

2.1.1 Equipment

Confocal microscope Zeiss LSM800	Carl Zeiss Microscopy (Munich, Germany)
Fluorescent microscope Zeiss Axiovert 200M	Carl Zeiss Microscopy (Munich, Germany)
Gel Imager: ChemiDoc XRS+	BioRad (Munich, Germany)
Gel Imager	Intas Science Imaging (Göttingen, Germany)
Homogenizer T10 Basic Ultra Turrax	IKA (Staufen, Germany)
iCycler	BioRad (Munich, Germany)
Light microscope	Leica Biosystems (Wetzlar, Germany)
Microplate spectrophotometer EON	BioTek (Bad Friedrichshall, Germany)
Mini-PROTEAN Tetra Vertical Electrophoresis Cell	BioRad (Munich, Germany)
Mini Trans-Blot Cell	BioRad (Munich, Germany)
Nanodrop ND-1000	Thermo Fisher Scientific (Munich, Germany)
Peristaltic pump	Ismatec (Wertheim, Germany)
Power Pack universal power supply	BioRad (Munich, Germany)
X-Ray Film processor	AGFA (Mortsel, Belgium)

2.1.2 Consumables

μ -Slide 8 Well Glass Bottom	Ibidi (Martinsried, Germany)
96- well qRT-PCR plates	VWR life science (Darmstadt, Germany)
Amersham Hybond PVDF (0.45 μ m)	GE life science (Munich, Germany)
Amersham Hyperfilm ECL	GE life science (Munich, Germany)

Any kD mini-PROTEAN TGX precast gel	BioRad (Munich, Germany)
Cell strainer 70 μ m	Greiner Bio-One (Frickenhausen, Germany)
Falcon cell scraper	BD Biosciences (Heidelberg, Germany)
General cell culture plastic ware	Sarstedt (Nürmbrecht, Germany)
General laboratory ware	Sarstedt (Nürmbrecht, Germany)
Superfrost Microscope slides	Thermo Fisher Scientific (Munich, Germany)
Whatman paper	VWR life science (Darmstadt, Germany)

2.1.3 Chemicals and reagents

β -mercaptoethanol	Sigma-Aldrich (Taufkirchen, Germany)
100 bp DNA ladder ready to load	Solis BioDyne (Tartu, Estonia)
4',6-diamidino-2-phenylindole	Thermo Fisher Scientific (Munich, Germany)
Acetic acid	Merck-Millipore (Darmstadt, Germany)
Antibiotics/Antimycotics	Sigma-Aldrich (Taufkirchen, Germany)
Benzaldehyde	Sigma-Aldrich (Taufkirchen, Germany)
Bovine serum albumine	Paesel-Lorei (Rheinberg, Germany)
Carbontetrachloride	Sigma-Aldrich (Taufkirchen, Germany)
Chloramine T	Merck-Millipore (Darmstadt, Germany)
Citric acid	Merck-Millipore (Darmstadt, Germany)
Collagenase	Sigma-Aldrich (Taufkirchen, Germany)
Dimethyl sulfoxide	Sigma-Aldrich (Taufkirchen, Germany)
Direct PCR Lysis Reagent	Peqlab (Erlangen, Germany)
Dithiothreitol	Thermo Fisher Scientific (Munich, Germany)
DMEM high glucose	Sigma-Aldrich (Taufkirchen, Germany)

DMEM low glucose	Sigma-Aldrich (Taufkirchen, Germany)
DNase I	Roche (Penzberg, Germany)
Eosine	Sigma-Aldrich (Taufkirchen, Germany)
Ethanol (96%)	Roth (Karlsruhe, Germany)
Ethanol absolute	Roth (Karlsruhe, Germany)
Ethylene glycol tetraacetic acid (Titrplex)	VWR life science (Darmstadt, Germany)
Fetal calf serum	Sigma-Aldrich (Taufkirchen, Germany)
Fluoromount G	Thermo Fisher Scientific (Munich, Germany)
Formaldehyde 4%	Otto Fischar (Saarbrücken-Scheidt, Germany)
Gel loading Dye	New England Biolabs (Frankfurt am Main, Germany)
GelRed Nucleic Acid Stain	Biotium (Fremont, CA, USA)
Glucose	Sigma-Aldrich (Taufkirchen, Germany)
Hank's Balanced Salt Sodium	Sigma-Aldrich (Taufkirchen, Germany)
HEPES	Merck-Millipore (Darmstadt, Germany)
Hydrochloric acid	Sigma-Aldrich (Taufkirchen, Germany)
Hydrogen chloride	Sigma-Aldrich (Taufkirchen, Germany)
Hydroxyproline	Sigma-Aldrich (Taufkirchen, Germany)
iQ SYBR Green Supermix	BioRad (Munich, Germany)
Isopropanol	Roth (Karlsruhe, Germany)
L-glutamine	Merck-Millipore (Darmstadt, Germany)
Leica CV Mount	Leica Biosystems (Wetzlar, Germany)
Lipofectamine RNAiMax	Thermo Fisher Scientific (Munich, Germany)
Lipopolysaccharide E.coli 055:B5	Sigma-Aldrich (Taufkirchen, Germany)
Magnesium chloride [50mM]	Thermo Fisher Scientific (Munich, Germany)

Methanol	Roth (Karlsruhe, Germany)
Methoxyethanol	Sigma-Aldrich (Taufkirchen, Germany)
Meyer's Hematoxyline	Roth (Karlsruhe, Germany)
Miglyol	Caesar & Loretz (Hilden, Germany)
Milk powder	Sigma-Aldrich (Taufkirchen, Germany)
Nycodenz	Thermo Fisher Scientific (Munich, Germany)
OptiMEM	Sigma-Aldrich (Taufkirchen, Germany)
Paraplast Plus	Roth (Karlsruhe, Germany)
PCR reaction buffer 10x	Thermo Fisher Scientific (Munich, Germany)
Penicillin-Streptomycin	Sigma-Aldrich (Taufkirchen, Germany)
Perchloric acid	Merck-Millipore (Darmstadt, Germany)
Phosphate-buffered saline tablets	VWR life science (Darmstadt, Germany)
Pikro Sirius Red	Morphisto (Frankfurt am Main, Germany)
Platinum Taq polymerase	Thermo Fisher Scientific (Munich, Germany)
Precision Plus Protein Dual Color	BioRad (Munich, Germany)
Pronase E	Merck-Millipore (Darmstadt, Germany)
Protease Inhibitor	Sigma-Aldrich (Taufkirchen, Germany)
Proteinase K	Roth (Karlsruhe, Germany)
Restore™ Western Blot Stripping Buffer	Thermo Fisher Scientific (Munich, Germany)
Retrieval solution	Agilent (Oberhaching, Germany)
RNAlater	Sigma-Aldrich (Taufkirchen, Germany)
RPMI	Sigma-Aldrich (Taufkirchen, Germany)
Sodium acetate	Merck-Millipore (Darmstadt, Germany)
Sodium hydroxide	Merck-Millipore (Darmstadt, Germany)
Tri-sodium citrate	Merck-Millipore (Darmstadt, Germany)

Trypsin (0.05%)	Thermo Fisher Scientific (Munich, Germany)
Tween 20	Sigma-Aldrich (Taufkirchen, Germany)
Weigerts hematoxyline	Morphisto (Frankfurt am Main, Germany)
Xylol	Sigma-Aldrich (Taufkirchen, Germany)

2.1.4 Buffers and solutions

2.1.4.1 General

Phosphate-buffered saline (PBS)

5 PBS tablets dissolved in 1l ddH₂O

PBS-T

PBS + 0,05% Tween

2.1.4.2 Immunostaining

IF buffer

3% BSA + 10% FCS in PBS

Sodium Citrate buffer (10nM, pH 6.0)

2.94 g Tri-sodium citrate in 1000 ml ddH₂O

2.1.4.3 Hydroxyproline assay

Citrate-acetate-buffer (CAP) pH = 6.0

25 g (238 mmol/l) Citric acid

Adjust pH with acetic acid

36.3 g (885 mmol/l) Sodium acetate

17 g (0.85 mol/l) Sodium hydroxide

500 ml ddH₂O

Chloramine-T solution

141 mg Chloramine T

2 ml ddH₂O

3 ml	2-Methoxyethanol
5 ml	CAP

4-(Dimethylamino)- benzaldehyde solution

2 g	4-(Dimethylamino)-benzaldehyde
10 ml	2-Methoxyethanol

Hydroxyproline stock solution

50 mg	Hydroxyproline
10 ml	ddH ₂ O

2.1.4.4 Isolation of murine hepatic stellate cells and Kupffer cells

HEPES pH 7.4

23.8 g	HEPES
100 ml	ddH ₂ O

Adjust pH with NaOH (1mol/l)

Hanks Balanced Salt Solution (HBSS)

5 ml	HEPES (1 mol/l, pH 7.4)
500 ml	Hanks Balanced Salt Solution

Nycodenz gradient solution

143.5 g	Nycodenz
100 mg	KCL
175 mg	NaHCO ₃
92.5 mg	CaCl ₂
50 mg	MgSO ₄
30 mg	KHPO ₄
24 mg	Na ₂ HPO ₄
fill to 1000 ml with	ddH ₂ O

Filter sterile through 0,2 µm filter

Store at 4 °C

Krebs-Ringer-Buffer (KRB)

0.75 g	Glucose
600 ml	ddH ₂ O
37.5 ml	20x KRB I
37.5 ml	20x KRB II
37.5 ml	20x KRB III
11.25 ml	HEPES (1 mol/l)

20x KRB Stock solution I

137.92 g	NaCl
7.16 g	7.16 g KCl
fill to 1000 ml with	ddH ₂ O
Store at 4°C	

20x KRB Stock solution II

3.27 g	KH ₂ PO ₄
5.92 g	MgSO ₄
fill to 1000 ml with	ddH ₂ O

20x KRB Stock solution III

5.59 g	CaCl ₂
fill to 1000 ml with	ddH ₂ O

Perfusion solution I

0.5 g	Glucose
95 mg	EGTA
425 ml	ddH ₂ O
25 ml	20x KRB I
25 ml	20x KRB II
7.5 ml	HEPES (1 mol/l)

Perfusion solution II

25 mg	Pronase E
-------	-----------

RAW264.7 cells were obtained from CLS (Eppelheim, Germany) and cultured in RPMI + 5% FCS + 1% P/S

Isolated mHSCs were cultured in DMEM low glucose + 10% FCS + 2% glutamine + 1% antibiotic/antimycotic solution

Isolated Kupffer cells were cultured in DMEM + 10% FCS + 1% P/S

2.1.6 Commercially available kits

CytoSelect 24- Well Cell Migration Assay (5 μ m, Fluorometric Format)	Cell Biolabs, Inc. (San Diego, CA, USA)
Human IL-6 Elisa Kit	BD Biosciences (Heidelberg, Germany)
Human IL-37 Elisa Kit	Adipogen (Liestal, Switzerland)
ImmPRESS-HRP-anti-rat	Vector Laboratories (Peterborough, UK)
ImmPRESS-HRP-anti-rabbit	Vector Laboratories (Peterborough, UK)
Liquid DAB+ Substrate Chromogen System	Agilent (Oberhaching, Germany)
Mouse IL-6 Elisa Kit	BD Biosciences (Heidelberg, Germany)
Pierce BCA Protein Assay Kit	Thermo Fisher (Munich, Germany)
Pierce ECL Western Blotting Substrate	Thermo Fisher (Munich, Germany)
Pikro Sirius Red	Morphisto (Frankfurt am Main, Germany)
ProcartaPlex 5-plex custom	Thermo Fisher (Munich, Germany)
ProcartaPlex Mouse TGF beta 1 Simplex	Thermo Fisher (Munich, Germany)
RNeasy Mini Kit	Qiagen (Hilden, Germany)
SuperScript II Reverse Transcriptase	Thermo Fisher (Munich, Germany)
TSA Cyanine 5 System	Perkin Elmer (Rodgau, Germany)
TSA Fluorescein System	Perkin Elmer (Rodgau, Germany)

2.1.7 Primary antibodies for western blotting

Name	Vendor	Dilution	Host species	Size [kD]
Icam1/CD54	R&D systems	1:1000	Goat	100
Bambi/NMA	R&D systems	1:1000	Goat	32
α -sma	Abcam	1:2500	Rabbit	42
β -actin	Cell signalling	1:2500	Rabbit	45
IL-37	Own production	1:1000	Mouse	25

2.1.8 Primary antibodies for immunohistochemistry/immunofluorescence

Name	Vendor	Dilution	Host species
α -sma	Abcam	1:100	Rabbit
Mac-2	Cederlane Labs	1:100	Rat
IL-37	Sigma-Aldrich	1:80	Rabbit

2.1.9 Secondary antibodies

Name	Vendor	Dilution
Alexa-fluor Cy5	Alexa Fluor	1:1000
Donkey-anti goat HRP	Santa Cruz	1:10000
Goat anti rabbit HRP	Agilent	1:2500
Goat anti mouse HRP	Agilent	1:2500

2.1.10 siRNAs

Name	Vendor	Concentration
Silencer select Negative control #1	Ambion	10-100 nM
IL37 silencer select siRNA	Ambion	10-100 nM

2.1.11 cmRNAs

Name	Company	Lot number
cmRNA ^{GFP}	Ethris, Planegg, Germany	141009-CA
cmRNA ^{Stop}	Ethris, Planegg, Germany	150722-SE/
cmRNA ^{IL37#1}	Ethris, Planegg, Germany	
cmRNA ^{IL37#2}	Ethris, Planegg, Germany	

2.1.12 Proteins/Cytokines

rhIFN- γ	Peptotech (Hamburg, Germany)
rhIL-1 β	Peptotech (Hamburg, Germany)
rh pro-IL-37	YBDY Biotechnology (Seoul, Korea)
rhTGF- β 1	R&D systems (Abingdon, UK)
rhTNF- α	Peptotech (Hamburg, Germany)

2.1.13 Primer qRT-PCR

2.1.13.1 Mouse primer

Gene of interest	Forward	Reverse
<i>Cxcl1</i>	<i>TGA AGG TGT TGC CCT CAG G</i>	<i>AAC CAA GGG AGC TTC AGG GT</i>
<i>Cxcl2</i>	<i>ACC AAC CAC CAG GCT ACA GG</i>	<i>CTC AAG CTC TGG ATG TTC TTG AAG</i>
<i>Cxcl10</i>	<i>CTG GGT CTG AGT GGG ACT CAA</i>	<i>TTC CCT ATG GCC CTC ATT</i>
<i>Ccl2</i>	<i>GTT GGC TCG CCA GAT</i>	<i>TGA TCC TCT TTA GCT CTC</i>

	<i>GCA</i>	<i>CAG C</i>
<i>Ccl3</i>	<i>CCA TGA CAC TCT GCA ACC AAG T</i>	<i>GAT GAA TTG GCG TGG AAT CTT C</i>
<i>Ccl4</i>	<i>CTC TC TCT CCT CTT GCT CGT GG</i>	<i>CGG GAG GTG TAA GAG AAA CAG C</i>
<i>Icam1</i>	<i>CGC ACA GAA CTG GAT CTC AGG</i>	<i>TTT GGG ATG GTA GCT GGA AGA</i>
<i>Vcam1</i>	<i>CCT GTC TGC AAA GGA CAC TGG</i>	<i>TCT CCC ATG CAC AAG TGG C</i>
<i>Bambi</i>	<i>CCA GCT ACT TCT TCA TCT GGC</i>	<i>GAT CTC TCC TTT GGT GAG CAG</i>
<i>TgfbβII</i>	<i>CAA GTC GGA TGT GGA AAT GGA</i>	<i>TGT TTC AGT GGA TGG ATG GTC</i>
<i>Il13</i>	<i>ACA TCA CAC AAG ACC AGA CTC</i>	<i>GAG ATG TTG GTC AGG GAA TC</i>
<i>Il6</i>	<i>ATT ACA CAT GTT CTC TGG G</i>	<i>GGA CTC TGG CTT TGT CTT</i>
<i>Tnfa</i>	<i>AGG CGG TGC CTA TGT CTC AG</i>	<i>GAC CGA TCA CCC CGA AGT T</i>
<i>Il1β</i>	<i>AAA TAC CTG TGG CCT TGG GC</i>	<i>ACA CTC TCC AGC TGC AGG GT</i>
<i>Timp1</i>	<i>CAA CTC GGA CCT GGT CATA A</i>	<i>GCT GGT ATA AGG TGG TCT CG</i>
<i>Colla1</i>	<i>CGG TAA CGA TGG TGC TGT T</i>	<i>CTT CAC CCT TAG CAC CAA CT</i>

<i>Acta2</i>	CCA TCT TTC ATT GGG ATG GAG	TAG CAT AGA GAT CCT TCC TGA
<i>Tgfb</i>	GCC AAC TTC TGT CTG GGA CC	CCG GGT TGT GTT GGT TGT AGA

2.1.13.2 Human primer

Gene of interest	Forward	Reverse
<i>CXCL1</i>	ATC CAA AGT GTG AAC GTG AAG TC	GCC TCT GCA GCT GTG TCT CT
<i>CXCL2</i>	CTG CAG GGA ATT CAC CTC AAG	CCT CTT CTG TTC CTG TA AGG GC
<i>CXCL10</i>	GCC ATT CTG ATT TGC TGC CT	TGC TGA TGC AGG TAC AGC GT
<i>CCL2</i>	AGA TGC AAT CAA TGC CCC AG	TTG TCC AGG TGG TCC ATG G
<i>CCL3</i>	ACT CGA GCC CAC ATT CCG T	GGA GGT GTA GCT GAA GCA GCA
<i>CCL4</i>	AAT ACC ATG AAG CTC TGC GTG AC	CCA CAA AGT TGC GAG GAA GC
<i>ACTA2</i>	TAC GAG TTG CCT GAT GGG C	CCA GCA GAC TCC ATC CCG
<i>ICAM1</i>	TGG AGC CAA TTT CTC GTG C	GGA CAA AGG TTG GAG CTG G
<i>IL37</i>	GGG AGA ACT CAG GAG TGA AAA T	TTT CAG CTT TGC AAA CTG GTT G
<i>VCAM1</i>	GGG AAC GAA CAC TCT TAC	TTC CTG TCT GCA TCC TCC AGA
<i>TGFβ</i>	TGC CCC GAG TGC TAC	AAC CCT CAT CTC CGA

	<i>TTT</i>	<i>AGG G</i>
<i>IL6</i>	<i>AAA GAG GCA CTG GCA GAA AA</i>	<i>CCA GGC AAG TCT CCT CAT TG</i>
<i>IL1β</i>	<i>TGA TGG CTT ATT ACA GTG GCA A</i>	<i>CAC TTC ATC TGT TTA GGG CCA</i>

2.1.13.3 House keeping genes

Gene of interest	Forward	Reverse
<i>Tbp</i>	<i>GCC CGA AAC GCC GAA TAT</i>	<i>CCG TGG TTC GTG GCT CTC T</i>
<i>Rpl13a</i>	<i>ATC CCT CCA CCC TAT GAC AA</i>	<i>AAG CAA ACT TTC TGG TAG GCT T</i>

2.1.14 Primer genotyping

2.1.14.1 IL-37tg

Gene of interest	Forward	Reverse
<i>IL37</i>	<i>GGG AGA ACT CAG GAG TGA AAA T</i>	<i>TTT CAG CTT TGC AAA CTG GTT G</i>

2.1.14.2 MDR2KO

Gene of interest	Forward	Reverse
<i>MDR2 wt</i>	<i>CAA CAC GCG CTG GAA</i>	<i>GAT GCT GCC TAG TTC AAA GTC G</i>
<i>MDR2 mut</i>	<i>TGT CAA GAC CGA CCT GTC CG</i>	<i>TAT TCG GCA AGC AGG CAT CG</i>

2.1.15 Animals

C57BL6/J mice were purchased from Jackson Laboratory (Sulzfeld, Germany). MDR2KO mice were purchased from Jackson Laboratory (Maine, USA). IL-10KO were purchased from Charles River Inc. (Boston, MA, USA)

2.1.16 Medication and sedation

Atipamezol	2.5 mg/kg
Buprenorphin	0.05 mg/kg
Fentanyl	0.05 mg/kg
Flumazenil	0.5 mg/kg
Ketamin	100 mg/kg
Medetomidin	0.5 mg/kg
Midazolam	5.0 mg/kg
Xylazin	10 mg/kg

2.1.17 Software

Adobe Photoshop CS6

Endnote X7.5.3

ImageJ 1.51s

ImageLab 6.0

Microsoft Office Suite for Mac 2011 (Version 14.1.0)

Prism 5 for Mac OS X

2.2 Methods

2.2.1 Tissue culture

2.2.1.1 General maintenance

All cell lines used in this work were cultivated in cell-specific media at 37 °C in a humidified atmosphere of 5% CO₂ in the air. All tissue culture work was performed under sterile conditions. To minimize the risk of cross contamination, different cell lines were handled independently. Media, trypsin and PBS were pre-warmed to 37 °C before use.

Thawing of cells

Vials of cryopreserved cells were taken from -80 °C storage and thawed quickly in a 37°C water bath for 1-2 minutes. To prevent any cytotoxic effect due to the DMSO cryoconservant, the cell suspension was rapidly transferred to 5 ml cell-specific medium. The cells were then centrifuged at 524 x g for 5 minutes and the cell pellet resuspended in cell-specific medium and transferred to a T25 tissue culture flask.

Passaging of cells

Cells were passaged when they reached 80% confluency by first washing them with PBS and then treating them with 0.05% trypsin/EDTA for approximately 5 minutes at 37 °C. Cell specific media was added to the flask and cell aggregates were dissolved by carefully pipetting up and down. Cells were split 1:3 to 1:10 every 2 to 4 days. Medium was changed every 2 to 3 days for all cell lines.

Cryoconservation of cells

For cryoconservation, cells were expanded in 75 cm² flasks to approximately 80% confluency. They were harvested from culture with 0.05% trypsin and then pelleted in 15 ml Falcon tubes by centrifugation at 524 x g for 5 minutes. The pellet was then resuspended in 800 µl of medium. Before the cells were transferred to the freezing vial, 100 µl of 10% FCS and 100 µl DMSO (10%) were added to the vial. The cells were transferred to the freezing vial and then placed in a freezing container filled with isopropanol and stored at -80 °C. After approximately 72 hours, the vials containing frozen cells were transferred to liquid nitrogen tanks (-196 °C) for long time storage.

2.2.1.2 cmRNA transfection

For IL-37 overexpression experiments A549 and RAW264.7 were plated in full culture media in 6-well plates. LX2 cells were plated in starvation media (DMEM + 0.5% FCS). Cells were transfected with 1 µg human IL-37 encoding chemically modified RNA (cmRNA^{IL37#1/#2}) or vehicle (cmRNA^{Stop/GFP}) using Lipofectamine RNAiMax. Subsequently, RAW264.7 were stimulated with LPS (100 ng/ml), A549 and LX2 with IL-1β (1ng/ml).

2.2.1.3 siRNA mediated knock down of IL-37

For siRNA mediated IL-37 knockdown LX2 cells were plated in starvation media in 6-well plates. Cells were transfected with a range (10-100nM) IL-37 targeting siRNA or vehicle (Scramble) using Lipofectamine RNAiMax and subsequently stimulated with IL-1β (1ng/ml). Level of knockdown was assessed 54h and 72h after transfection.

2.2.1.4 Recombinant human IL-37 treatment

For recombinant human IL-37 treatment LX2 cells were plated in starvation media (DMEM + 0.5% FCS) and exposed to a range of rhIL-37 for 24h. Subsequently, cells were stimulated with IL-1β (1ng/ml). Total RNA was collected 6h after stimulation. Supernatant was tested for IL-6 by Elisa 24h after stimulation.

2.2.1.5 Cell harvest

For protein or RNA extraction, cells were detached as described above or collected using ice-cold PBS and cell scrapers. Cells were pelleted at 524 x g at 4 °C for 5 minutes. Pellets for RNA extraction were immediately processed, whereas pellets for protein analysis were stored at -20°C until further use.

2.2.2 Protein analysis

2.2.2.1 Whole cell lysis and organ lysis

Cell pellets were resuspended in 80 – 100 µl Pierce IP lysis buffer (Thermo Fisher Scientific, Munich, Germany) containing protease inhibitors depending on the size of the pellet. 10 mg of liver tissue was homogenized in organs lysis buffer (PBS + 0.1% Triton). Cells/tissue were

frozen at -20°C for 1 hour. After the freeze and thaw cycle the lysed cells/tissue were centrifuged for 10 minutes at 13000 x g. The protein- containing supernatant was transferred to a fresh tube and stored at -80 °C until further use.

2.2.2.2 Protein quantification

Protein quantification was performed using the BCA kit from Thermo Fischer. Samples were diluted 1:2 to 1:5 depending on original sample size.

2.2.2.3 Western blot

Between 5 and 35 µg of protein sample were loaded into each lane of an any kD Mini-PROTEAN TGX Precast Protein Gel. 5µL BIO-RAD Precision Plus Protein Dual Color Standard was loaded as a marker for protein size. The gel was run using the BioRad electrophoresis system for 90 minutes at 120 V. The samples were then blotted onto PVDF membrane using BioRad blotting chamber for 1h at 180 mA. The membranes were briefly washed in PBS-T and then transferred to 5% milk in PBS-T for 1 hour. After blocking, membranes were probed with antibodies listed under 2.1.7 diluted in 5% milk over night at 4 °C. After washing the membranes for 3 x 5 minutes in PBS-T the next day, the blots were exposed to secondary antibodies diluted in 5% milk in PBS-T for one hour. The membranes were washed 3 x 10 minutes in PBS-T before being developed using Amersham ECL Prime Western Blotting Detection Reagent. Bands were imaged using either the AGFA film developer or ChemiDoc XRS+.

2.2.2.4 Secondary probing

For re-probing of western blot membranes with different primary antibodies, membranes were incubated in stripping buffer for 15 minutes at RT. After washing the membranes 3 times 5 minutes with PBS-T, membranes were either stored in PBS or re-probed as described above.

2.2.3 Nucleic acid analysis

2.2.3.1 RNA extraction and quality control

RNA was extracted from cell pellets or 30 mg liver tissue using the RNeasy mini kit. RNA amount was measured using the Nanodrop. RNA purity was assessed by reviewing the

260/280 ratio, RNA degradation was excluded by loading native RNA on to a 1.5% Agarose gel.

2.2.3.2 cDNA

Between 500 ng – 1 µg RNA was transcribed to cDNA using the SuperScript™ II Reverse Transcriptase kit from Thermo Fischer.

2.2.3.3 qRT-PCR

Gene expression level was measured by quantitative RT-PCR using SYBR Green Supermix and 50 – 100 ng cDNA per well. Gene specific primers were designed using PrimerExpress and ordered from Eurofins MWG (Ebersberg, Germany) with purification grade HPLC. qRT-PCR reactions were performed in doubles in a 96-well format (BioRad iCycler). Fold changes of mRNA expression were calculated and normalized to house keeping gene *Rpl13a* or *Tbp* using the $\Delta\Delta C_t$ -method (41). The sequences of the gene specific primers used are listed under 2.1.13. Non-template control was run alongside.

2.2.4 Histology

2.2.4.1 Preservation, embedding and sectioning of samples

After euthanization, livers were explanted and the big right liver lobe was transferred to 4% formaldehyde for 24h for fixation. To remove PFA residue, specimen was washed twice with PBS, dehydrated and prepared for embedding according to following scheme:

Time	Chemical	Concentration
10 minutes	PBS	
10 minutes	Ethanol	70%
10 minutes	Ethanol	80%
10 minutes	Ethanol	96%
10 minutes	Ethanol	100%
20 minutes	Ethanol	100%
15 Minutes	Ethanol (100%) / Xylol	2:1
15 Minutes	Ethanol (100%) / Xylol	1:1

15 Minutes	Ethanol (100%) / Xylol	1:2
15 Minutes	Xylol	100%
15 Minutes	Xylol	100%
15 Minutes	Xylol	100%
30 minutes	Xylol / Paraffine	2:1
30 minutes	Xylol / Paraffine	1:1
30 minutes	Xylol / Paraffine	1:2
1-2 h	Paraffine	100%
Over night	Paraffine	100%

Samples were embedded the following day and let to rest overnight. 5 µm sections were cut using the Leica microtome (Wetzlar, Germany), placed on slides and then in an incubator over night at 37°C. Slides were mounted using Leica CV Mount. For Immunohistochemistry, slides were embedded using Fluoromount G (Thermo Fisher Scientific, Munich, Germany) and stored at -20°C.

2.2.4.2 Hematoxylin/Eosine staining

5 µm liver sections were deparaffinised, stained and dehydrated according to following scheme:

Time	Chemical
10 minutes	Xylol
10 minutes	Xylol
5 minutes	Ethanol (100%)
5 minutes	Ethanol (96%)
5 minutes	Ethanol (70%)
1 minute	Aqua dest.
4 minutes	Meyers Hemytoxyline
5 minutes	Running tap water
3 minutes	Eosine
2-3 seconds	Ethanol (70%)
2-3 seconds	Ethanol (96%)

2-3 seconds	Ethanol (100%)
5 minutes	Xylol
5 minutes	Xylol

Slides were mounted using Leica CV Mount.

2.2.4.3 Pikro Sirius Red Staining

5 µm liver sections were deparaffinised, stained and dehydrated according to following scheme:

Time	Chemical
10 minutes	Xylol
10 minutes	Xylol
4 minutes	Ethanol (100%)
4 minutes	Ethanol (96%)
4 minutes	Ethanol (70%)
8 minutes	Weigerts Hematoxyline
5 seconds	Aqua dest.
10 minutes	Running tap water
1 minutes	Aqua dest.
1 hour	Pikro Sirius Red
1 minute	Acetic acid (30%)
1 minute	Acetic acid (30%)
4 minutes	Ethanol (96%)
4 minutes	Ethanol (100%)
10 minutes	Xylol
10 minutes	Xylol

2.2.4.4 Immunohistochemistry

All immunohistochemical stainings for CD3 were performed by the Institute of Pathology, Munich. Stainings for α -Sma and Mac-2 were performed using the ImpressKit from Vector Laboratories. First the slides were deparaffinised according to following scheme:

Time	Chemical
10 minutes	Xylol
10 minutes	Xylol
5 minutes	Ethanol (100%)
5 minutes	Ethanol (96%)
5 minutes	Ethanol (70%)
5 minutes	Aqua dest.

Antigen retrieval was performed by pressure-cooking the slides in citrate buffer (pH 9.0) for 9 minutes and then let to cool to RT. After washing the slides twice for 5 minutes in PBS-T slides were exposed to 3% H₂O₂ in ddH₂O for 30 minutes, followed by two times 7 minutes washing in PBS-T (0.05%). Non-specific binding was blocked by horse serum for 30 minutes. Antibody detection was performed according to following scheme:

Time	Procedure
Overnight (4°C)	Primary antibody diluted in serum
3 x 5 minutes	Washing PBS-T
30 minutes	Secondary antibody
3 x 7 minutes	Washing PBS-T
2-3 minutes	DAB staining
10 minutes	Running tap water
1-2 minutes	hematoxyline
10 minutes	Running tap water
10 seconds	Ethanol (100%)
2 x 5 minutes	Xylol

2.2.4.5 Immunofluorescence

All immunofluorescent stainings for α -sma or IL-37 were performed using the TSA Cyanine 5 or Fluorescein Kit (Perkin Elmer). First the slides were deparaffinised according to following scheme:

Time	Chemical
10 minutes	Xylol

10 minutes	Xylol
5 minutes	Ethanol (100%)
5 minutes	Ethanol (96%)
5 minutes	Ethanol (70%)
5 minutes	Aqua dest.

Antigen retrieval was performed by pressure-cooking the slides in Dako Retrieval buffer for 30 minutes and then letting them cool to RT. After washing the slides twice for 5 minutes in PBS-T slides were exposed to 7.5% H₂O₂ for 10 minutes. The slides were then washed twice for 5 minutes under running water followed by blocking in horse serum. Detection was performed as follows:

Time	Procedure
1 hour	Primary antibody diluted in serum
3 x 5 minutes	Washing in PBS-T
30 minutes	Secondary antibody
3 x 7 minutes	Washing in PBS-T
5 minutes	Perkin Elmer substrate (in the dark)
2 x 5 minutes	Washing PBS-T (in the dark)
10 minutes	Dapi staining (in the dark)

2.2.4.6 Quantification

The average number of positive cells was determined by counting stained cells in four randomly chosen high power fields (HPF). Sirius Red staining was quantified using ImageJ.

2.2.5 Biochemical analysis

2.2.5.1 Liver serum values

After euthanization blood was collected and centrifuged at 300 x g for 10 minutes, followed by a second centrifugation step at 300 x g for 10 minutes. Serum was then diluted 1:4 in PBS. Liver serum values were determined by routine laboratory medicine methods.

2.2.5.2 Hydroxyproline measurement

For hydroxyproline measurement 200 mg liver was homogenized in 4 ml HCL using a dounce-homogenizer (IKA, Staufen, Germany). The samples were heated to 110°C, vortexed after 30 minutes and hydrolysed for 16-24h at 110°C. The cooled samples were filtrated into a 50 ml falcon. 50 µl lysate was neutralized by adding 450 µl NaOH solution.

The calibration curve was pipetted by adding 12 µl hydroxyproline stock solution to 10 ml Citrat-Acetate-buffer pH 6.0 (CAP) and then diluted 2-fold in serial dilution steps diluted in CAP.

Then 250 µl chloramine T solution was added to every sample, shortly vortexed and incubated for 20 minutes at RT. After that, 250 µl perchloric acid (70%) was added to the samples, vortexed briefly and incubated at RT for 12 minutes. Finally, 250 µl 4-(dimethylamine)-benzaldehyde solution was added to the tubes, vortexed briefly and incubated at 60°C for 20 minutes.

The absorption was measured at 565 nm and the hydroxyproline content calculated by linear regression of the calibration samples.

2.2.5.3 Cytokine measurement

IL-6 secretion was measured using the IL-6 Elisa kit obtained from BD Biosciences. Unstimulated samples were diluted 1:10, 1:20, 1:40 and 1:80, whereas stimulated samples were diluted 1:20, 1:40, 1:80 and 1:160.

IL-10, IL-1 β , CCL2, CCL4, TNF- α and TGF- β , were measured in supernatant of mHSCs using specially designed ProcartaPlex from Thermo Fischer.

IL-12p40, G-CSF, CCL2, KC, Rantes, CCL4, IL-10 and IL-12 were measured in supernatant of KCs using specially designed Bioplex Assay from BioRad.

2.2.6 Isolation of human PBMCs

After collection, blood sample was diluted 1:2 in NaCl (0.9%) in a 50 ml tube. 15 ml Ficol was added to a fresh tube and overlaid with 30-35 ml blood. NaCl was added up to 50 ml total volume. Samples were centrifuged at 1800 rpm for 10 minutes without brakes. Lymphocytes appearing as a white ring were gently aspirated and transferred to a fresh tube. NaCl was added to collected lymphocytes and centrifuged at 1100 rpm for 10 minutes with brakes. Cell pellet was washed twice with NaCl before being resuspended in RPMI + 10% serum.

2.2.7 Primary cell culture

2.2.7.1 Isolation and cultivation of murine hepatic stellate cells

Quiescent hepatic stellate cells were isolated from wt and IL37tg mice (C57BL/6 background) according to standard methods as described by Reiter et al. (76). After sedation the portal vein was cannulated and flushed with EGTA-containing buffer. Subsequently the liver was flushed with pronase E solution to digest the tissue followed by collagenase solution. Afterwards the liver was removed from the peritoneal cavity, cut into small pieces and stirred for 20 minutes at 37°C in solution containing pronase E, collagenase and DNase I. The cell suspension was filtered through 70 µm cell strainer into 50 ml falcon tube and centrifuged for 7 minutes at 450 g at 4°C. Cells were washed in HBSS and then resuspended in 10ml DNase-I containing HBSS. 8.5ml nycodenz solution (28.7%) was added. Cell suspension was gently overlaid with 6 ml HBSS and centrifuged at 4°C and 1400 g for 22 min without brakes. Subsequently mHSCs appearing as a white ring of the interphase, were gently aspirated, added to 20 ml culture media and centrifuged for 10 minutes at 450 g. Cell pellets were resuspended in 10ml culture media (DMEM low glucose) and plated in 6-well TC plates with or without rh-IL37 (10,100,1000 ng/ml). Media and rhIL-37 was replaced every 2 days and tested for spontaneous IL-6 secretion by Elisa. In addition, cells were stimulation with LPS (100ng/ml) on day 8 and TGF-β1 (100 pg/ml) on day 9. RNA analysis was performed on day 2, 6h after LPS stimulation or on Day 3 after LPS and TGF-β1 stimulation.

2.2.7.2 Isolation of murine Kupffer cells

Murine Kupffer cells were isolated according to the same process as described under 2.2.6.1. After gradient centrifugation cells appearing as a white milky coloured ring were gently aspirated, added to 50 ml GBSS/B and centrifuged at 45 x g at 4 °C for 2 minutes. Supernatant was carefully transferred to a fresh falcon and centrifuged at 4 °C for 5 minutes at 700 x g. Cell pellet was resuspended in cell culture media plated for cell staining or migration assay.

2.2.7.3 Cell staining

mHSCs

After isolating mHSCs cells count was adjusted to 150.000/ml. 300 µl cell suspension was pipetted into the chambers of an Ibidi µ-Slide and cultured for 12 days until cells were fully

activated stellate cells. Cells were washed twice with PBS before being fixed with 3.7% formaldehyde solution (in PBS) for 20 minutes at RT. Formaldehyde solution was removed, cells were washed twice with PBS and then incubated in PBS + glycine (0.1 M) for 10 minutes.

Fixed cells were permeabilised with 0.5% Triton X-100 in PBS for 10 minutes at RT. Cells were blocked with IF buffer for 30 minutes at RT. Primary antibody α -sma was diluted 1:150 in IF buffer and incubated for 1 hour at RT followed by three washes with PBS. Secondary antibody was incubated for 30 minutes in the dark, followed by three washes with PBS. Cell nuclei were stained with DAPI solution for 15 minutes at RT. Finally, cells were washed with PBS and preserved with 150 μ l Mounting Media.

KCs

After isolating KCs cells count was adjusted to 150.000/ml. 300 μ l cell suspension was pipetted into the chambers of an Ibidi μ -slide and cultured for 24 hours. Kupffer cell staining was performed as described under 2.2.6.3.1. using the primary antibody Mac-2 diluted 1:150 in IF buffer.

2.2.7.4 Migration assay

Media conditioning

Hepatic stellate cells were isolated from wt and IL37tg mice, plated in petri dishes and stimulated with 100 ng/ml LPS on day 8, followed by stimulation with TGF- β 1 (100 pg/ml). 24h after TGF- β 1 stimulation, supernatant was collected and used for Kupffer cell migration assay.

Kupffer cell migration

Equal number of freshly isolated KCs from wt or IL37tg mice were plated into the upper chamber of the CytoSelect Migration Kit. DMEM, or conditioned media from IL37tg or wt stimulated mHSCs was placed in the lower chamber. KCs were incubated for 8h to migrate through the 5 μ m pore inserts. Cell count was determined using the CytoSelect Cell Migration Assay.

2.2.8 *In-vivo* studies

2.2.8.1 Animals

Animals were housed in specific-pathogen free condition at a controlled temperature with light/dark cycles with free access to food and water and were acclimatized for 2 weeks before being studied.

IL-37tg (C57BL/6J Background)

IL37 transgenic mice were generated using the full-length precursor cNDA of IL37b isoform driven by the CMV promotor for constitutive expression, as this promotor is commonly used to drive expression in most cells. There is no obvious phenotype, however compared to wt mice, IL37tg mice are protected against LPS challenge. C57BL/6J mice expressing human IL-37 have been described previously (36). Homozygous IL-37tg mice were selected by genotyping.

IL-10KO/IL-37tg

IL-10KO mice were crossbred with C57BL/6J-IL-37tg mice to create IL-10KO/IL-37tg mice. IL-10KO mice were obtained from Charles River Inc. (Boston, MA, USA). Homozygous IL-10KO/IL-37tg mice were selected by genotyping.

MDR2KO (FVB.129P2-*Abcb4*^{tm1Bor}/J)

MDR2KO mice were purchased from Jackson Laboratory (Maine, USA). The mice fail to secrete phospholipid into the bile from the liver. They develop portal inflammation followed by hepatocellular carcinoma. Detailed genetics and disease phenotype have been described previously (77). Homozygous MDRKO mice were selected by genotyping.

2.2.8.2 Genotyping of animals

For genotyping of animals, tails biopsies were lysed in 100 µl Direct PCS Lysis Reagent with 5 µl proteinase K over night at 55°C followed by an inactivation step of 30 min at 75°C. DNA was precipitated by adding 200 µl conc. EtOH and 10 µl 3M NaN₃ to the lysed tails. The probes were placed on -20°C for 60 minutes followed by 15 min. centrifugation at 13,000 x g at 4°C. Supernatant was mixed with 1 ml 70% EtOH and centrifuged for further 5 min at full speed and 4°C. Supernatant was carefully removed and DNA pellet let to dry. DNA was then dissolved in 25 µl HPLC H₂O and concentration measured using the Nanodrop.

After running the PCR the product was run on a 1.5% agarose gel and imaged using the Intas Gel Imager. Positive and negative controls were run alongside at all times.

IL-37tg

IL-37tg genetics were determined by adjusting DNA input to 25 ng and adding following PCR components:

H ₂ O + 25ng DNA	13.6 µl
MgCl ₂ [50nM]	0.8 µl
10x Buffer	2.0 µl
dNTPs [10nM]	0.4 µl
Forward primer	1.0 µl
Reverse primer	1.0 µl
Taq Platinum	0.2 µl

Homozygous IL37tg mice were genotyped using following endpoint PCR program:

95 °C	3 min	
95 °C	30 sec	40 cycles
58 °C	45 sec	
72 °C	2 min	
72 °C	7 min	
4 °C	hold	

Heterozygous IL37tg mice were genotyped using following semi-quantitative PCR program:

95 °C	3 min	
95 °C	30 sec	28 cycles
58 °C	45 sec	
72 °C	2 min	
72 °C	7 min	
4 °C	hold	

MDR2

wt, heterozygous or knockout mice were genotyped using the following reaction components:

10x Buffer	2.5 μ l
MgCl ₂ [50nM]	1.25 μ l
DMSO	2.5 μ l
Forward Primer (wt/KO)	1 μ l
Reverse Primer (wt/KO)	1 μ l
dNTPS [10nM]	0.3 μ l
Taq Platinum	0.25 μ l
ddH ₂ O	15.2 μ l
DNA	2 μ l

2.2.8.3 Animal models

Chemically induced liver fibrosis mouse model

CCl₄ (0.6 ml/kg in Miglyol) or Miglyol was administered twice a week via intra-peritoneal injection into 6-8-week-old female C57BL/6 or IL37tg mice for 6-10 weeks. At the end of the experiment mice were sacrificed via terminal bleeding, serum was collected and liver preserved for further evaluation.

Bile duct ligation induced liver fibrosis

Male wt, IL37tg or rhIL-37 treated (5 μ g) mice underwent ligation of the common bile duct under general anaesthesia at the age of 6-8 weeks as described in (78). After disinfection with 70% Ethanol a midline upper-abdominal incision was made and the abdominal wall retracted. The common bile duct was identified, isolated and double ligated with 6-0 braided silk sutures and divided between the ligatures. The fascia and skin of the midline abdominal incision will be closed with the same silk sutures. Control mice underwent sham operations in which the common bile duct was exposed but not ligated. For analysis of early fibrosis markers, mice were sacrificed 3 days after bile-duct ligation. To analyse effect of rhIL37 in early fibrosis mice were injected with rhIL-37 1 hour before the operation and once again on day 2. To study the effects of IL-37 in the long-term bile duct ligation model, mice were sacrificed 14 days after ligation. Mice were sacrificed by terminal bleeding, serum was collected and liver preserved for further evaluation.

MDR2KO mouse model

Male, 2-week-old MDR2 KO mice were injected 3 times per week with 5 µg chemically modified Stop or IL37 RNA for 4 weeks. At the end of the experiment mice were sacrificed by terminal bleeding, serum was collected and liver preserved for further evaluation.

Colitis associated liver disease

We recently described the protective role of IL-37 against colon inflammation and carcinogenesis during chronic colitis in IL-10KO mice (74). Livers of homozygous IL-10KO and IL-10KO/IL-37tg mice from this study were analysed by histology for fibrosis and by qPCR for gene expression after a 6 months course of chronic colitis.

Animal protocols were approved by the review board of the Federal Government of Bavaria, Germany (Az. 55.2-1-54-2532-3-2017) and (Az. 55.2.1.54-2532-77-11).

2.2.9 Statistical analysis

Results are expressed as mean ± SEM. All samples were tested for normal distribution by Kolmogorov-Smirnov test and analysed by unpaired t-test. Samples without normal distribution were analysed by Mann-Whitney test. Statistical analysis was performed with Prism 8 Version 3.0d for Macintosh.

3. RESULTS

3.1 IL-37 modulates liver inflammation and fibrosis in liver fibrosis mouse models

Sustained inflammation is a common characteristic of chronic liver injury and induces liver fibrogenesis. It has been reported that anti-inflammatory IL-37 interacts with Smad3 and we therefore hypothesize that IL-37 interferes with the signalling cascade of pro-fibrogenic TGF- β to modulate liver inflammation and fibrogenesis. To test this hypothesis, we investigated the immunomodulatory and anti-fibrogenic properties of IL-37 in four different mouse models of liver fibrosis.

3.1.1 Bile duct ligation-induced liver fibrosis

Underlying causes of liver inflammation and fibrosis are very heterogenic. To examine whether IL-37 modulates liver fibrosis in a cholestatic setting we performed bile duct ligation on wt, IL-37tg and wt mice treated with rhIL-37 by i.p. injection.

3.1.1.1 Pro-fibrogenic gene expression increases after bile duct ligation

To establish an end point for our subsequent experiments, wt mice underwent bile duct ligation and were bled either 10 or 21 days after ligation. *Acta2*, *Tgf β* , *Tgf β RII*, *Cxcl10* and *Cxcl11* gene expression in the liver was upregulated already 10 days after BDL (Fig. 4).

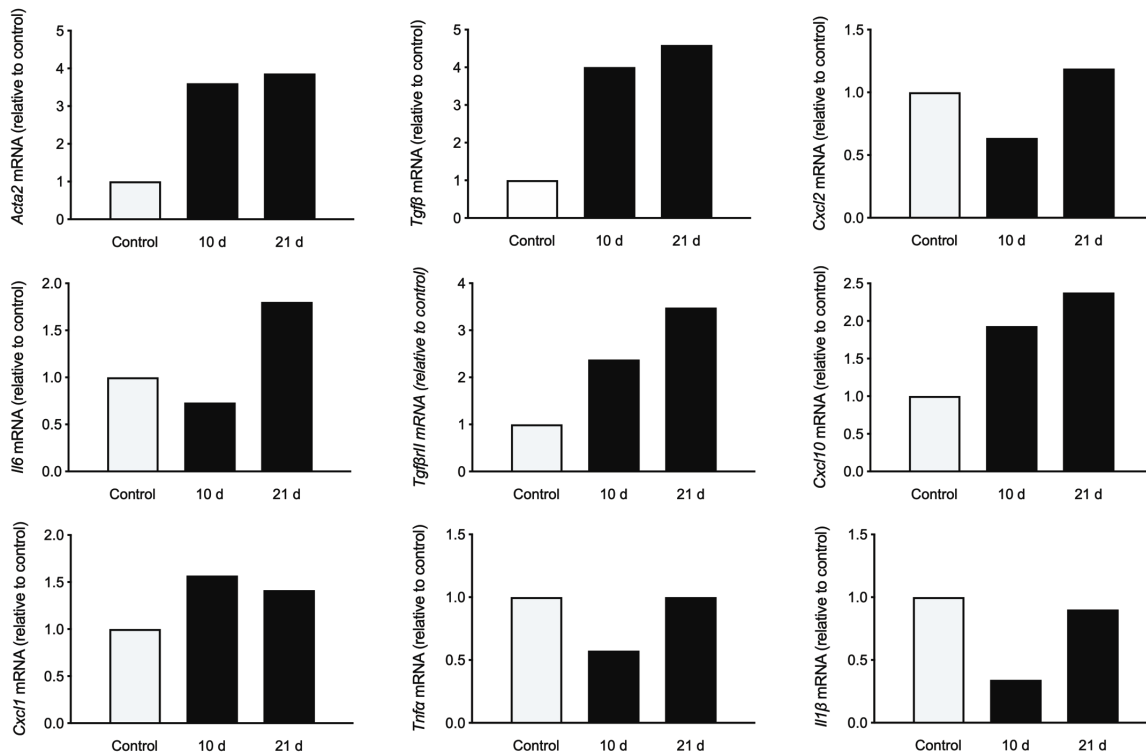


Figure 4: Pro-fibrogenic gene expression increases after bile duct ligation. Wt mice underwent ligation of the common bile duct (n=2) or sham (n=1) operation. BDL mice were bled after 10 (n=1) or 21(n=1) days. Sham control (n=1) was bled after 21 days. Hepatic mRNA levels were measured by qPCR. *Rpl13a* was run as normalization input. N=1.

3.1.1.2 Transgene IL-37 expression improves survival and serum biochemistry in bile duct ligated mice

To investigate the impact of IL-37 on liver fibrosis, we performed bile duct ligation in wt and IL-37tg mice and planned termination of the experiment after 15 days in accordance to the preliminary experiment (Fig. 4). By day 6 after BDL, 5/10 wt mice unexpectedly had died (n=2) or had to be sacrificed due to a high morbidity score (n=3), whereas only one IL-37tg mouse had to be sacrificed on day 13 due to significant loss of body weight (Fig. 5A). Spleen weight was higher in IL-37tg mice (Fig. 5B). Total serum bilirubin, aspartate aminotransferase (GOT), alkaline phosphatase (AP) and alanine aminotransferase (GPT) were normal in sham-operated mice and significantly higher in mice after 15 days of BDL. IL-37tg mice had lower GOT levels and there was a trend of reduced serum bilirubin (45.8% reduction, $p = 0.06$) and AP (40.1% reduction, $p = 0.25$) compared to wt mice after bile duct ligation (Fig. 5C). Gene expression levels of *Colla1*, *Acta2* and *Icam1* were increased in BDL mice compared to sham operated mice, though there was no difference between wt and IL-37tg mice (Fig. 5D).

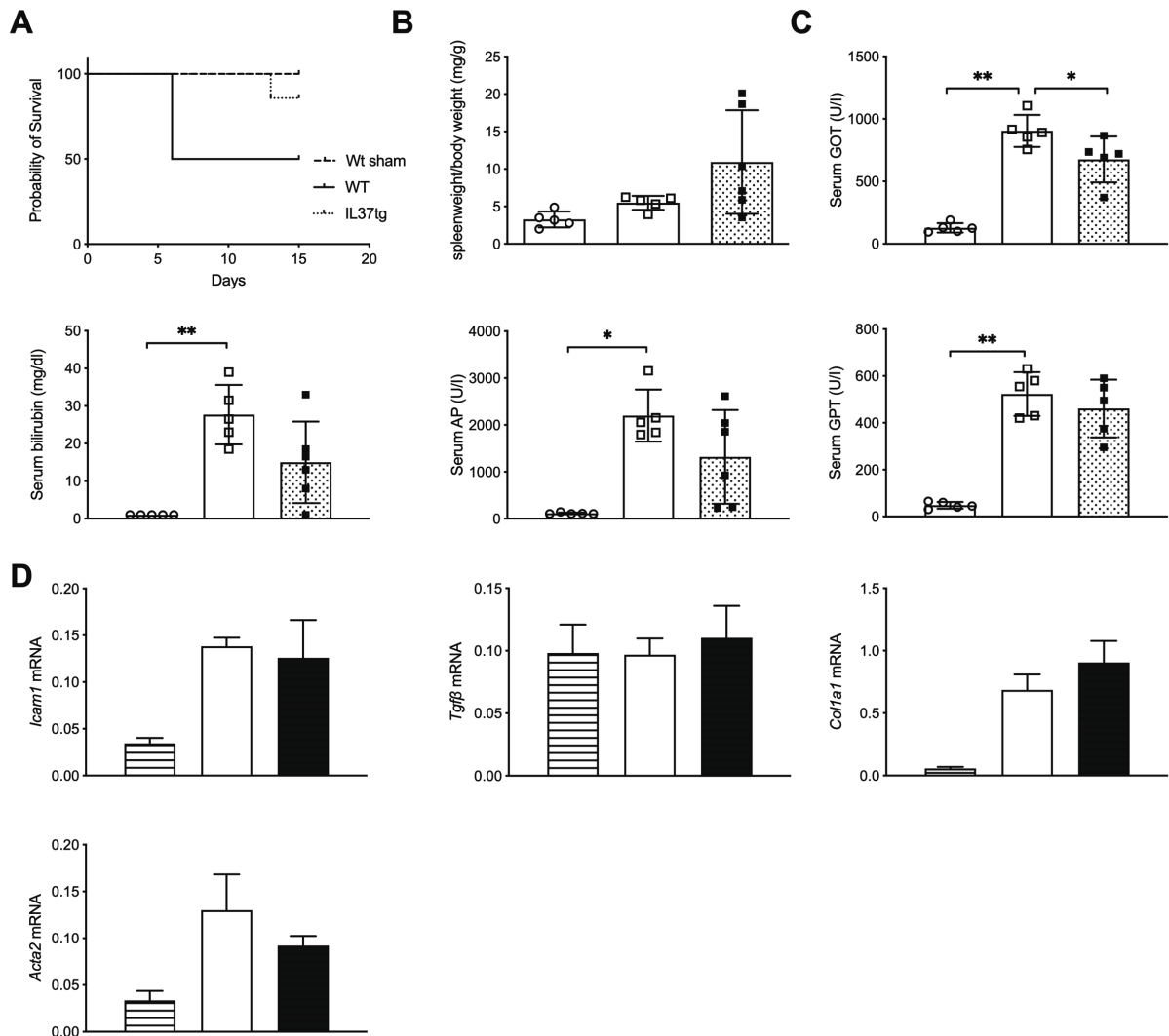


Figure 5: Transgene IL-37 expression improves survival and serum biochemistry in bile duct ligated mice Wt and IL-37tg mice underwent bile duct ligation or sham operation. Mice were bled 14 days after procedure. **(A) Survival curve.** **(B) Spleen weight** **(C) Serum liver values.** Bilirubin, GOT, GPT and AP were measured by routine methods. **(D) Gene expression.** Hepatic mRNA levels were measured by qPCR. *Rpl13a* was run as normalization input. Open circles/dashed column: Wt-sham (n=5), Open boxes/column: Wt (n=5), Closed boxes/column: IL-37tg (n=6). *p< 0.05, **p< 0.01.

3.1.1.3 Transgene IL-37 expression reduces fibrosis in bile duct ligated mice

After 15 days IL-37tg mice showed less histologically-proven liver fibrosis and, concomitantly, less collagen deposition compared to wt mice as determined by Sirius Red staining (Fig. 6A, 6D). Hydroxyproline content was low in sham-operated mice but similarly elevated in bile duct-ligated wt and IL-37tg mice (Fig. 6E). Hepatic infiltration of Mac-2-positive cells after BDL was similar in IL-37tg and wt mouse livers despite a significant increase in comparison to sham-operated mice (Fig. 6A, 6B), though CD3-positive cells were less in IL-37tg mice compared to wt mice (Fig. 6A, 6C).

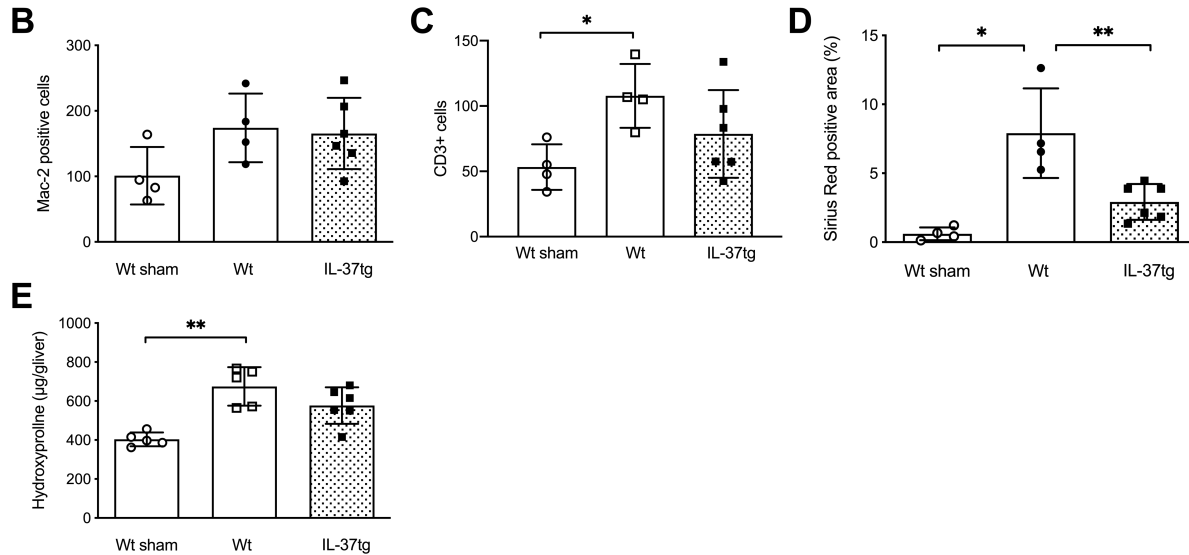
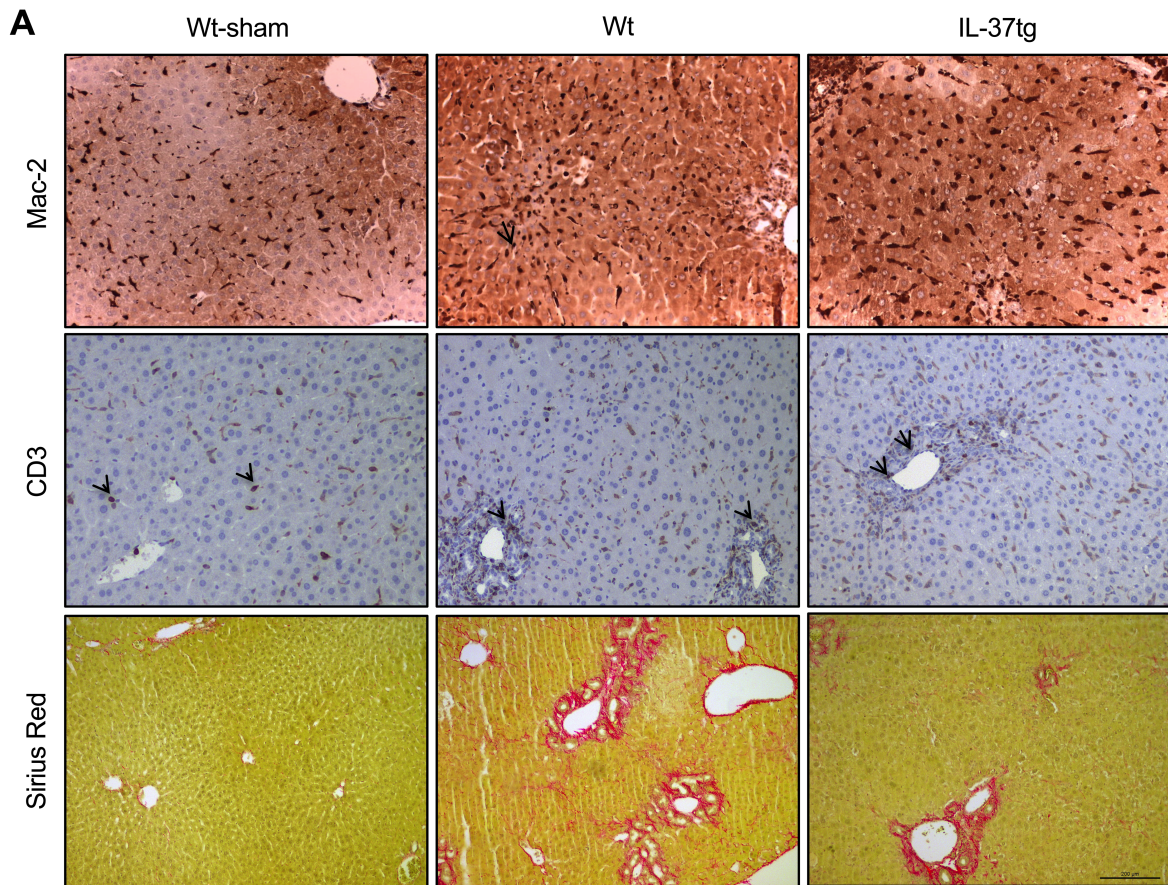


Figure 6: Transgene IL-37 expression reduces fibrosis in bile duct ligated mice. Wt and IL-37tg mice underwent bile duct ligation or sham operation. Mice were bled 14 days after procedure. **(A) Histology.** Liver sections were stained for fibrosis using Sirius Red and for cellular infiltrate using Mac-2 and CD3. **(B) Mac-2 quantification:** Liver sections were stained for Mac-2 and quantified by counting positively stained cells. **(C) CD3 quantification:** Liver sections were stained for CD3 and quantified by counting positively stained cells. **(D) Sirius Red quantification.** Liver sections were stained for fibrosis and then quantified for fibrosis positive area. **(E) Hydroxyproline measurement.** 200 mg wet liver was used to assess hydroxyproline content in the liver according to previously established method by Edwards et al. Open circles: Wt-sham (n=5), Open boxes: Wt (n=5), Closed boxes: IL-37tg (n=6). *p< 0.05, **p< 0.01.

3.1.1.4 Transgene IL-37 expression shows trend towards reduced pro-inflammatory and pro-fibrotic gene expression 3 days after bile duct ligation

To investigate early markers of liver fibrosis IL-37tg and wt mice were sacrificed already 3 days after BDL. Wt mice showed significant higher mRNA levels of *Cxcl2* than sham-operated mice. IL-37 expression was associated with lower, but not significantly reduced gene expression levels of *Tgfb* (36.8% reduction), *Colla1* (64.4% reduction), *Tnfa* (53.7% reduction), *Il6* (45.1% reduction), *Acta2* (55.9% reduction) and *Cxcl2* (48.9% reduction) compared to wt mice after BDL (Fig. 7).

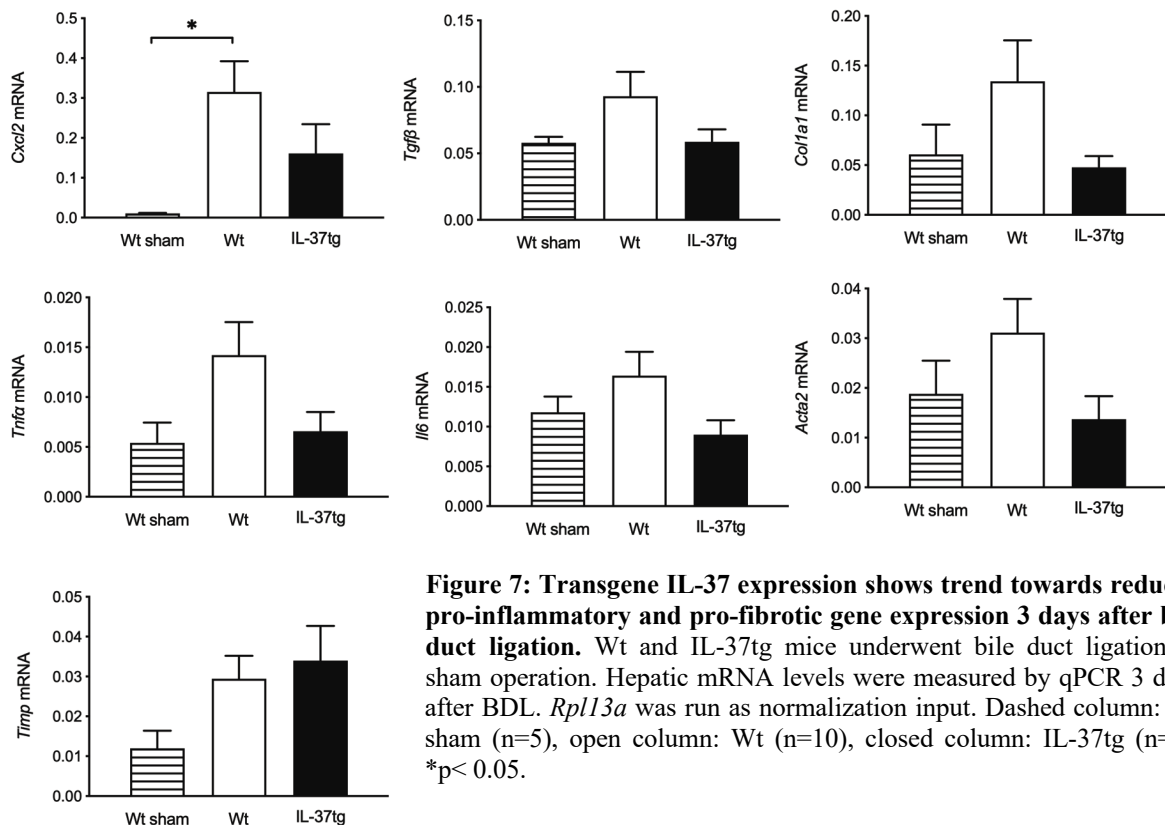


Figure 7: Transgene IL-37 expression shows trend towards reduced pro-inflammatory and pro-fibrotic gene expression 3 days after bile duct ligation. Wt and IL-37tg mice underwent bile duct ligation or sham operation. Hepatic mRNA levels were measured by qPCR 3 days after BDL. *Rpl13a* was run as normalization input. Dashed column: Wt sham (n=5), open column: Wt (n=10), closed column: IL-37tg (n=8). *p < 0.05.

3.1.1.5 Low dose, short term rhIL-37 (1 µg) treatment shows no effect on fibrosis associated gene expression in bile duct ligated mice

The i.p. administration of 1 µg rhIL-37 was shown to be effective in reducing ischemia-reperfusion damage of the liver (57). To assess whether recombinant, i.p. administered IL-37 is sufficient to modulate early inflammation markers in liver tissue after BDL, mice were injected with 1 µg rhIL-37 prior to BDL. Gene expression analysis of *Acta2*, *Tnfa*, *Il13*, *Tgfb*, *Cxcl2*, *Il6*, *Cxcl10*, *Il1β*, *Cxcl1* and *Tgfb β RII* showed no difference between PBS and rhIL-37 treated mice (Fig.8A). Also, hydroxyproline content in the liver was comparable in both groups (Fig. 8B).

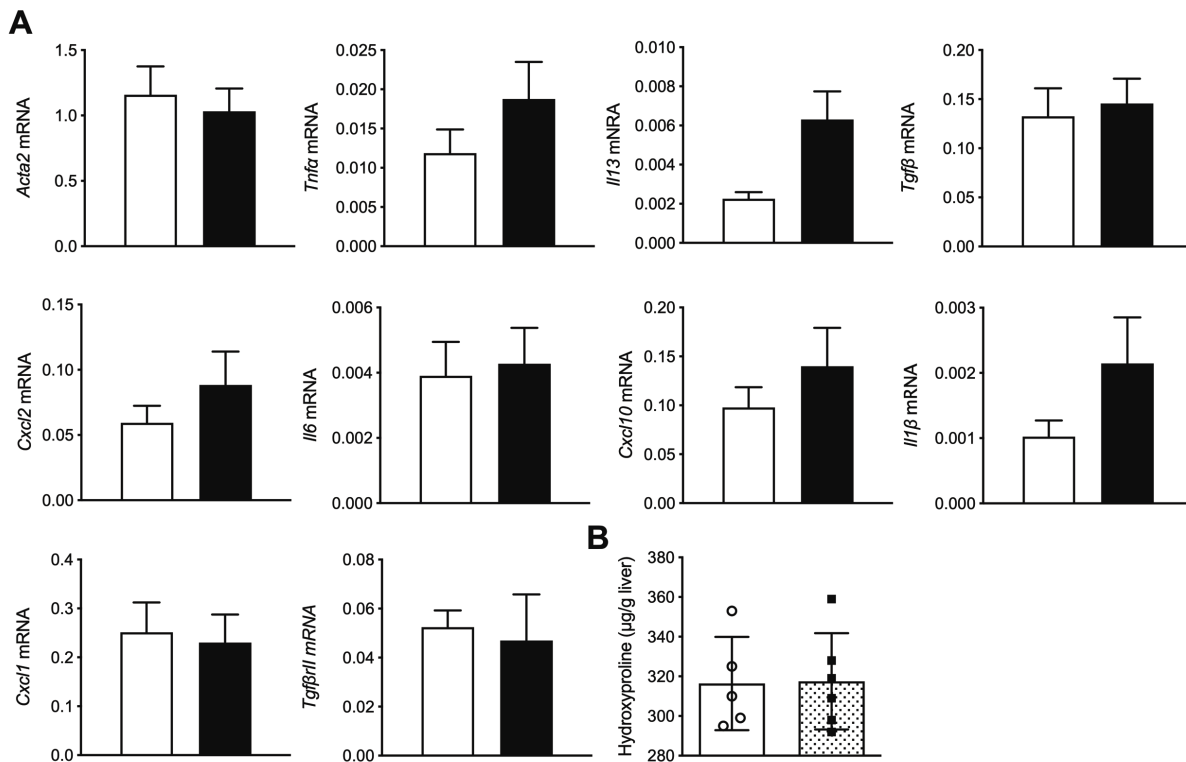


Figure 8: Low dose, short term rhIL-37 (1 µg) treatment shows no effect on fibrosis associated gene expression in bile duct ligated mice. Wt C57BL/6 mice were injected with 1 µg rhIL-37 or PBS prior to undergoing bile duct ligation. **(A) Gene expression.** Hepatic mRNA levels were measured by qPCR 3 days after BDL. *Rpl13a* was run as normalization input. **(B) Hydroxyproline measurement.** Hydroxyproline content was measured using 200 mg wet liver according to previously established method by Edwards et al. Open bars/triangles: PBS (n=5), closed bars/boxes: rhIL-37 (n=6).

3.1.1.6 High dose, short term rhIL-37 (2x5 µg) treatment shows no effect on fibrosis associated gene expression in bile duct ligated mice

Since 1 µg rhIL-37 was not sufficient to modulate markers of inflammation and fibrosis, we increased the dose to 5 µg rhIL-37 which we injected prior to BDL and the day after. Total serum bilirubin, GOT, GPT, γGT and AP levels were comparable in PBS treated and rhIL-37 treated mice (Fig. 9A). Also, gene expression levels of *Acta2*, *Colla1*, *Timp1* and *Cxcl2* showed no difference between the groups (Fig. 9B).

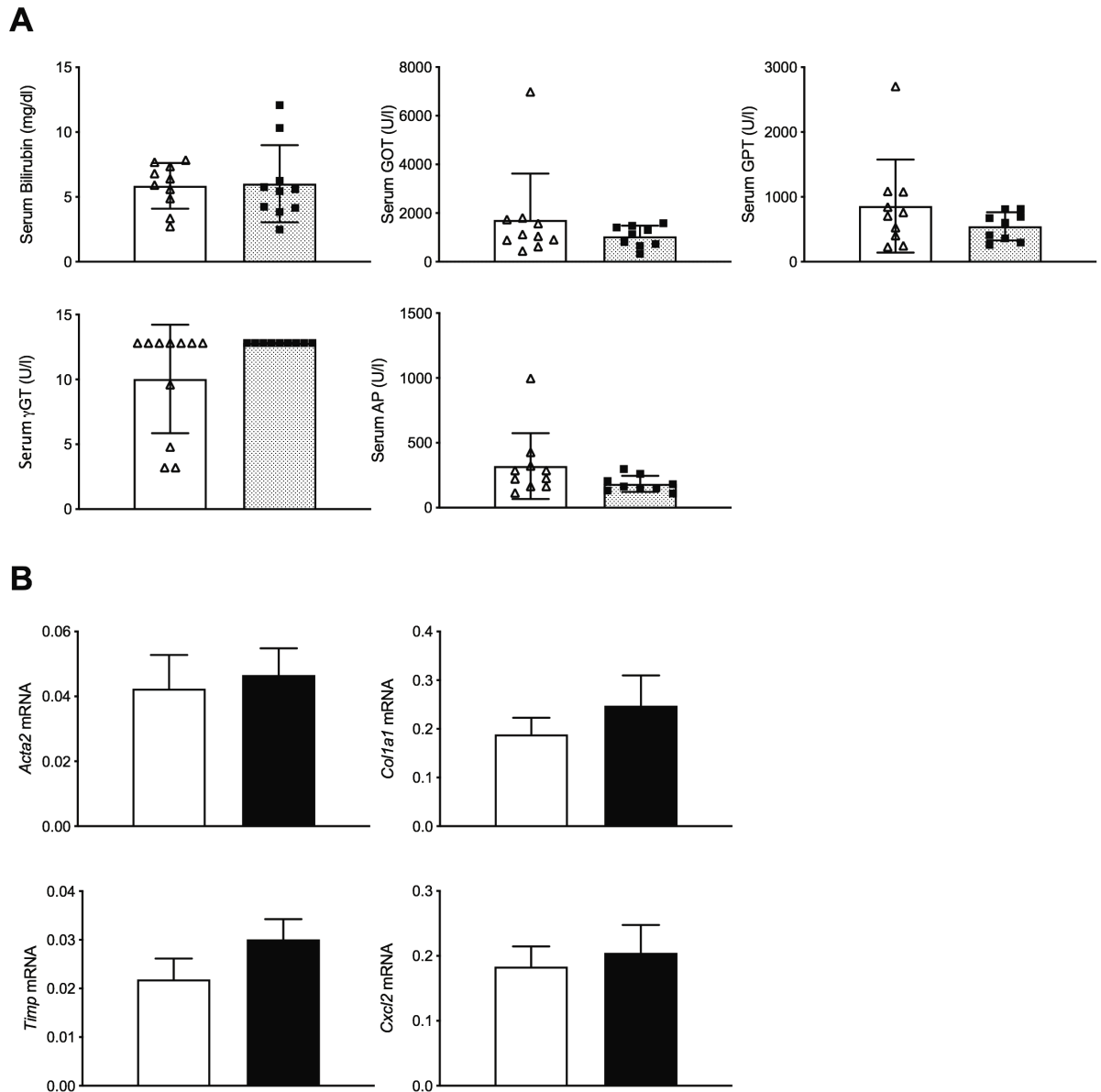


Figure 9: High dose, short term rhIL-37 (2x5 μ g) treatment shows no effect on fibrosis associated gene expression in bile duct ligated mice. Wt C57BL/6 mice were injected with 5 μ g rhIL-37 or PBS prior to undergoing bile duct ligation and again on day 2. **(A) Serum liver values.** Bilirubin, GOT, GPT, γ GT and AP were measured by routine methods. **(B) Gene expression.** Hepatic mRNA levels were measured by qPCR 3 days after BDL. *Rpl13a* was run as normalization input. Open bars/triangles: PBS (n=12), closed bars/boxes: rhIL-37 (n=10).

3.1.2 CCl₄-induced liver fibrosis

3.1.2.1 CCl₄ injected mice develop fibrosis after 6 weeks

Before analysing the effect of transgene IL-37 expression in mice subjected to CCl₄-induced liver fibrosis, we needed to establish the dose and length of injections. It was the aim to induce mild liver damage enabling us to detect also subtle changes in liver inflammation and fibrosis by transgene IL-37 expression.

Mice injected with CCl₄ show signs of fibrosis after 6 weeks of bi-weekly injections. Sirius Red and α -Sma staining showed fibrotic tissue after 6 weeks of injections, which increased in severity over 8 and 10 weeks (Fig 10A). The overall tissue integrity shown in HE staining worsened after 8 weeks of CCl₄ injections (Fig 10A). Quantification of Sirius Red positive area shows an increase from 0.5% to 2.1% after 6 weeks. Sirius Red positive area was increased to 3.0% and 1.8% after 8 and 10 weeks CCl₄ injections (Fig. 10B). Macrophage infiltration determined by Mac-2 staining showed an increase from 346 positive cells in the control group to 811 positive cells per high-power field after 8 weeks of CCl₄ injections (Fig. 10C). Hydroxyproline content of the liver increased from 3.5 μ g to 5.1 μ g after 6 weeks, 5.2 μ g after 8 weeks and 4.5 μ g after 10 weeks CCl₄ injections (Figure 10D). Pro-fibrogenic genes *Acta2* and *Tgfb* were upregulated in mice injected with CCl₄ for 6 weeks compared to control group, whereas there was no alteration in pro-inflammatory genes *Cxcl1*, *Cxcl2*, *Tnfa* and *Il1 β* (Fig. 10E).

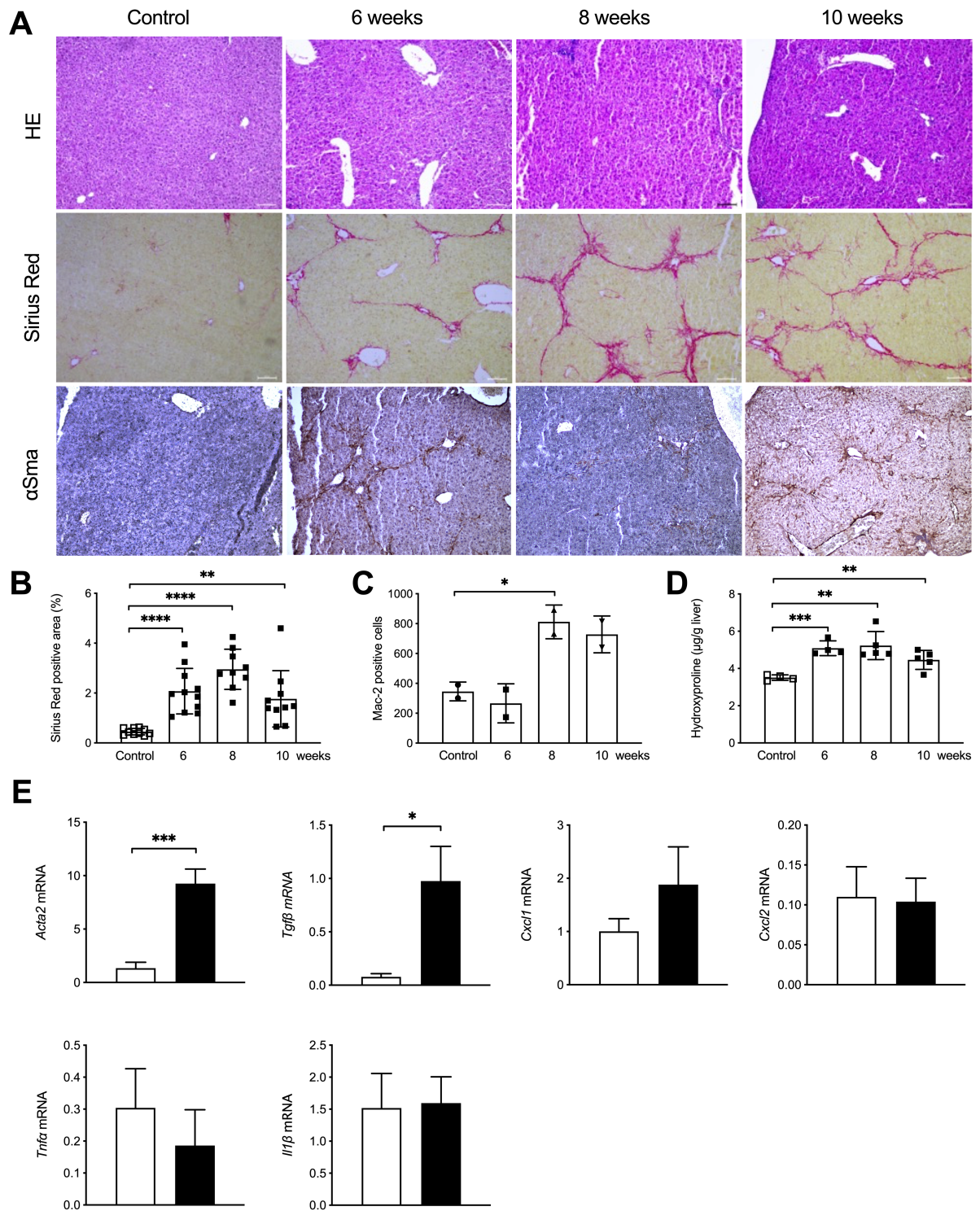


Figure 10: CCl₄-injected mice develop fibrosis after 6 weeks. 8-week-old female C57BL/6 mice were injected with CCl₄ or oil twice a week for 6, 8 and 10 weeks. **(A) Immunohistochemistry.** Liver sections were stained for HE, Sirius Red and α -Sma. **(B) Fibrosis quantification.** Liver sections stained for Sirius Red were quantified. **(C) Cellular infiltrate.** Liver sections underwent immunohistochemical staining for Mac-2 and were subsequently quantified. **(D) Hydroxyproline.** Hydroxyproline content was analysed using 200 mg wet liver according to previously established method by Edwards et al. **(E) Gene expression.** Hepatic mRNA was measured by qPCR. *Rpl13a* was run as normalization input. Wt control (N=5), closed boxes/bars: Wt CCl₄ (N=5), **p* < 0.05, ***p* < 0.01, ****p* < 0.001, *****p* < 0.0001.

3.1.2.2 Transgene IL-37 expression reduces inflammatory markers in CCl₄-treated mice

To investigate whether IL-37 modulates liver fibrosis we evaluated the effect of IL-37 in CCl₄-induced toxic liver injury. After a 6 weeks course of bi-weekly i. p. CCl₄-injections wt mice showed a reduced body weight compared to oil treated mice (Fig. 11A). IL-37tg mice showed no significant weight loss over this time (Fig. 11A). Overall bilirubin levels were low, however serum bilirubin was increased in CCl₄ treated wt mice compared to control, though there was no difference in treated and untreated IL-37tg mice (Fig. 11B). Similarly, this was observed for γ GT (Fig. 11B). AP was slightly reduced in both oil and CCl₄-treated IL-37tg mice compared to control (Fig. 11B). *Ilf6* mRNA concentration was increased in CCl₄ treated wt mice versus control but lower in CCl₄-injected IL-37tg mice (Fig. 11C). *Tgfb* mRNA was higher in wt mice after CCl₄. IL-37tg mice had increased baseline *Tgfb* mRNA expression levels compared to wt mice but lower levels after CCl₄ treatment compared to wt mice. There was no difference in *Acta2* expression between the groups (Fig. 11C).

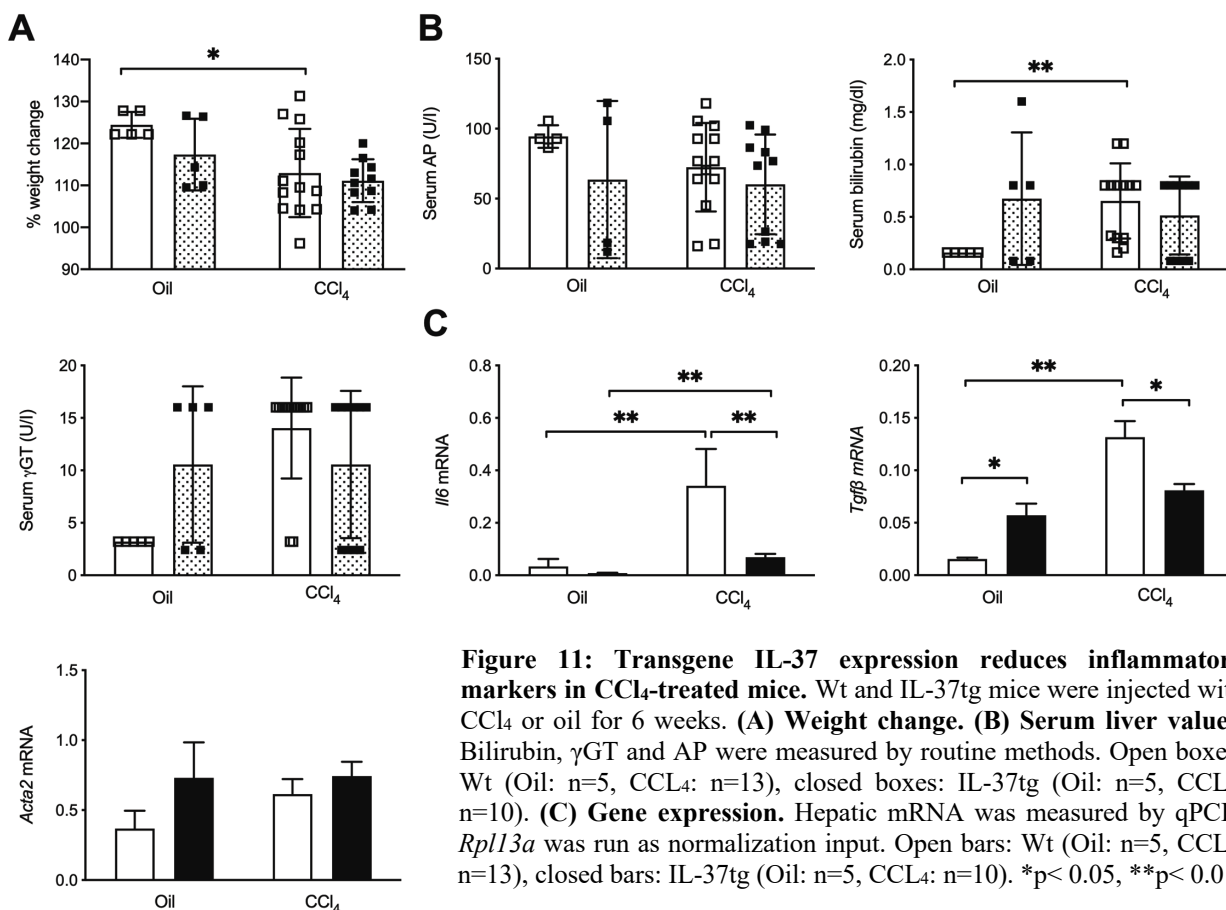


Figure 11: Transgene IL-37 expression reduces inflammatory markers in CCl₄-treated mice. Wt and IL-37tg mice were injected with CCl₄ or oil for 6 weeks. **(A) Weight change.** **(B) Serum liver values.** Bilirubin, γ GT and AP were measured by routine methods. Open boxes: Wt (Oil: n=5, CCL₄: n=13), closed boxes: IL-37tg (Oil: n=5, CCL₄: n=10). **(C) Gene expression.** Hepatic mRNA was measured by qPCR. *Rpl13a* was run as normalization input. Open bars: Wt (Oil: n=5, CCL₄: n=13), closed bars: IL-37tg (Oil: n=5, CCL₄: n=10). *p< 0.05, **p< 0.01.

3.1.2.3 Transgene IL-37 expression reduces fibrosis in CCl₄-treated mice

Hydroxyproline content in the liver was increased in CCl₄-treated mice, though there was no difference between wt and IL-37tg CCl₄ injected mice (Fig. 12A). Quantification of collagen deposition by Sirius Red staining showed an increase in CCl₄ treated mice compared to oil treated mice (Fig. 12B), but slightly reduced levels in livers of IL-37tg mice (27.9% reduction, p=0.12, Fig. 12B, 12C).

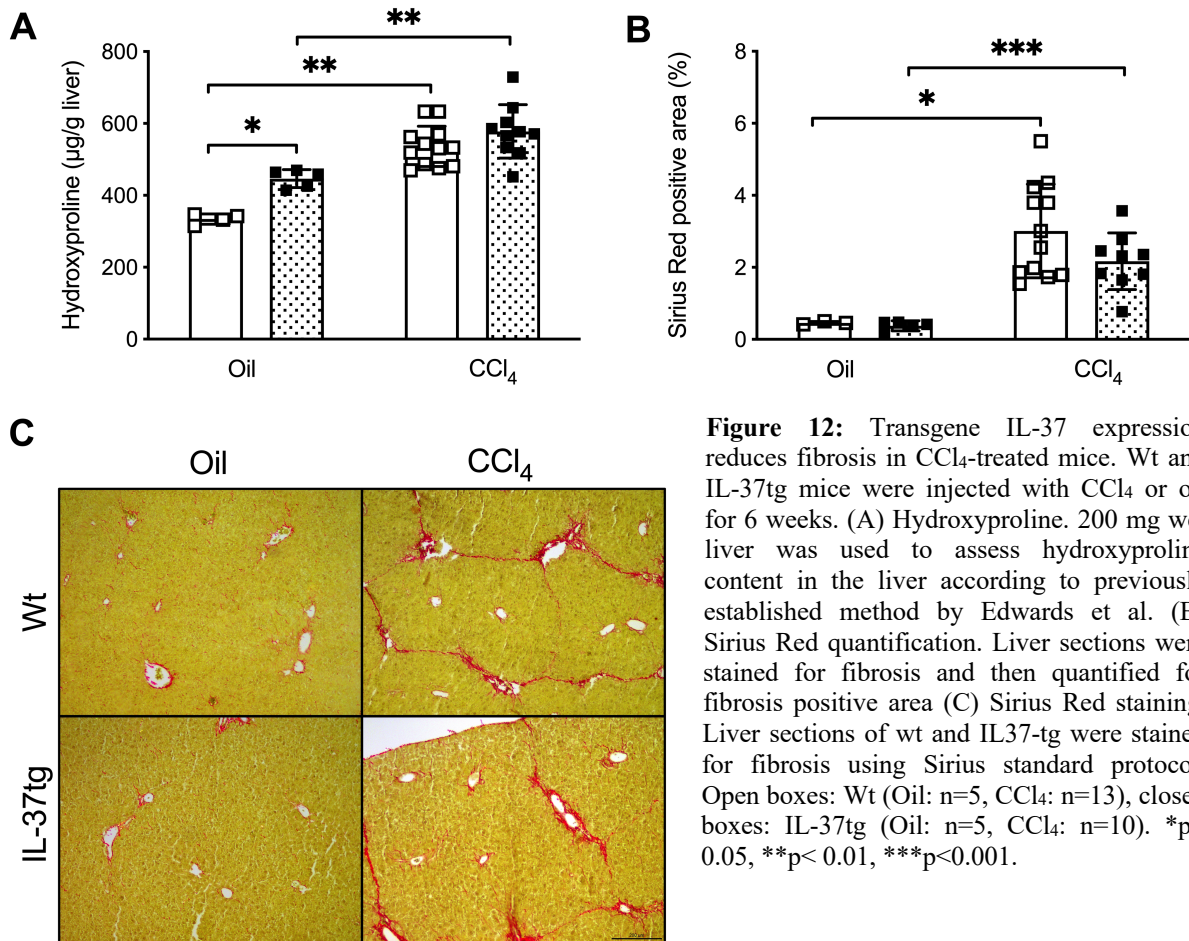


Figure 12: Transgene IL-37 expression reduces fibrosis in CCl₄-treated mice. Wt and IL-37tg mice were injected with CCl₄ or oil for 6 weeks. (A) Hydroxyproline. 200 mg wet liver was used to assess hydroxyproline content in the liver according to previously established method by Edwards et al. (B) Sirius Red quantification. Liver sections were stained for fibrosis and then quantified for fibrosis positive area (C) Sirius Red staining. Liver sections of wt and IL37-tg were stained for fibrosis using Sirius standard protocol. Open boxes: Wt (Oil: n=5, CCl₄: n=13), closed boxes: IL-37tg (Oil: n=5, CCl₄: n=10). *p<0.05, **p<0.01, ***p<0.001.

3.1.3 Transgene IL-37 expression reduced colitis associated liver inflammation and fibrosis

IBD may be associated with liver inflammation and fibrosis (79, 80). Here we evaluated whether transgene IL-37 expression reduces liver inflammation and fibrosis in the IL-10KO mouse model of chronic colitis which we recently published (74). IL-10KO mice developed colon carcinomata secondary to chronic colitis and showed mild liver inflammation and fibrosis with the age of 6 months. Gene expression levels in the livers showed that the pro-inflammatory cytokines *Cxcl2*, *Cxcl10*, *Ccl2*, *Ccl3*, *Il6* and *Tnfa* were downregulated in IL-

10KO/IL-37tg mice compared to IL-10KO mice, as are the pro-fibrotic genes *Icam1* and *Acta2* (Fig 13A). IL-37 expressing IL-10KO mice were protected from colon carcinogenesis and showed a reduced histological liver fibrosis score compared to IL-10KO mice (Fig. 13B, 13E), though there was no difference to IL-10KO mice in regards to liver inflammation (Fig. 13B, 13D) or hydroxyproline content (Fig. 13C).

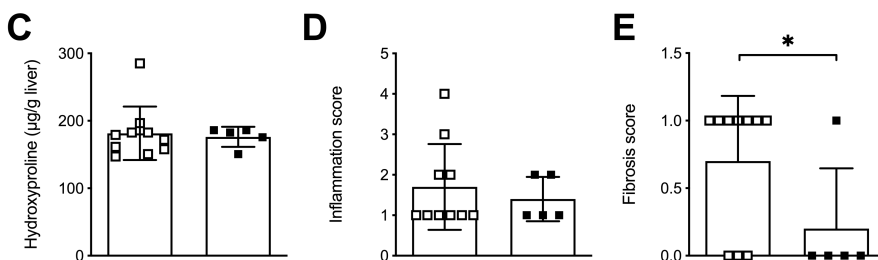
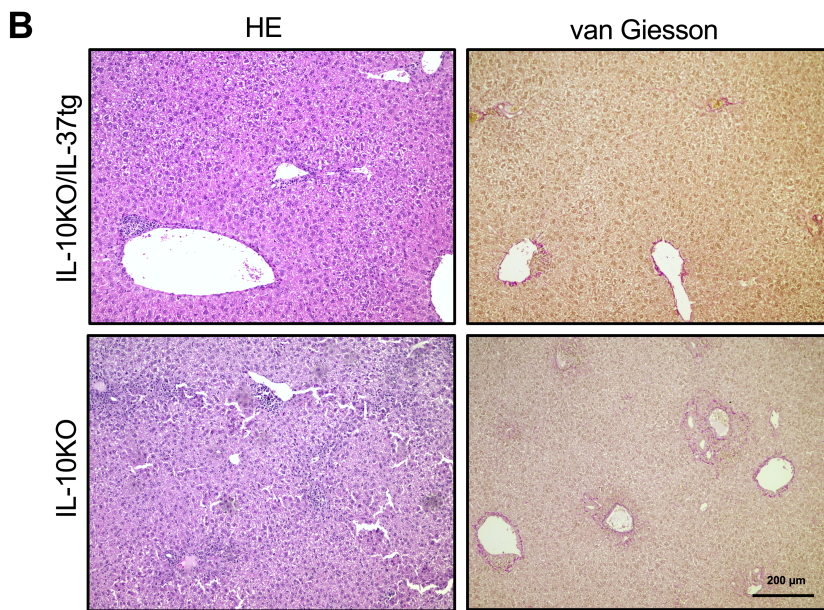
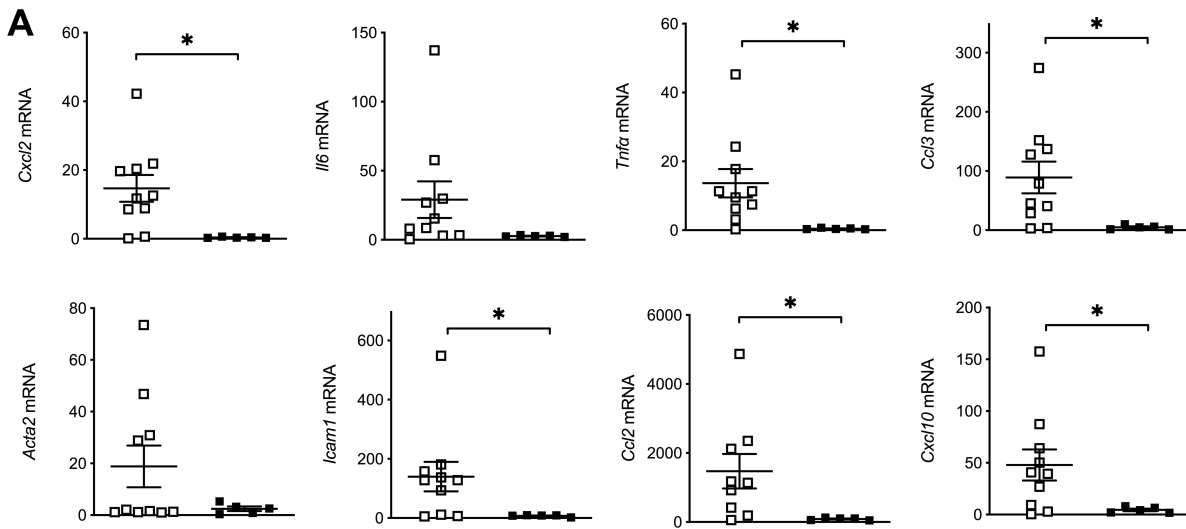


Figure 13: Transgene IL37 expression reduces colitis associated liver inflammation. (A) Gene expression. Hepatic mRNA was measured by qPCR. TBP was run as normalization input. **(B) Histology.** Paraffin embedded liver sections of IL-10KO and IL-10/IL-37tg mice were stained with HE and van Gieson. **(C) Hydroxyproline measurement.** 200 mg wet liver was used to assess hydroxyproline content in the liver according to previously established method by Edwards et al **(D) Inflammation score.** Level of inflammation in the liver was assessed by a pathologist using the HAI scoring system. **(E) Fibrosis score.** Level of fibrosis was assessed by a pathologist using the HAI scoring system. Open boxes/column: IL-10KO (n=5), closed boxes/column: IL-10KO/IL-37tg (n=10), *p< 0.05

3.1.4 Role of IL-37 in the MDR2KO model of liver fibrosis

Liver fibrogenesis in MDRKO mice resembles human PSC and is therefore a particular interesting fibrosis model. MDR2KO mice lack the canicular phospholipid flipase and develop severe cholestasis in the first weeks of life due to the absence of phospholipids from the bile (75). In order to study the functional impact of IL-37 in the MDR2KO model, we decided to induce overexpression of IL-37 by chemically modified RNAs (cmRNA). Crossbreeding of MDR2KO with IL-37tg mice would have been problematic because of potential infertility of mice. The administration of rh IL-37 protein for many weeks would have been extremely costly.

3.1.4.1 IL-37 overexpression by chemically modified RNAs (cmRNA) in cell lines

Therapies with chemically modified RNAs are improving and emerging as a new alternative for protein replacement therapies (81). In a pilot study we overexpressed IL-37 in RAW264.7, A549 and LX2 cells to confirm expression and functionality of the cmRNAs before applying this technique to the MDR2KO mouse model. Since under physiological conditions IL-37 expression is only upregulated after stimulation, cells were stimulated with either LPS or IL-1 β throughout the experiments.

IL-37 overexpression reduces pro-inflammatory markers in RAW264.7 cells after LPS stimulation

In RAW264.7 cells, successful transfection was confirmed by western blotting (Fig. 14A). Stimulating cells with LPS showed no alteration of protein expression compared to unstimulated cells indicating that IL-37 cmRNA does not undergo spontaneous degradation as described for wildtype IL-37 mRNA (43) (Fig. 14A). Cells transfected with IL-37 cmRNA showed reduced IL-6 secretion (Fig. 14B). *Cxcl10* gene expression was reduced after LPS stimulation (Fig. 14C).

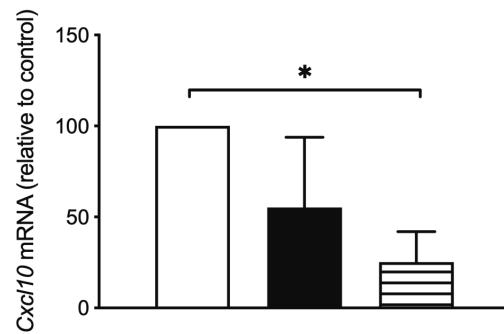
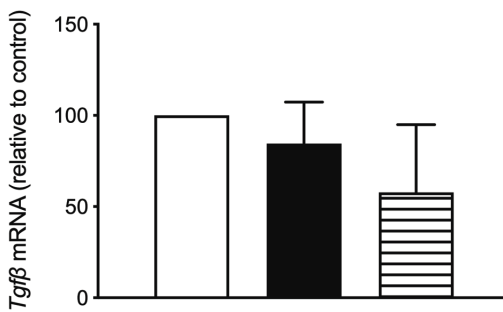
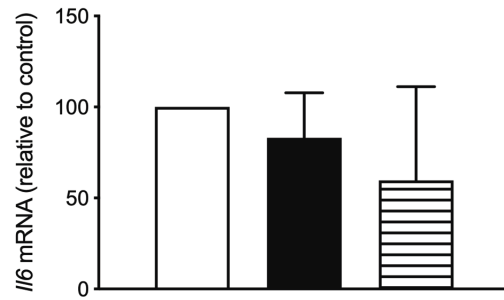
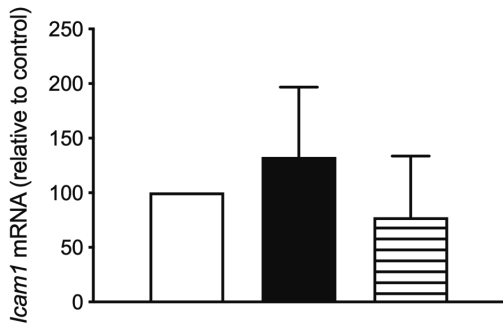
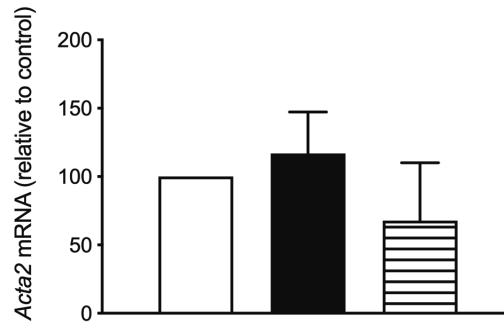
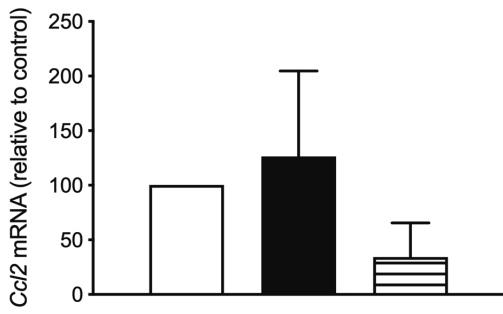
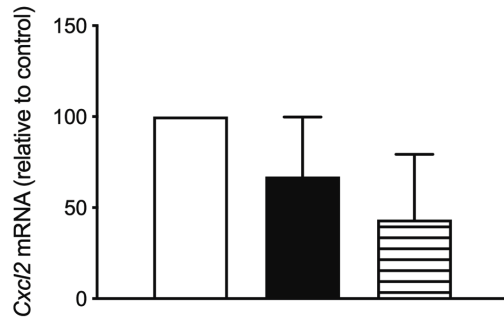
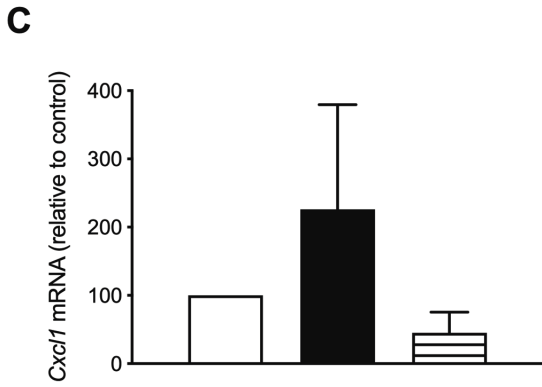
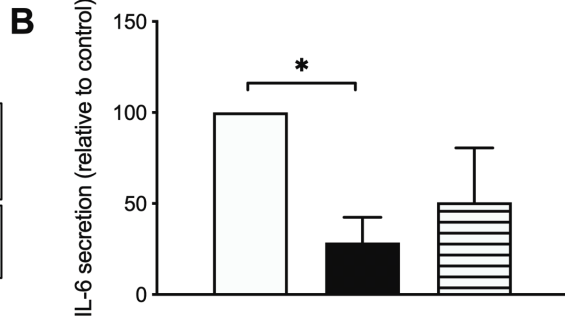
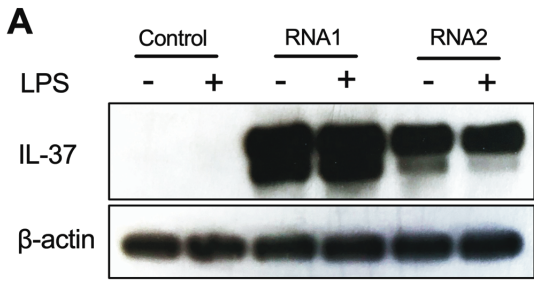


Figure 14: IL-37 overexpression reduces pro-inflammatory markers in RAW264.7 cells after LPS stimulation. Cells were transfected with 1 µg control RNA, RNA1 or RNA2 using Lipofectamine RNAiMax. 24h after transfection cells were stimulated with LPS (100 ng/ml). **(A) Protein expression.** Protein was extracted from cell pellets 24h after stimulation. Equal amounts of protein were run and probed for IL-37. β -actin was run as a loading control. **(B) IL-6 secretion.** IL-6 was measured in supernatants 24h after LPS stimulation. **(C) Gene expression.** Total RNA was extracted from cell pellets 6h after LPS stimulation and transcribed to cDNA. mRNA was measured by qPCR. *TBP* was run as normalization input. Open columns: Control, closed columns: RNA1, dashed columns: RNA2. N=3, *p<0.05.

IL-37 overexpression reduces inflammation markers in A549 cells after IL-1 β stimulation

After successful over expression of IL-37 (Fig. 15A), cells expressing IL-37 secreted less IL-6 compared to control cells (Fig. 15B). Gene expression analysis showed a reduction of *CXCL1*, *CXCL10*, *CCL2*, *IL6* and *TGF β* expression levels after stimulation (Fig. 7C).

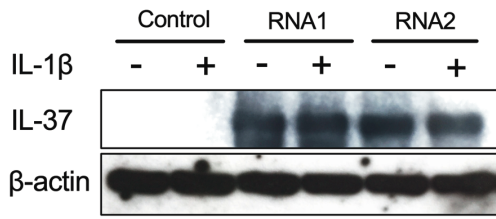
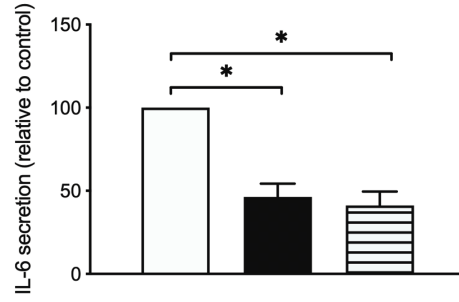
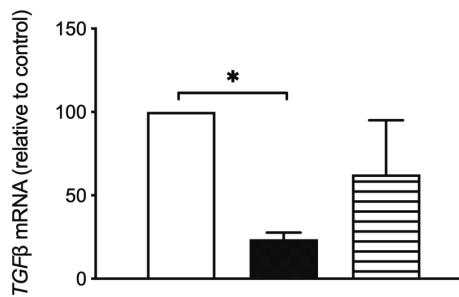
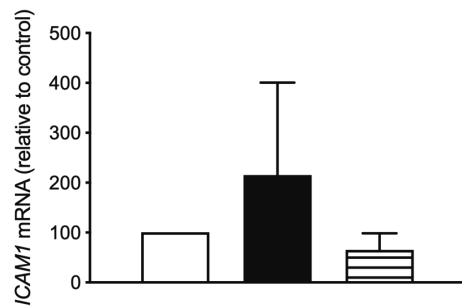
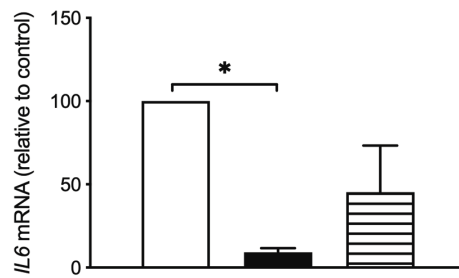
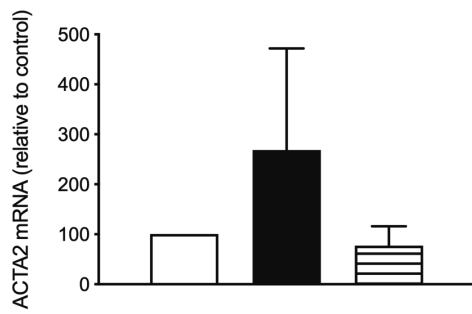
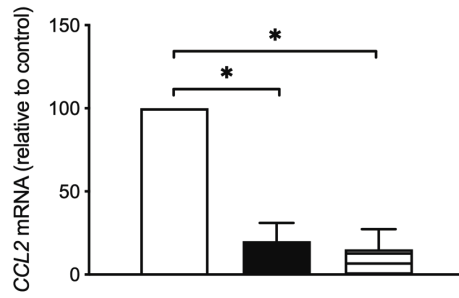
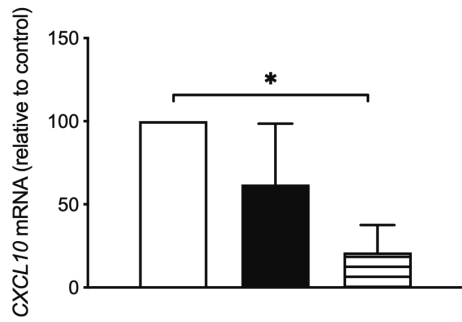
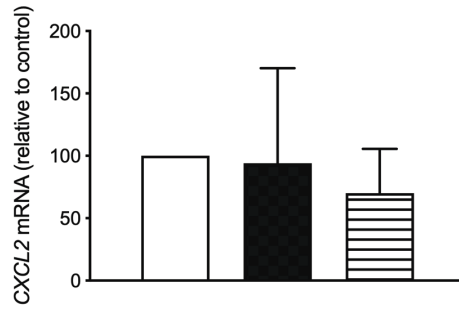
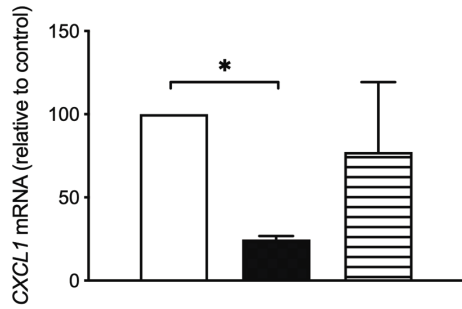
A**B****C**

Figure 15: IL-37 overexpression reduces inflammation markers in A549 cells after IL-1 β stimulation. Cells were transfected with 1 μ g control RNA, RNA1 or RNA2 using Lipofectamine RNAiMax. 24h after transfection cells were stimulated with IL-1 β (1ng/ml). **(A) Protein expression.** Protein was extracted from cell pellets 24h after stimulation. Equal amounts of protein were run and probed for IL-37. β -actin was run as loading control. **(B) IL-6 secretion.** IL-6 was measured in supernatants 24h after IL-1 β stimulation. **(C) Gene expression.** Total RNA was extracted from cell pellets 6h after IL-1 β stimulation and transcribed to cDNA. mRNA was measured by qPCR. *TBP* was run as normalization input. Open columns: Control, closed columns: RNA1, dashed columns: RNA2. N=3, *p<0.05.

IL-37 overexpression reduces inflammation markers in LX2 cells after IL-1 β stimulation

Hepatic stellate cells are the main source of extracellular matrix proteins in liver fibrosis. In order to analyse the impact of IL-37 on HSC function we overexpressed IL-37 in human LX-2 stellate cells by chemically modified RNA (Fig. 16A). Transfection efficiency of about 95% was reached in these experiments (Fig. 16B). To confirm that IL-37 was translated successfully we tested cell supernatant for circulating IL-37. IL-37 transfected cells had 6 pg/ml IL-37, whereas in control transfected cells, IL-37 could not be detected (Fig. 16C). When LX2 cells were transfected with RNA1 or RNA2 less IL-6 was secreted after stimulation (Fig. 16D). *CXCL10* gene expression was reduced in RNA2 transfected cells (Fig.16E).

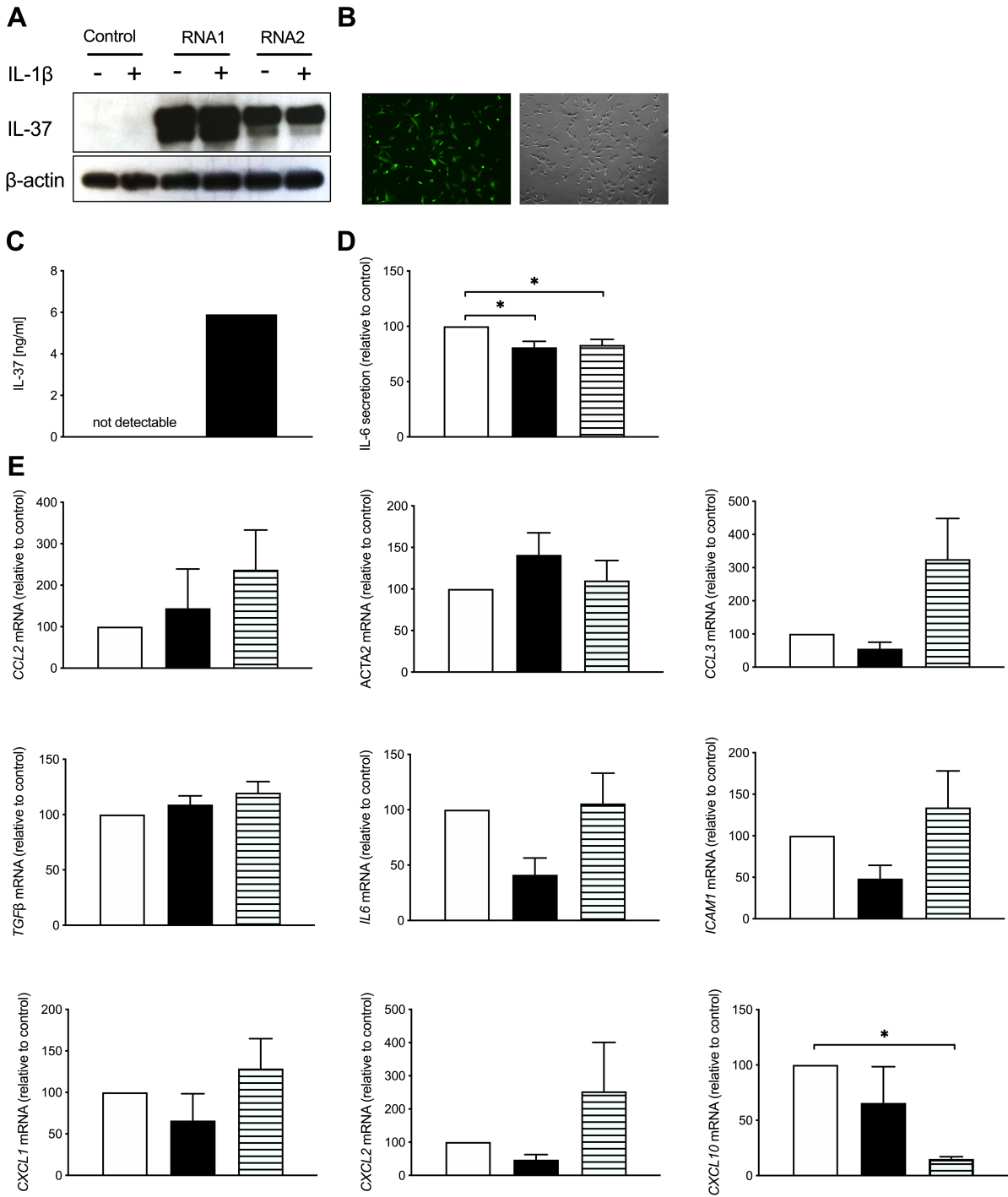


Figure 16: IL-37 overexpression reduces inflammation markers in LX2 cells after IL-1 β stimulation. Cells were transfected with 1 μ g control RNA, RNA1 or RNA2 using Lipofectamine RNAiMax. 24h after transfection cells were stimulated with IL-1 β (10 ng/ml). **(A) Protein expression.** Protein was extracted from cell pellets 24h after stimulation. Equal amounts of protein were run and probed for IL-37. β -actin was run as loading control **(B) cmRNA transfection efficiency.** Cells were transfected with 1 μ g GFP encoding cmRNA using Lipofectamine RNAiMax. Transfection efficiency was imaged 24h after transfection using a fluorescent microscope. **(C) cmRNA translation efficiency.** Cells were transfected with 1 μ g control RNA or RNA1 using Lipofectamine RNAiMax. Supernatants were tested for IL-37 48h after transfection. **(D) IL-6 secretion.** IL-6 was measured in supernatants 24h after IL-1 β stimulation. **(E) Gene expression.** Total RNA was extracted from cell pellets 6h after IL-1 β stimulation and transcribed to cDNA. mRNA was measured by qPCR. *TBP* was run as normalization input. Open columns: Control, closed columns: RNA1, dashed columns: RNA2. N=3, *p<0.05.

3.1.4.2 MDR2KO-mice develop bridging fibrosis at the age of 5 weeks

To study the effects of injecting chemically modified IL-37 expressing RNAs, we first needed to establish the MDR2KO mouse model. Sirius Red stained liver sections showed that mice start developing signs of fibrosis from the age of 4 weeks. By week 5, knock out mice develop bridging fibrosis and by 8 weeks big parts of the liver is fibrotic (Figure 17).

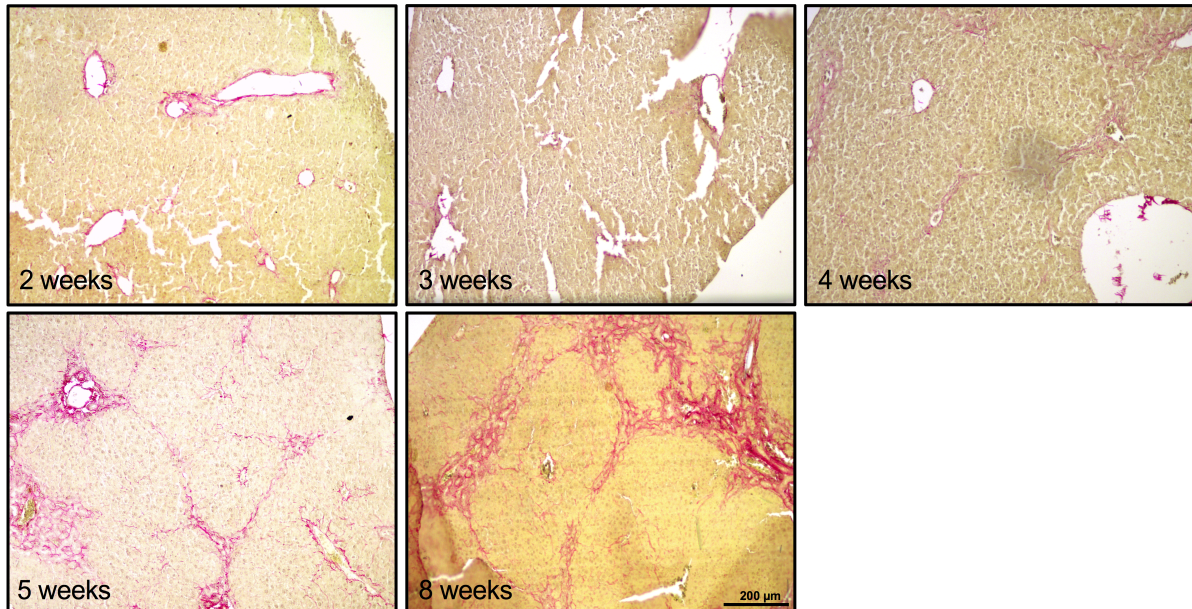
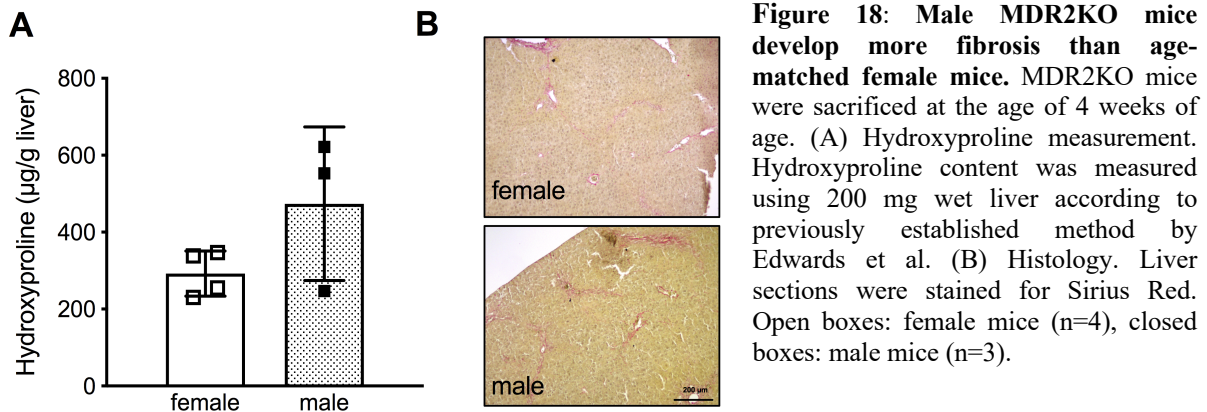


Figure 17: MDR2KO mice develop bridging fibrosis at the age of 5 weeks. MDR2KO mice were sacrificed at the age of 2, 3, 4, 5 and 8 weeks of age. Liver sections were stained for Sirius Red. N=1.

3.1.4.3 Male mice develop more fibrosis than age-matched female mice

Since many publications differ in regards to gender specific developments of fibrosis in the MDR2KO model, we wanted to analyse the level of fibrosis in our male and female mice. Analysis of collagen content showed 4-week-old female mice had an average of 392.5 µg hydroxyproline per g wet liver, whereas male age matched mice had 473.7 µg hydroxyproline in the liver (Fig. 18A). This finding was also reflected in Sirius Red staining of liver specimen (Fig. 18B).



3.1.4.4 Low dose chemically-modified (cm) RNA injections show no effect on reducing fibrosis factors in MDR2KO mice

After bi-weekly injections of 1 µg cmRNA or vehicle there was no difference in spleen weight as a surrogate parameter of chronic liver disease between IL-37 RNA injected mice and controls (Fig. 19A) or hydroxyproline content in the liver (Fig. 19B). *Acta2*, *Tgfb* and *Il6* mRNA was comparable in both groups (Fig. 19C).

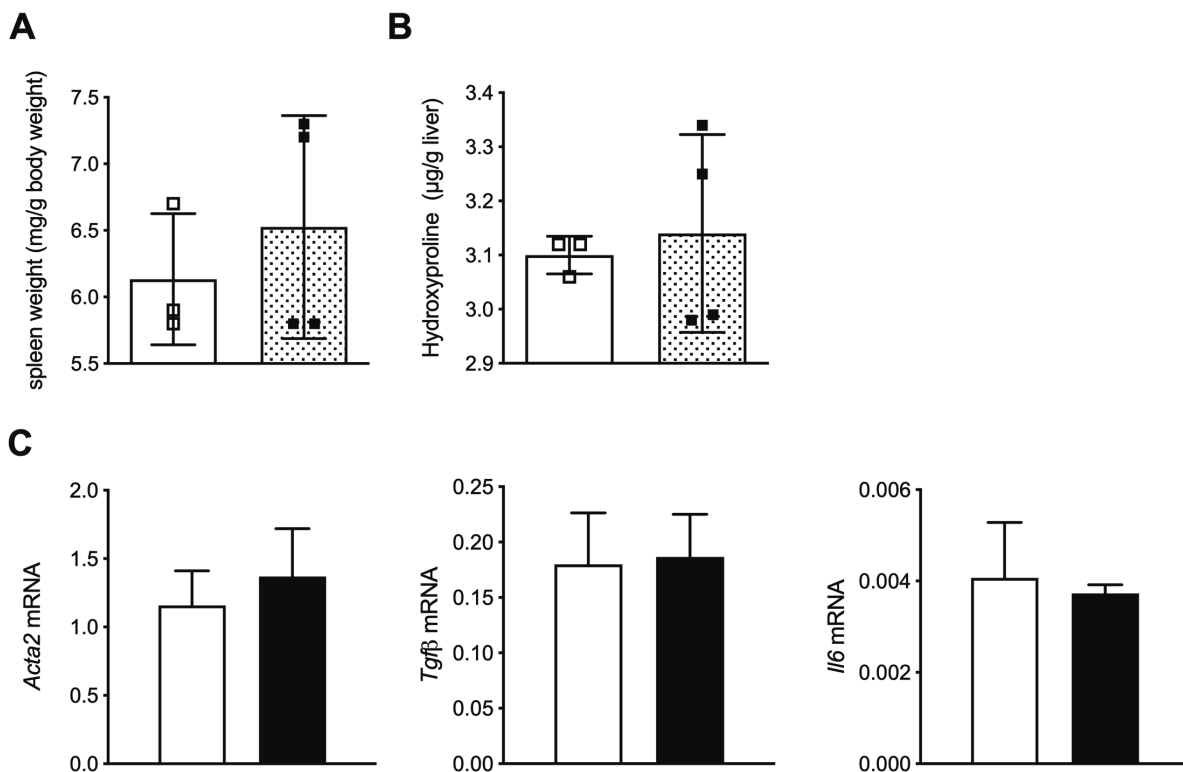


Figure 19: Low dose cmRNA injections show no effect on reducing fibrosis factors in MDR2KO mice. 2-week-old, male MDR2KO mice were injected with 1 µg RNA1 or control RNA 2 times a week. After 2 weeks, at the age of 4 weeks, mice were sacrificed, and spleen and liver were explanted. (A) Spleen weight. (B) Hydroxyproline. (C) mRNA levels.

Hydroxyproline. Hydroxyproline content was measured using 200 mg wet liver according to previously established method by Edwards et al. **(C) Gene expression.** Hepatic mRNA was measured by qPCR. *Rpl13a* was run as normalization input. Open boxes/bars: Control RNA (n=3). Closed boxes/bars: RNA1 (n=4).

3.1.4.5 High dose cmRNA injections show now effect on reducing fibrosis factors in MDR2KO mice

Since 1 µg cmRNA was not sufficient to modulate liver fibrosis, we increased the treatment to 5 µg cmRNA three times per week.

Spleen weight in control RNA and RNA1 injected mice was comparable (Fig. 20A). There was no difference in serum GOT, GPT, γGT, bilirubin or AP between the two groups (Fig. 20D). Furthermore, evaluation of pro-inflammatory and pro-fibrotic gene expression showed similar expression levels in both groups (Fig. 20E). Quantification of Sirius Red positive area revealed no difference between control and IL-37 injected group (Fig. 20B, 20F). Also, hydroxyproline levels were comparable in both groups (Fig. 20C).

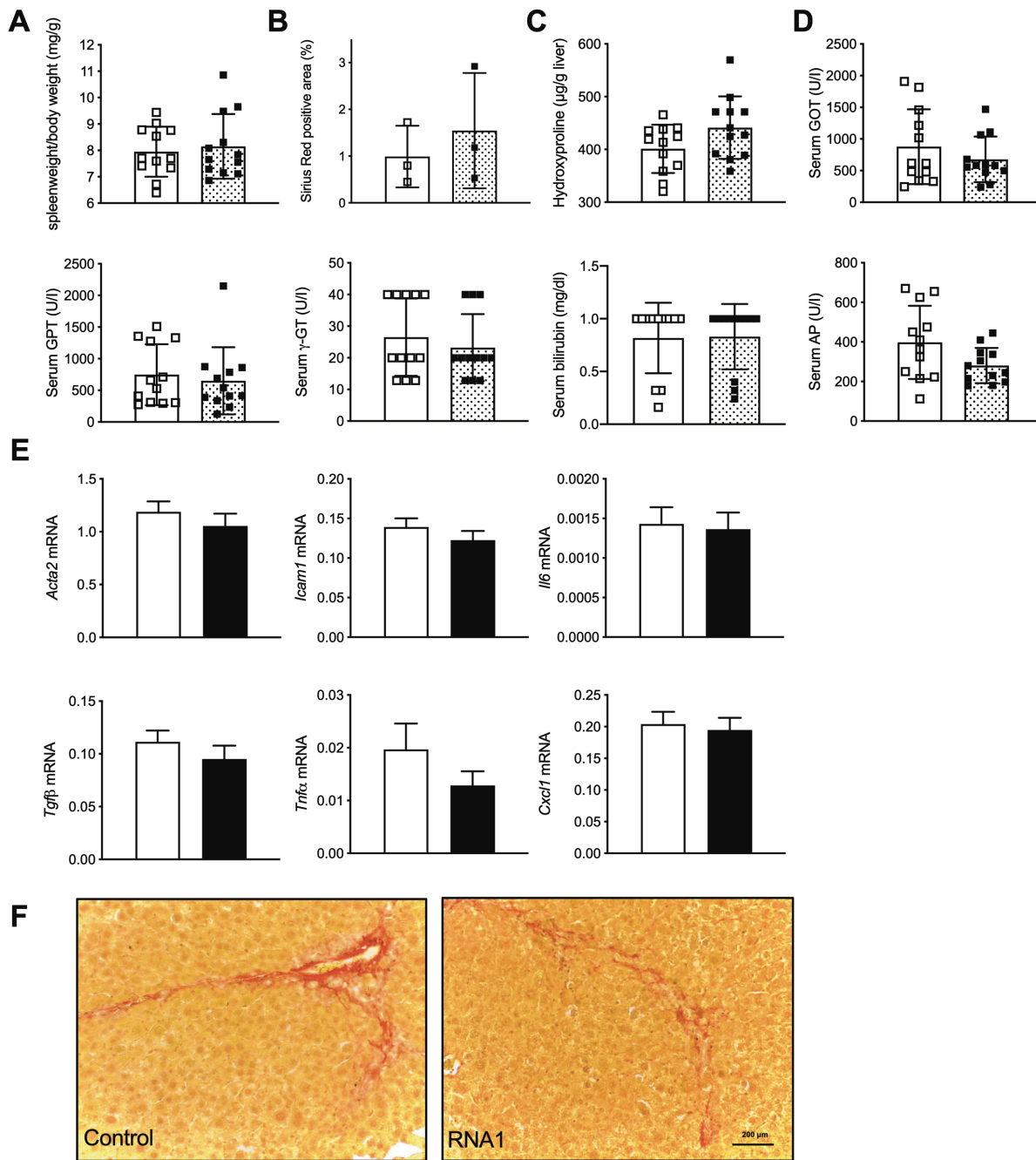


Figure 20: High dose cmRNA injections show no effect on reducing fibrosis factors in MDR2KO mice. 2-week-old, male MDR2KO mice were injected with 5 µg RNA1 or control RNA 3 times a week. After 2 weeks, at the age of 4 weeks, mice were sacrificed, and spleen and liver were explanted. **(A) Spleen weight.** Spleen weight in relation to body weight at the time of spleen removal. **(B) Sirius Red quantification.** Liver sections were stained for fibrosis and then quantified for fibrosis positive area. **(C) Hydroxyproline.** Hydroxyproline content was measured using 200 mg wet liver according to previously established method by Edwards et al. **(D) Serum liver values.** Bilirubin, GOT, GPT, γ GT and AP were measured by routine methods. **(E) Gene expression.** Hepatic mRNA was measured by qPCR. *Rpl13a* was run as normalization input. **(F) Histology.** Liver sections were stained for Sirius Red. Open boxes/bars: Control RNA, Closed boxes/bars: RNA1. N=12.

3.1.4.6 IL-37 cmRNA-injected mice produce antibodies against IL-37

To further investigate why the cmRNA injections did not show any effect on liver inflammation or fibrosis we measured circulating IL-37 by Elisa and tested for antibodies

against IL-37. All mice injected with RNA1 had an increased IL-37 antibody production in comparison to controls (Fig. 21A) and, however, only marginally detectable levels of circulating IL-37 protein (Fig. 21B).

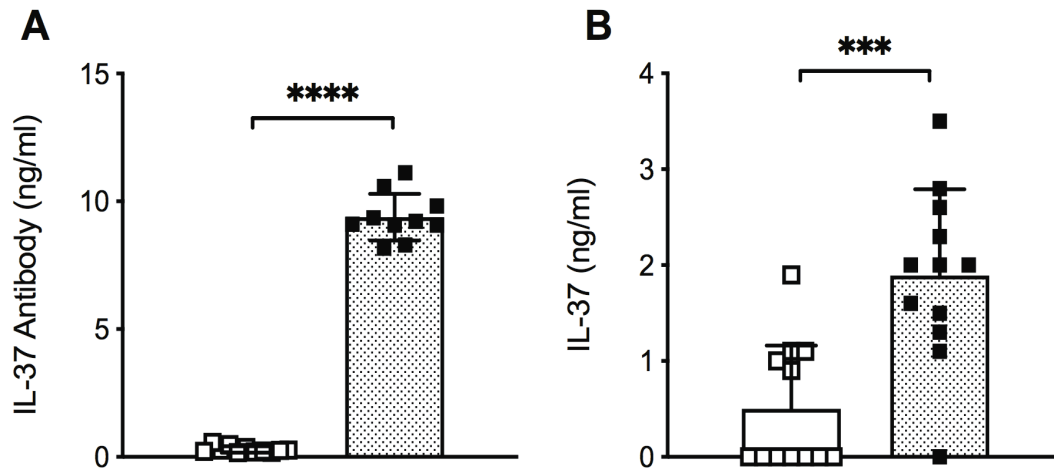


Figure 21: IL-37 cmRNA injected mice develop IL-37 antibodies and produce IL-37. MDR2KO mice were injected with 5 μ g RNA1 or control RNA 3 times a week. IL-37AB (A) and IL-37 (B) was measured by Elisa. Open boxes: Control RNA, closed boxes: RNA1. N=12. *** p <0.001, **** p <0.0001.

3.2 Impact of IL-37 on human hepatic stellate cell function

Activated hepatic stellate cells and Kupffer cells are the main driver in the development of fibrosis. To unravel the molecular link between inflammation and fibrosis, we examined the molecular function of IL-37 in (murine) hepatic stellate and murine Kupffer cells.

3.2.1 Overexpression of IL-37 in human stellate cell line LX2

As shown above, overexpression of IL-37 decreased IL-6 secretion and *CXCL10* expression in LX2 cells. Since IL-37 has intra- and extracellular functionality in immune cells, we also studied the effect of exogenously administered recombinant human IL-37 in the cells.

3.2.2 Recombinant human IL-37 reduces gene expression of pro-fibrotic *ACTA2*

After confirming that LX2 cells express the IL-37 receptor complex consisting of SIGIRR and IL-18R α (Fig. 22A), we exposed the cells to 100 ng/ml or 1 μ g/ml rhIL-37 for 24h. There was no change in IL-6 secretion (Fig. 22B). Gene expression analysis showed a reduction in *ACTA2*, though there was no difference in *CXCL1*, *CXCL2*, *CXCL10*, *IL6*, *TNF α* , *TGF β* , *TGF β RII* or *IL13* expression (Fig 22C).

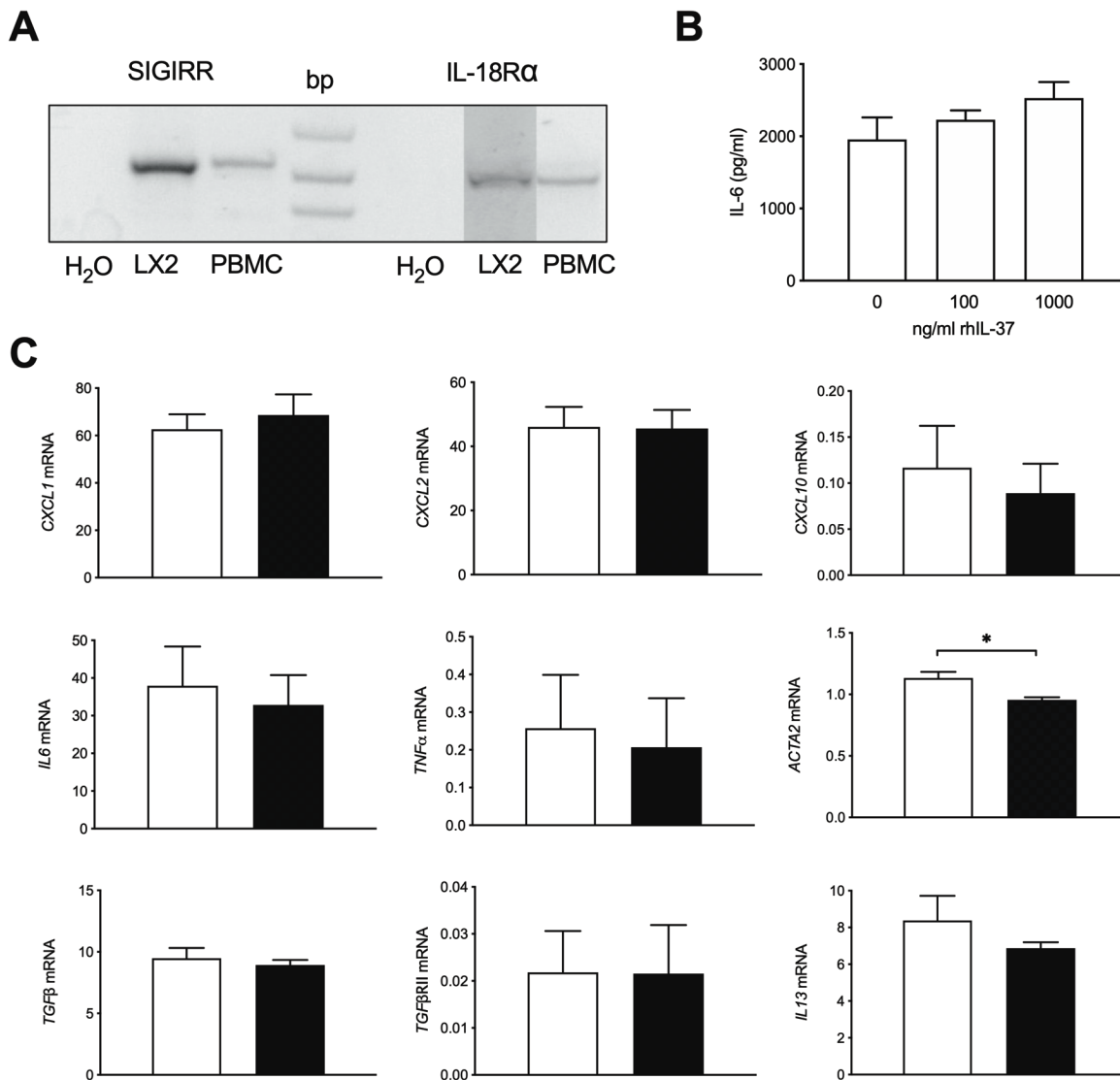


Figure 22: Recombinant human IL-37 reduces pro-fibrogenic gene expression. (A) Expression of SIGIRR and IL-18Rα. SIGIRR and IL-18Rα specific mRNA was detected by RT-PCR in LX2 and human PBMCs. (B) IL-6 secretion. Cells were exposed to recombinant human IL-37 (100 or 1000 ng/ml) or PBS, and stimulated with IL-1β (10 ng/ml) 24h later. IL-6 was measured in supernatants 24h after IL-1β stimulation (C) Gene expression. Cells were exposed to recombinant human IL-37 (100 or 1000ng/ml) and stimulated with IL-1β (10 ng/ml) 24h later. Total RNA was from cell pellets extracted 6h after IL-1β stimulation and transcribed to cDNA. mRNA was measured by qPCR. *Rpl13a* was run as normalization input. Open columns: PBS, closed columns: rhIL-37. N=3, *p<0.05.

3.2.3 siRNA-mediated knockdown of endogenous IL-37 in LX2 cells

Since overexpression of IL-37 downregulated the inflammatory and profibrogenic response of LX-2 cells, we hypothesized that, vice versa, knockdown of endogenous IL-37 will upregulate the cellular response. We tested different concentrations of siRNA for functional IL-37 knockdown. With 5 nM siRNA no knockdown of IL-37 mRNA was achieved. Using 10nM, 50 nM and 100 nM siRNA *IL37* expression was reduced. Best results were achieved using 10 nM siRNA for 72h (Fig. 23).

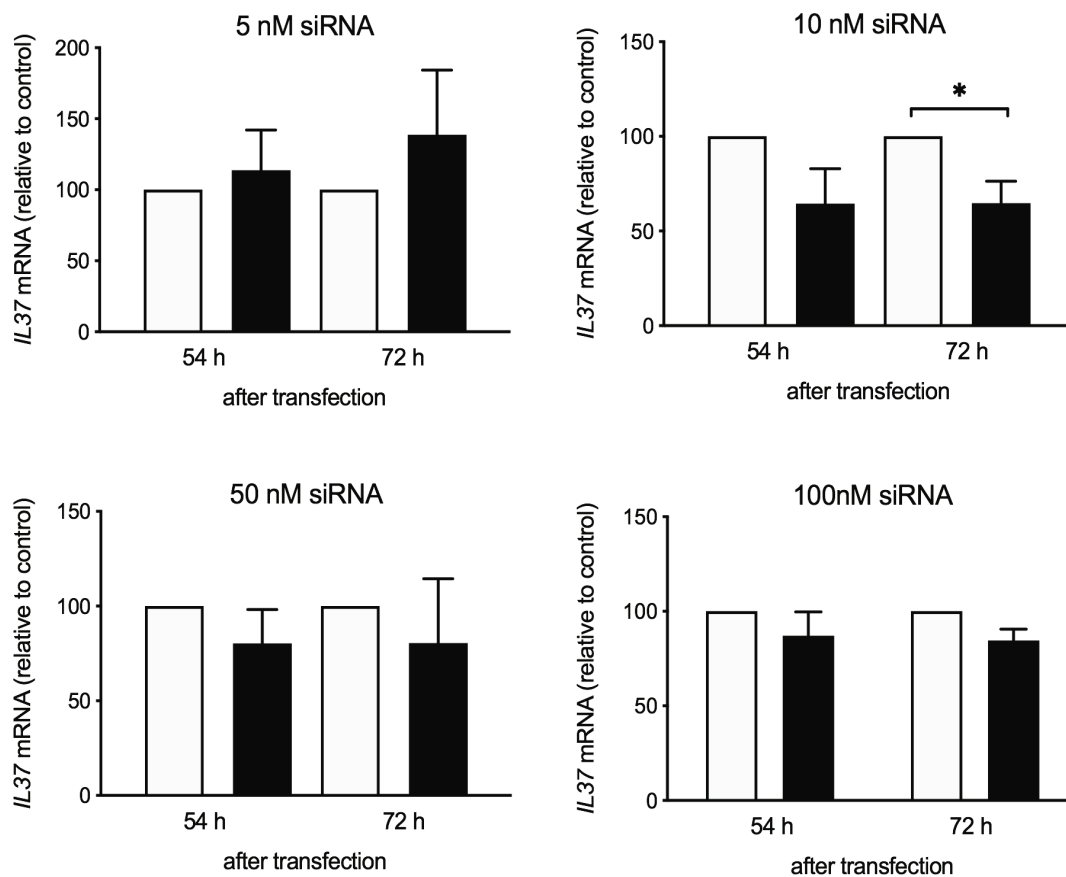


Figure 23: 10nM IL-37 siRNA downregulates IL-37 after IL-1 β stimulation. LX2 cells were transfected with 5 nM, 10 nM, 50 nM or 100 nM IL-37 *siRNA* or *scr* RNA using RNAiMax. Total RNA was extracted from cell pellets and transcribed to cDNA 54h and 72h post transfection after being stimulated for 6h with IL-1 β (10 ng/ml). mRNA was measured by qPCR. *Rpl13a* was run as normalization input. Open columns: *Scr*, closed columns: *siRNA*. N=3, *p<0.05.

To examine whether IL-37 knockdown increases the inflammatory response, LX-2 cells were transfected with 10nM siRNA and subsequently stimulated with IL-1 β . In a pilot experiment IL-6 secretion from IL-37siRNA transfected cells was increased (Fig. 24A), though there was no IL-37 knockdown in transfected cells (Fig. 24B). Since specific knockdown of endogenous IL-37 could not be replicated in several other experiments under different conditions, we stopped this line of experiments and shifted our focus to primary mouse stellate cells from livers of wt and IL-37tg mice.

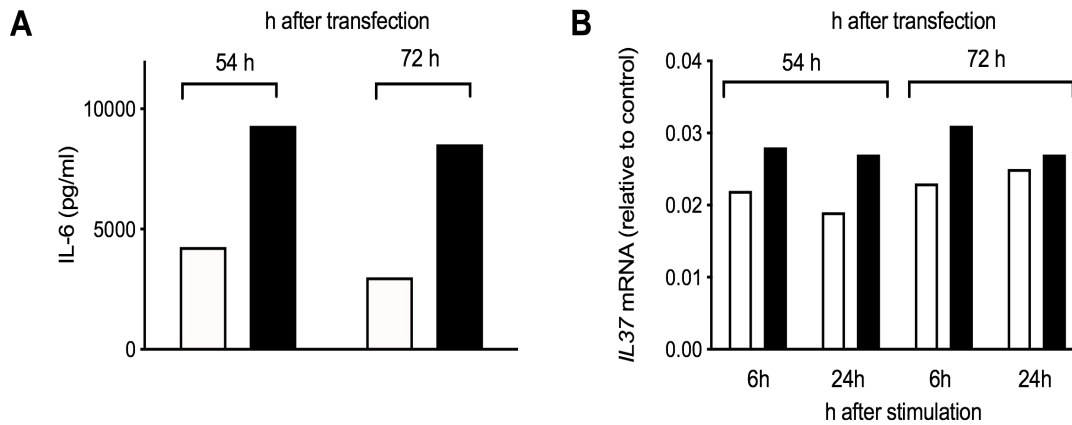


Figure 24: IL-37 knockdown in LX2 cells. LX2 cells were transfected with 10 nM IL-37 *siRNA* or *scr* using RNAiMax. Total RNA was extracted from cell pellets and transcribed to cDNA 54h and 72h post transfection after being stimulated with IL-1 β (10 ng/ml) for 6h. **(A) IL-6 secretion.** IL-6 was measured in supernatants 24h after IL-1 β stimulation. **(B) Gene expression.** Total RNA was extracted 6h and 24h after IL-1 β stimulation from cell pellets and transcribed to cDNA. mRNA was measured by qPCR. *Rpl13a* was run as normalization. Open columns: *Scr*, closed columns: *siRNA*. N=1

3.3 The functional role of IL-37 in mouse hepatic stellate cells

3.3.1 Spontaneous activation of wt murine hepatic stellate cell in culture

To estimate at what point after isolation mHSC differentiate into activated stellate cells, we monitored spontaneous IL-6 release from cultured mHSC over a period of 15 days. IL-6 secretion begins to increase on day 5, reaching a maximum of about 600 pg/ μ g IL-6 on day 9. After day 10, IL-6 in supernatant declines (Fig. 25A). mHSC cells express α -Sma on day 12 as a marker for activation and myofibroblast activation (Fig. 25B). α -Sma protein expression is elevated on day 11, and then reduced on day 15 (Fig. 25C).

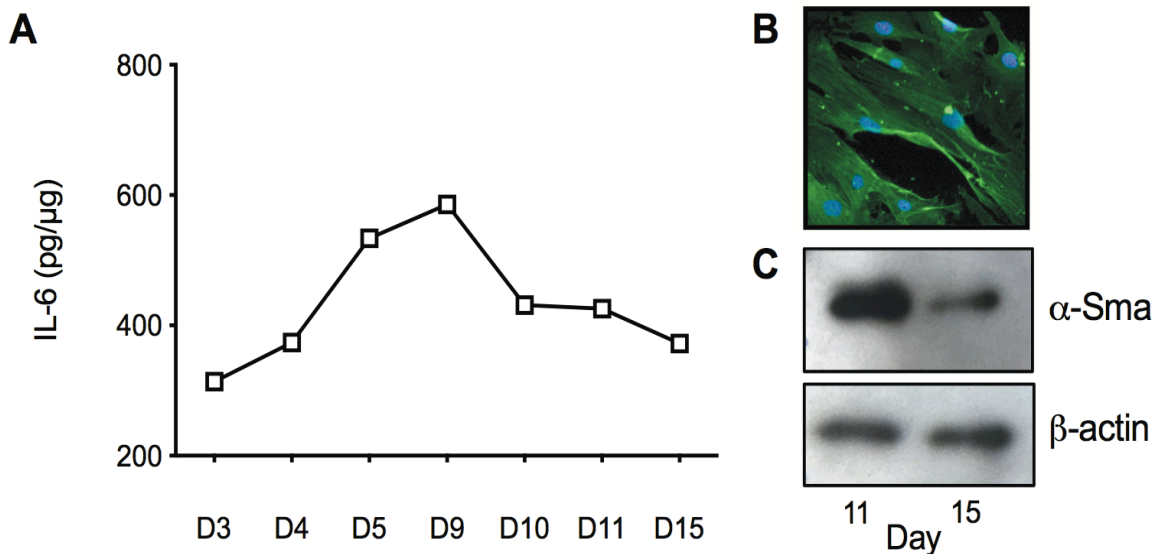


Figure 25: Wt murine hepatic stellate cell activate spontaneously. Wt murine hepatic stellate cells were isolated according to standard procedures and cultivated for 15 days. **(A) IL-6 secretion.** Cell culture media was collected every second day and tested for spontaneous IL-6 release. **(B) α -Sma staining.** Cells were fixed on day 12 after isolation and stained for α -SMA. **(C) Protein expression.** Cells were harvested on day 11 and day 15, lysed and probed for α -Sma. β -actin was run as loading control. N=1.

3.3.2 Transgene IL-37 expression reduces pro-inflammatory response in mHSC

Next, we isolated hepatic stellate cells from wt and IL-37tg mice. Spontaneous IL-6 secretion over a 12-day period in culture was markedly lower in IL-37tg HSC compared to wt HSC (Fig. 26A). *In-vitro* differentiated IL-37tg HSC also released less IL-6 in response to LPS and the costimulation with LPS and TGF- β (Fig. 26B). CCL2 was also lower in supernatants of IL-37tg HSC before and after stimulation with LPS and LPS/TGF- β ($p=0.1$), whereas there was no difference in the release of IL-10 (Fig. 26C). After LPS stimulation gene expression of *Cxcl1* and *Icam1* were reduced in IL-37tg HSC compared to control. *Bambi* expression showed a trend in reduction in IL-37tg HSC (Fig. 26D). α -Sma protein expression was lower in IL-37tg mHSC compared to wt HSC after LPS and TGF- β stimulation (Fig. 26E). *Icam1* protein was also reduced but without significant difference ($p=0.1$). Unstimulated HSC showed no difference in protein expression for α -SMA and *Icam1* (Fig. 26E).

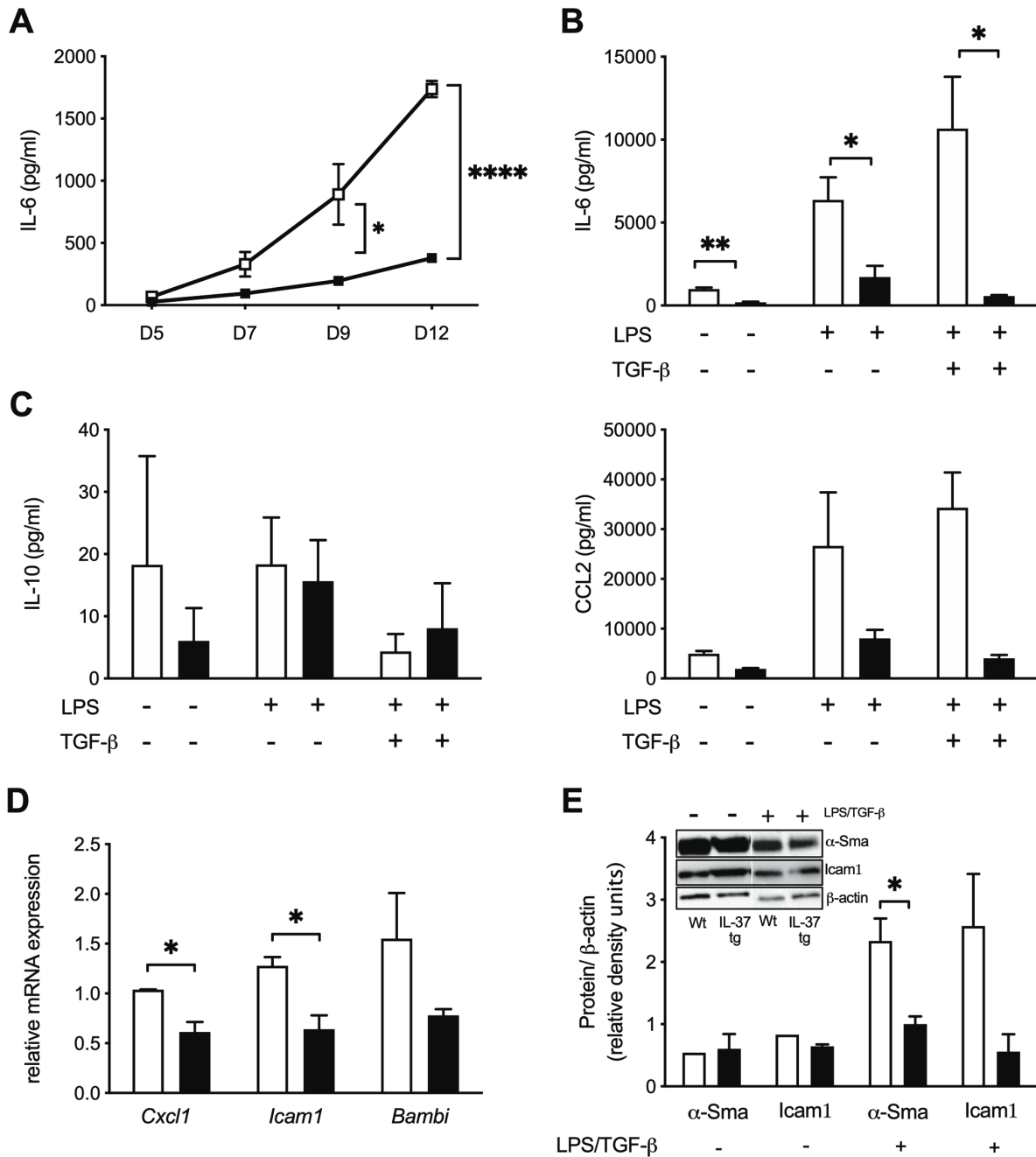


Figure 26: Transgene IL-37 expression reduces pro-inflammatory response in mHSC. Murine hepatic stellate cells were isolated according to standard procedures. **(A) Spontaneous IL-6 release.** Supernatant was collected on day 5,7,9 and 12 and tested for spontaneous IL-6 release. **(B) IL-6 secretion after stimulation.** Cells were stimulated with LPS (100 ng/ml) on day 8, and TGF-β (100 pg/ml) on day 9. Cells were harvested on day 12 and supernatant tested for IL-6. **(C) Bioplex Assay.** Cells were stimulated as described in (B). Supernatant was tested for IL-10 and CCL2 using ProcartaPlex Assay. **(D) Gene expression after LPS stimulation.** After isolation mHSC were cultured overnight and then stimulated with LPS (100 ng/ml) the next day. Total RNA was collected 6h after stimulation and transcribed to cDNA. mRNA was measured by qPCR. *Rpl13a* was run as normalization input. **(E) Protein expression.** Cells were stimulated as described in (B). On day 12 cells were harvested, lysed and probed for Icam1 and α-Sma. β-actin was run as loading control. Quantification was performed using Image Lab software from BioRad. Open boxes/bars: Wt, closed boxes/bars: IL-37tg. N=3, *p< 0.05, **p< 0.01, ****p< 0.0001.

3.3.3 Recombinant IL-37 does not modulate the pro-inflammatory response of mHSC

To further investigate whether extracellular IL-37 is sufficient to modulate the immune response of HSC, we exposed freshly isolated wt cells to IL-37 protein and monitored spontaneous IL-6 secretion. There was no difference between treated and untreated cells (Fig. 27A). Gene expression levels of pro-inflammatory and pro-fibrotic genes after rh-IL37 exposure and LPS stimulation were similar in both groups (Fig. 27B). Recombinant IL-37 had no effect on IL-6 secretion after LPS and TGF- β stimulation (Fig. 27C).

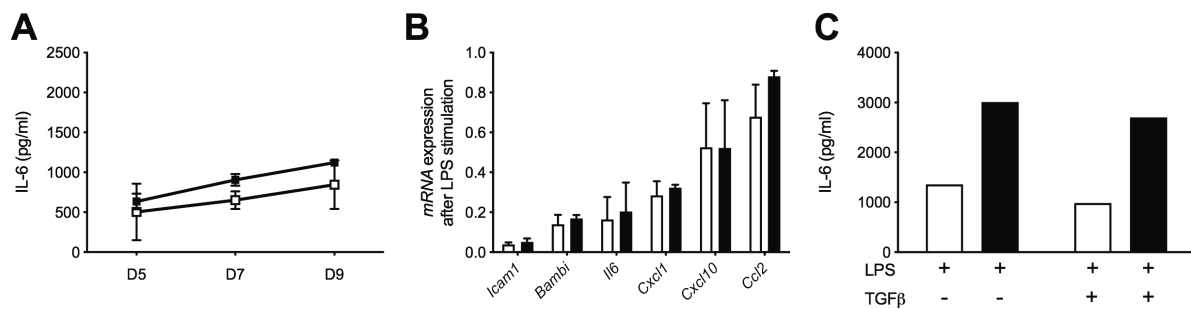


Figure 27: Recombinant IL-37 does not influence pro-inflammatory response in mHSC. Murine hepatic stellate cells were isolated according to standard procedures. **(A) Spontaneous IL-6 release.** Recombinant IL-37 was added every second day along with fresh media. Supernatant was collected on day 5, 7 and 9 and tested for spontaneous IL-6 release. N=2. **(B) Gene expression after LPS stimulation.** After isolation mHSC were cultured with 1 μ g/ml rhIL-37 overnight and then stimulated with LPS (100 ng/ml) the next day. Total RNA was collected 6h after stimulation and transcribed to cDNA. mRNA was measured by qPCR. *Rpl13a* was run as normalization input. N=3. **(C) IL-6 secretion after stimulation.** Recombinant IL-37 was added every second day along with fresh media. Cells were stimulated with LPS (100 ng/ml) on day 8, and TGF- β (100 pg/ml) on day 9. Cells were harvested on day 12 and supernatant tested for IL-6. Open boxes/column untreated, closed boxes/column: rhIL-37 treated cells. N=1.

3.4 The functional role of IL-37 in murine Kupffer cells

3.4.1 Transgene IL-37 expression reduces pro-inflammatory response in KC

Kupffer cells are the second major cell type of the liver to induce fibrosis via the activation of HSC. Therefore, we next investigated whether KC isolated from IL-37tg mice exhibit a reduced pro-inflammatory response. After LPS stimulation KC isolated from IL-37tg mice showed a trend in reduced cytokine secretion (IL-12p40, G-CSF, CCL2, KC, Rantes and CCL4) (Fig. 28A). Similar to IL-37tg HSC, KC isolated from IL-37tg mice showed reduced IL-6 secretion after LPS stimulation (Fig. 28B).

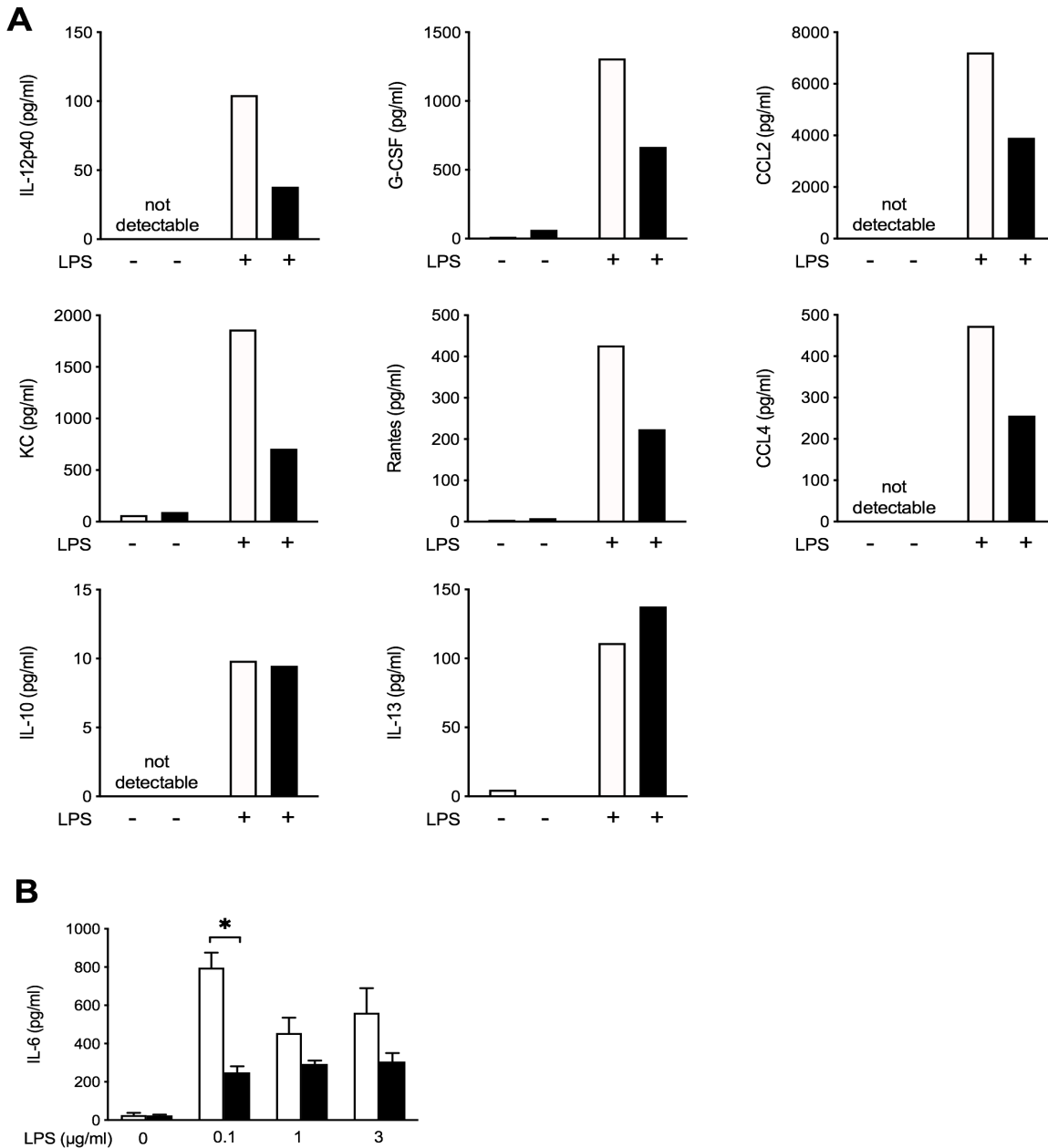


Figure 28: Transgene IL-37 expression reduces pro-inflammatory response in KC. Kupffer cells were isolated according to standard procedures. **(A) Cytokine secretion.** Cells were isolated and then stimulated with LPS (100 ng/ml). Supernatant from 3 individual experiments was pooled and tested for cytokine secretion. **(B) IL-6 secretion after LPS stimulation.** Cells were stimulated with increasing concentration of LPS (0.1, 1, 3 µg/ml). Supernatant was collected 24h thereafter and tested for IL-6 release. N=3, *p< 0.05.

3.4.2 The impact of transgene IL-37 on KC migration

Since the migration of KC towards HSC is essential for their activation, we analysed whether IL-37tg expression alters the migratory behaviour. First, we isolated wt KC to show that the isolated cells migrate towards conditioned media (Fig. 29A). As shown in figure 29B, neither transgene IL-37 expression in KC nor the supernatant of IL-37tg HSC modulated migration of freshly isolated KC (Fig. 29B).

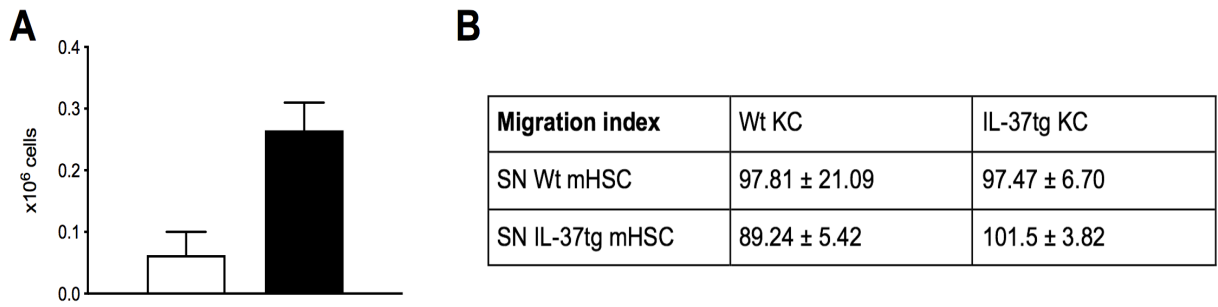


Figure 29: Transgene IL-37 expression does not affect Kupffer cell migration. Kupffer cells were isolated according to standard procedures. **(A) Wt Kupffer cell migration.** Kupffer cells isolated from wt mice were placed in the upper chamber of a Boyden chamber assay. Pure media or supernatant from LPS and TGF- β stimulated IL-37tg mHSCs was placed in the lower chamber. Migration index was assessed after 8h. **(B) Kupffer cell migration.** Kupffer cells from wt and IL-37tg animals were isolated and placed in the upper chamber of a Boyden Chamber Migration assay. Supernatant from LPS and TGF- β stimulated wt or IL-37tg mHSCs was placed in the lower chamber. Migration index was assessed after 8h. Open column: pure media, closed column: conditioned media. N=3.

4. DISCUSSION

Chronic inflammation is an important trigger of liver fibrogenesis. Although well described, inflammatory pathways have received little attention as therapeutic targets for chronic liver diseases (11). IL-37 has proven to exert broad-spectrum anti-inflammatory effects *in vitro* and *in vivo* (82). Furthermore, IL-37 interferes with the TGF- β signaling pathway by interaction with Smad3 (36, 37, 47, 83, 84). Since TGF- β is a core cytokine involved in liver fibrogenesis we hypothesized that IL-37 modulates liver fibrosis by functional interaction with the TGF- β signaling pathway (4). Here, we show that IL-37 improves the clinical outcome and downregulates liver inflammation and fibrogenesis in various models of liver fibrosis as well as the activation of Kupffer- and stellate cells.

Obstructive cholestasis in patients induces the release of serum transaminases, alkaline phosphatase and bilirubin (85). In consistence we show that wt and IL-37tg mice showed elevated GOT, GPT, AP and bilirubin serum levels after BDL. Interestingly, IL-37tg mice had lower GOT levels than wt mice indicating reduced hepatocellular damage. In addition to its protective effects on hepatocellular damage the transgene IL-37 expression also markedly improved survival after BDL. Weight loss was the main indication for premature sacrifice of wt mice. Weight loss is well described in CCl₄-induced liver inflammation and fibrosis (86) was similarly less in IL-37tg mice indicating an improved clinical condition by IL-37tg expression.

In parallel to the mitigated clinical outcome, IL-37tg mouse livers showed less fibrosis compared to wt mice after BDL as assessed by Sirius red staining. In CCl₄-induced liver injury we observed a trend towards less liver fibrosis in IL-37tg mice as shown by Sirius Red stainings of liver tissue. An impression that is underlined by a significant lower *Tgfb* mRNA expression in IL-37tg mice compared to wt mice after CCl₄ treatment.

As a third model we examined livers of IL-10KO and IL-10KO/IL-37tg mice during chronic colitis, since hepatobiliary involvement in IBD is common and affects 20% to 30% of children and adults with IBD (79, 80, 87). Liver inflammation in this model was low, however, IL-37tg expression was associated with even less hepatic mRNA expression of proinflammatory genes. These anti-inflammatory effects were associated with significant less fibrosis assessed by histological evaluation in IL-10KO/IL-37tg mice compared to IL-10KO

controls. Thereby, we can summarize that the IL-37 expression showed hepatoprotective effects in three different models of liver injury indicating its protective value for different entities of chronic liver diseases such as cholestatic-, toxin mediated- and immune-driven liver diseases. As a fourth model, we wanted to test the function of IL-37 during spontaneous liver fibrosis in MDR2KO mice. However, the intraperitoneal expression of IL-37 by cmRNA induced the generation of IL-37 specific antibodies in these mice. Most likely, this explains why IL-37 expression in this model was not sufficient to modulate liver fibrogenesis.

When analyzing the hepatic immune cell infiltrate, we found that numbers of Mac-2-positive hepatic macrophages after BDL were similar in both IL-37tg and wt mice. However, we observed a trend of lower numbers of CD3 positive lymphocytes in livers of IL-37tg mice indicating less hepatocellular inflammation. When activated, liver infiltrating macrophages and T-lymphocytes secrete cytokines such as IL-6 and TGF- β to stimulate, in concert with KCs, the proliferation and activation of HSCs resulting in ECM deposition (88, 89). Since overexpression of IL-37 downregulates the pro-inflammatory response of immune cells *in vitro* and *in vivo* we hypothesized that pro-inflammatory mediators are also lower in livers of IL-37tg mice (82). Indeed, in CCl₄-induced liver fibrosis levels of hepatic *Il6* and *Tgfb* gene expression were markedly lower in IL-37tg mice compared to wt mice. Similarly, there was a trend of reduced expression of pro-inflammatory and pro-fibrogenic genes in IL-37tg mouse livers in the early course after BDL. Most strikingly was the reduction of *Tnfa*, *Cxcl10* and other pro-inflammatory and pro-fibrogenic genes in livers of IL-37tg mice during chronic colitis suggesting that IL-37 modulates fibrosis both by inhibiting inflammation and downregulating fibrosis-inducing pathways.

I.p. injected rhIL-37 reduces ischemia/reperfusion-induced liver damage (57). However, in our model of BDL, the systemic administration of rhIL-37, acting primarily by binding to the membrane receptor, was not sufficient to limit pro-inflammatory or pro-fibrogenic gene expression at day 3 after BDL. Therefore, we speculate that in BDL intracellular IL-37 plays a more dominant role in modulating cholestasis-induced liver inflammation and fibrosis than extracellular IL-37.

The liver damage in MDR2KO mice resembles human PSC. Since crossbreeding of MDR2KO mice with IL-37tg mice and the backcrossing of homozygous mice would have been an extremely time consuming and uncertain process because of infertility of

homozygous MDR2KO mice, we overexpressed IL-37 using cmRNAs in the MDR2KO mouse model. mRNA-based therapeutics are improving and are enhancing the potential of mRNA as a new alternative for protein replacement therapies (81). Certain liver diseases including urea cycle disorder (90), Crigler-Najjar syndrome type 1 (91), Alpha-1 antitrypsin deficiency (92), thrombotic thrombocytopenic purpura (93), glycogen storage disease (94), acute intermittent porphyria (95) and factor IX deficiency haemophilia B (96, 97) are already in preclinical studies using transcript therapy.

We first tested the function of IL-37 expressed by two different cmRNAs in RAW264.7, LX2 and A549 cells. Our results show that overexpression of IL-37 by cmRNA reduces the release of pro-inflammatory mediators such as IL-6 in response to LPS or IL-1 β stimulation by all three cell lines. Also pro-inflammatory cytokine *Cxcl10*, which is secreted by hepatocytes in areas of lobular inflammation in various types of liver injury was downregulated in cells overexpressing IL-37 (98, 99).

After establishing that MDR2KO mice develop fibrosis from the age of 4 weeks, we injected the mice with cmRNA from only 2 weeks of age three times a week to intervene with the progression of spontaneous liver fibrosis as early as possible. The injection of IL-37 cmRNAs induced transcription and secretion of barely detectable levels of IL-37 in circulation, indicating successful expression and systemic distribution. However, we detected antibodies against human IL-37 in all mice treated with IL-37-coding cmRNA most likely neutralizing circulating IL-37. Therefore, the administration of IL-37 cmRNA did not result in the modulation of liver fibrosis in MDR2KO mice. Although mRNA therapies show a great potential for future application, a different experimental approach is needed to study whether IL-37 is capable to modulate liver fibrogenesis in the robust model of MDR2KO mice resembling human PSC.

The crosstalk between KC and HSC is crucial for the activation of HSC and the initiation of liver fibrogenesis. Therefore, we next tested the impact of IL-37 on the function of human LX2 stellate cells and primary mouse KC and HSC. KC secrete pro-inflammatory cytokines in response to danger signals such as endotoxin (100). In turn, these cytokines activate and thereby initiate proliferation and myofibroblast differentiation of HSCs, which then produce components of ECM as well as adhesion molecules like α -SMA and Icam1 (10, 101, 102).

After studying the effect of IL-37 overexpression we next attempted to knockdown endogenous IL-37 in human LX2 cells. Under physiological conditions, IL-37 expression is very low. Only upon stimulation with TLR ligands or pro-inflammatory cytokines IL-37 expression is upregulated in immune cells (43). Accordingly, we also detected only low levels of IL-37 in resting LX2 cells. Only after IL-1 β stimulation we were able to see an increase in IL-37 mRNA expression. During the pilot experiments it was extremely difficult to obtain reliable and reproducible results of the siRNA-mediated IL-37 knockdown and we therefore discontinued this part of experiments with LX2 cells. In future, analysing the intracellular role of IL-37 in cell lines could be achieved by using CRISPR-CAS9 method.

However, despite the expression of the receptor, treatment of LX2 cells with rhIL-37 had no effect indicating that intracellular expression of IL-37 is mandatory for its function in LX-2 cells. Similar results were obtained in mouse HSC-derived myofibroblasts, where only transgene IL-37 but not rhIL-37 protein reduced spontaneous, LPS or LPS/TGF- β -induced IL-6 secretion and pro-inflammatory gene expression. Common markers of HSC activation such as Icam1 and α -Sma were also reduced in HSC-derived myofibroblasts isolated from IL-37tg mice compared to wt cells after LPS or LPS/TGF- β stimulation. These results show that IL-37 overexpression reduces both the inflammatory response and ECM deposition by HSC. Notably, there was no difference in IL-10 secretion from IL37tg and wt HSCs before or after stimulation with LPS or LPS plus TGF- β . This stands in accordance with previously published observations that the immunomodulatory function of IL-37 in macrophage cells or PBMC is not mediated by IL-10 (36, 83).

Previous studies have shown that IL-37 inhibits the formation of macrophage pseudopodia and has the capacity to suppress the migration of human cervical cancer cells (36, 103). Activated liver HSC/myofibroblasts release a range of chemokines including CCL2, CCL3 and CXCL10 to attract lymphocytes (104). Our results show that HSC-derived myofibroblasts isolated from IL-37tg mouse livers secreted less KC activating chemokine CCL2 compared to wt HSC. Although we showed that KCs migrate towards the supernatant of stimulated HSC, neither transgene IL-37 in KCs nor the supernatant of stimulated IL-37tg HSC modulated the migration behaviour of KC. Therefore, we assume that reduced liver fibrosis in IL-37tg mice is unlikely to be explained by alterations of the spatial proximity of KC and HSC.

Zhao et al. reported that increased IL-37 expression in human HCC was linked to better overall survival and disease-free survival. IL-37 expression in the tumor was associated with the higher density of tumor-infiltrating CD57+ natural killer cells, but not with CD3+ and CD8+ T cells, indicating that IL-37 expression increased NK recruitment to the tumor-microenvironment and, thereby, downregulates tumor growth (61). Although IL-37 did not impact KC migration in our experiments, IL-37 possibly modulates the inflammatory microenvironment within the liver by inhibition of the recruitment of infiltrating lymphocytes as seen in our BDL model.

At the molecular level we reported that intracellular IL-37 interacts with Smad3 to reduce inflammation (36). Smad3 itself is activated by phosphorylation at the C-terminus (pSmad3C) or at the linker domain (pSmad3L) through TGF- β type I receptor or TGF- β -dependent c-Jun N-terminal kinase (105). The pSmadC pathway inhibits growth of normal cells as a tumor suppressor, whereas pSmadL-mediated signaling promotes ECM deposition and subsequent fibrosis, as well as tumor cell invasion as a tumor promoter during human HCC and ulcerative colitis-associated carcinogenesis (105-107). In a human HCC cell line, transfected IL-37 directly targets pSmad3L/c-myc signaling to suppress oncogenic pSmadL signalling and to promote tumor-suppressive pSmad3C signaling (63). In line with this observation, our yet unpublished, confocal microscopy data show that IL-37 colocalizes with pSmad3L in liver fibrosis.

In collaboration we found in >300 patients with chronic liver disease increased IL-37 serum levels correlating with the degree of cirrhosis and Child Pugh score (Mountford J. Hepatol 2020, MS submitted). A similar phenomenon has been described for IL-1 receptor antagonist, another anti-inflammatory IL-1 family member (108). This might reflect the frustrating response of the host to fight against overwhelming hepatic inflammation and consecutive fibrosis.

In summary, here we show that transgene expression of IL-37 reduces liver inflammation and fibrosis in BDL-, CCl₄- and colitis-associated liver disease of mice. We suggest that predominantly intracellular IL-37 modulates liver fibrosis in two definite ways. Firstly, the interaction of IL-37 with pSmad3L directly targets the fibrotic pathway. Secondly, IL-37 downregulates liver inflammation and subsequent HSC activation by limiting the release of pro-inflammatory and pro-fibrogenic cytokines from infiltrating lymphocytes, macrophages

and KC. Thus IL-37-dependent mechanisms may represent a future target for the treatment of inflammatory and fibrosing liver diseases. The correlation of serum IL-37 with disease severity of liver cirrhosis in humans indicates the clinical relevance of our experimental findings.

5. ABSTRACT

Sustained inflammation is a common characteristic of chronic liver injury inducing liver fibrosis, cirrhosis and potentially liver cancer. Liver Kupffer cells (KC) are key modulators of hepatic stellate cell (HSC) function by secretion of immunologically active proteins such as TGF- β . TGF- β promotes liver fibrosis via the activation of Sma- and Mad-related protein 3 (Smad3). Interleukin (IL)-37 is an IL-1 family cytokine with intra- and extracellular functionality and broadly suppresses innate and adaptive immune responses. Intracellularly, IL-37 interacts with Smad3 and we hypothesize that IL-37 interferes with the signalling cascade of pro-fibrogenic TGF- β .

Here we demonstrate that transgene (tg) expression of IL-37 in mice is associated with prolonged survival, reduced hepatic damage and early fibrosis markers as well as less histologically proven liver fibrosis after bile duct ligation (BDL). IL-37tg mice were also protected against CCl₄-induced liver inflammation. In addition, colitis-associated liver inflammation and fibrosis was less severe in IL-10 knockout mice expressing IL-37. Spontaneous as well as LPS/TGF- β -induced cytokine release and pro-fibrogenic gene expression was lower in hepatic stellate and Kupffer cells isolated from IL-37tg mice and IL-37 overexpressing, IL-1 β - or LPS-stimulated human LX-2 stellate, RAW264.7 and A549 cells. However, administration of recombinant human (rh) IL-37 did not modulate fibrosis pathways after BDL in mice, in LX2 cells or murine HSCs.

We conclude that predominantly intracellular IL-37 down-regulates pathways of liver inflammation and fibrosis and may represent a novel target to modulate the clinical course of chronic liver diseases.

6. ZUSAMMENFASSUNG

Das Hauptmerkmal chronischer Leberverletzungen sind anhaltende Entzündungsvorgänge, die zu Fibrose, Zirrhose und schließlich Leberkrebs führen können. Die entscheidenden Modulatoren für eine Progression der Krankheit sind die Kupffer-Zellen der Leber, da sie immunologisch aktive Proteine wie z.B. profibrogenes TGF- β sezernieren. TGF- β aktiviert durch die Interaktion mit Sma- und Mad-assoziierten Proteinen 3 (Smad3) die profibrogene Signalkaskade und aktiviert dadurch die Haupteffektorzellen der Leberfibrogenese – die hepatischen Sternzellen. Interleukin (IL)-37 ist ein Zytokin der IL-1 Familie und hemmt durch intra- und extrazelluläre Mechanismen die angeborene und adaptive Immunantwort. Da IL-37 intrazellulär mit Smad3 interagiert, war es die Hypothese und das Ziel dieser Arbeit zu prüfen, ob IL-37 auf diese Weise in die profibrogene Signalkaskade eingreift und dadurch die Ausbildung der Leberfibrose moduliert.

Wir untersuchen den Einfluss von IL-37 in drei verschiedenen Mausmodellen zur Leberfibrose. Die transgene (tg) IL-37 Expression schützte Mäusen nach Ligatur der Gallengänge und war mit besserem Überleben, reduziertem Leberschaden, geringerer Expression früher Fibrosemarker sowie reduzierter Leberfibrose assoziiert. IL-37tg Mäuse hatten auch im Modell der CCl₄-induzierten Leberfibrose weniger Entzündung der Leber. Zusätzlich wiesen IL-37tg Mäuse eine geringere Beteiligung der Leber im Rahmen eines chronischen Kolitismodells auf und waren im Vergleich zu IL-10KO Mäusen vor Leberentzündung und -fibrose geschützt. Die Überexpression von IL-37 durch chemisch-modifizierte RNA-Moleküle reduzierte die spontane und LPS/TGF- β induzierte Zytokinausschüttung sowie Expression profibrogenen Gene in Stern- und Kupffer-Zellen von IL-37tg Mäusen, RAW264.7 und A549 Zellen. Allerdings hatte die Gabe von rekombinantem (rh) IL-37 bei Mäusen nach Gallengangligatur oder stimulierten LX2 Zellen und hepatischen Sternzellen keinen Effekt auf Ausschüttung von Entzündungs- und Fibrosemarkern.

Dies bedeutet, dass vorrangig intrazelluläres IL-37 das Ausmaß von Leberentzündung und -fibrose moduliert. Die Modulation der IL-37-Expression oder IL-37-abhängiger Signalwege könnte damit in Zukunft zur Therapie chronischer Lebererkrankungen genutzt werden.

7. REFERENCES

1. Pellicoro A, Ramachandran P, Iredale JP, Fallowfield JA. Liver fibrosis and repair: immune regulation of wound healing in a solid organ. *Nat Rev Immunol* 2014;14:181-194.
2. Robinson MW, Harmon C, O'Farrelly C. Liver immunology and its role in inflammation and homeostasis. *Cell Mol Immunol* 2016;13:267-276.
3. Luedde T, Schwabe RF. NF-kappaB in the liver--linking injury, fibrosis and hepatocellular carcinoma. *Nat Rev Gastroenterol Hepatol* 2011;8:108-118.
4. Bataller R, Brenner DA. Liver fibrosis. *The Journal of clinical investigation* 2005;115:209-218.
5. Iredale JP. Models of liver fibrosis: exploring the dynamic nature of inflammation and repair in a solid organ. *The Journal of clinical investigation* 2007;117:539-548.
6. Gines P, Cardenas A, Arroyo V, Rodes J. Management of cirrhosis and ascites. *N Engl J Med* 2004;350:1646-1654.
7. Fattovich G, Stroffolini T, Zagni I, Donato F. Hepatocellular carcinoma in cirrhosis: incidence and risk factors. *Gastroenterology* 2004;127:S35-50.
8. Fallowfield JA, Iredale JP. Reversal of liver fibrosis and cirrhosis--an emerging reality. *Scott Med J* 2004;49:3-6.
9. Iredale JP. Cirrhosis: new research provides a basis for rational and targeted treatments. *BMJ* 2003;327:143-147.
10. Seki E, De Minicis S, Osterreicher CH, Kluwe J, Osawa Y, Brenner DA, Schwabe RF. TLR4 enhances TGF-beta signaling and hepatic fibrosis. *Nature medicine* 2007;13:1324-1332.
11. Seki E, Schwabe RF. Hepatic inflammation and fibrosis: functional links and key pathways. *Hepatology* 2015;61:1066-1079.
12. Racanelli V, Rehermann B. The liver as an immunological organ. *Hepatology* 2006;43:S54-62.
13. Friedman SL. Molecular regulation of hepatic fibrosis, an integrated cellular response to tissue injury. *J Biol Chem* 2000;275:2247-2250.
14. Mackay IR. Hepatoimmunology: a perspective. *Immunol Cell Biol* 2002;80:36-44.
15. Gale RP, Sparkes RS, Golde DW. Bone marrow origin of hepatic macrophages (Kupffer cells) in humans. *Science* 1978;201:937-938.
16. Gao B, Jeong WI, Tian Z. Liver: An organ with predominant innate immunity. *Hepatology* 2008;47:729-736.
17. MacPhee PJ, Schmidt EE, Groom AC. Evidence for Kupffer cell migration along liver sinusoids, from high-resolution in vivo microscopy. *Am J Physiol* 1992;263:G17-23.
18. Smedsrod B, De Bleser PJ, Braet F, Loviseti P, Vanderkerken K, Wisse E, Geerts A. Cell biology of liver endothelial and Kupffer cells. *Gut* 1994;35:1509-1516.
19. Duffield JS, Forbes SJ, Constandinou CM, Clay S, Partolina M, Vuthoori S, Wu S, et al. Selective depletion of macrophages reveals distinct, opposing roles during liver injury and repair. *The Journal of clinical investigation* 2005;115:56-65.
20. Geerts A. History, heterogeneity, developmental biology, and functions of quiescent hepatic stellate cells. *Semin Liver Dis* 2001;21:311-335.
21. Paik YH, Schwabe RF, Bataller R, Russo MP, Jobin C, Brenner DA. Toll-like receptor 4 mediates inflammatory signaling by bacterial lipopolysaccharide in human hepatic stellate cells. *Hepatology* 2003;37:1043-1055.

22. Pradere JP, Kluwe J, De Minicis S, Jiao JJ, Gwak GY, Dapito DH, Jang MK, et al. Hepatic macrophages but not dendritic cells contribute to liver fibrosis by promoting the survival of activated hepatic stellate cells in mice. *Hepatology* 2013;58:1461-1473.
23. Dooley S, ten Dijke P. TGF-beta in progression of liver disease. *Cell Tissue Res* 2012;347:245-256.
24. Fabregat I, Fernando J, Mainez J, Sancho P. TGF-beta signaling in cancer treatment. *Curr Pharm Des* 2014;20:2934-2947.
25. Bauer M, Schuppan D. TGFbeta1 in liver fibrosis: time to change paradigms? *FEBS letters* 2001;502:1-3.
26. Kremer M, Perry AW, Milton RJ, Rippe RA, Wheeler MD, Hines IN. Pivotal role of Smad3 in a mouse model of T cell-mediated hepatitis. *Hepatology* 2008;47:113-126.
27. Tilg H, Diehl AM. Cytokines in alcoholic and nonalcoholic steatohepatitis. *N Engl J Med* 2000;343:1467-1476.
28. Hammerich L, Tacke F. Interleukins in chronic liver disease: lessons learned from experimental mouse models. *Clin Exp Gastroenterol* 2014;7:297-306.
29. Dinarello CA. Introduction to the interleukin-1 family of cytokines and receptors: Drivers of innate inflammation and acquired immunity. *Immunol Rev* 2018;281:5-7.
30. Barbier L, Ferhat M, Salame E, Robin A, Herbelin A, Gombert JM, Silvain C, et al. Interleukin-1 Family Cytokines: Keystones in Liver Inflammatory Diseases. *Front Immunol* 2019;10:2014.
31. Tsutsui H, Cai X, Hayashi S. Interleukin-1 Family Cytokines in Liver Diseases. *Mediators Inflamm* 2015;2015:630265.
32. Kamari Y, Shaish A, Vax E, Shemesh S, Kandel-Kfir M, Arbel Y, Olteanu S, et al. Lack of Interleukin-1alpha or Interleukin-1beta Inhibits Transformation of Steatosis to Steatohepatitis and Liver Fibrosis in Hypercholesterolemic Mice. *Journal of hepatology* 2011.
33. Petrasek J, Bala S, Csak T, Lippai D, Kodys K, Menashy V, Barrieau M, et al. IL-1 receptor antagonist ameliorates inflammasome-dependent alcoholic steatohepatitis in mice. *J Clin Invest* 2012;122:3476-3489.
34. Marvie P, Lisbonne M, L'Helgoualc'h A, Rauch M, Turlin B, Preisser L, Bourd-Boittin K, et al. Interleukin-33 overexpression is associated with liver fibrosis in mice and humans. *J Cell Mol Med* 2010;14:1726-1739.
35. McHedlidze T, Waldner M, Zopf S, Walker J, Rankin AL, Schuchmann M, Voehringer D, et al. Interleukin-33-dependent innate lymphoid cells mediate hepatic fibrosis. *Immunity* 2013;39:357-371.
36. Nold MF, Nold-Petry CA, Zepp JA, Palmer BE, Bufler P, Dinarello CA. IL-37 is a fundamental inhibitor of innate immunity. *Nat Immunol* 2010;11:1014-1022.
37. Nold-Petry CA, Lo CY, Rudloff I, Elgass KD, Li S, Gantier MP, Lotz-Havla AS, et al. IL-37 requires the receptors IL-18Ralpha and IL-1R8 (SIGIRR) to carry out its multifaceted anti-inflammatory program upon innate signal transduction. *Nat Immunol* 2015;16:354-365.
38. Kumar S, Hanning CR, Brigham-Burke MR, Rieman DJ, Lehr R, Khandekar S, Kirkpatrick RB, et al. Interleukin-1F7B (IL-1H4/IL-1F7) is processed by caspase-1 and mature IL-1F7B binds to the IL-18 receptor but does not induce IFN-gamma production. *Cytokine* 2002;18:61-71.

39. Boraschi D, Lucchesi D, Hainzl S, Leitner M, Maier E, Mangelberger D, Oostingh GJ, et al. IL-37: a new anti-inflammatory cytokine of the IL-1 family. *Eur Cytokine Netw* 2011;22:127-147.
40. Bufler P, Azam T, Gamboni-Robertson F, Reznikov LL, Kumar S, Dinarello CA, Kim SH. A complex of the IL-1 homologue IL-1F7b and IL-18-binding protein reduces IL-18 activity. *Proc Natl Acad Sci U S A* 2002;99:13723-13728.
41. Weidlich S, Bulau AM, Schwerd T, Althans J, Kappler R, Koletzko S, Mayr D, et al. Intestinal expression of the anti-inflammatory interleukin-1 homologue IL-37 in pediatric inflammatory bowel disease. *J Pediatr Gastroenterol Nutr* 2014;59:e18-26.
42. Gao W, Kumar S, Lotze MT, Hanning C, Robbins PD, Gambotto A. Innate immunity mediated by the cytokine IL-1 homologue 4 (IL-1H4/IL-1F7) induces IL-12-dependent adaptive and profound antitumor immunity. *J Immunol* 2003;170:107-113.
43. Bufler P, Gamboni-Robertson F, Azam T, Kim SH, Dinarello CA. Interleukin-1 homologues IL-1F7b and IL-18 contain functional mRNA instability elements within the coding region responsive to lipopolysaccharide. *The Biochemical journal* 2004;381:503-510.
44. Ballak DB, van Diepen JA, Moschen AR, Jansen HJ, Hijmans A, Groenhof GJ, Leenders F, et al. IL-37 protects against obesity-induced inflammation and insulin resistance. *Nat Commun* 2014;5:4711.
45. Coll-Miro M, Francos-Quijorna I, Santos-Nogueira E, Torres-Espin A, Bufler P, Dinarello CA, Lopez-Vales R. Beneficial effects of IL-37 after spinal cord injury in mice. *Proc Natl Acad Sci U S A* 2016;113:1411-1416.
46. McNamee EN, Masterson JC, Jedlicka P, McManus M, Grenz A, Collins CB, Nold MF, et al. Interleukin 37 expression protects mice from colitis. *Proceedings of the National Academy of Sciences of the United States of America* 2011;108:16711-16716.
47. Li S, Neff CP, Barber K, Hong J, Luo Y, Azam T, Palmer BE, et al. Extracellular forms of IL-37 inhibit innate inflammation in vitro and in vivo but require the IL-1 family decoy receptor IL-1R8. *Proc Natl Acad Sci U S A* 2015.
48. Lunding L, Webering S, Vock C, Schroder A, Raedler D, Schaub B, Fehrenbach H, et al. IL-37 requires IL-18Ralpha and SIGIRR/IL-1R8 to diminish allergic airway inflammation in mice. *Allergy* 2015.
49. Moretti S, Bozza S, Oikonomou V, Renga G, Casagrande A, Iannitti RG, Puccetti M, et al. IL-37 inhibits inflammasome activation and disease severity in murine aspergillosis. *PLoS Pathog* 2014;10:e1004462.
50. Wu B, Meng K, Ji Q, Cheng M, Yu K, Zhao X, Tony H, et al. Interleukin-37 ameliorates myocardial ischaemia/reperfusion injury in mice. *Clin Exp Immunol* 2014;176:438-451.
51. Ye Z, Wang C, Kijlstra A, Zhou X, Yang P. A possible role for interleukin 37 in the pathogenesis of Behcet's disease. *Curr Mol Med* 2014;14:535-542.
52. Ballak DB, Li S, Cavalli G, Stahl JL, Tengesdal IW, van Diepen JA, Kluck V, et al. Interleukin-37 treatment of mice with metabolic syndrome improves insulin sensitivity and reduces pro-inflammatory cytokine production in adipose tissue. *J Biol Chem* 2018;293:14224-14236.
53. Cavalli G, Justice JN, Boyle KE, D'Alessandro A, Eisenmesser EZ, Herrera JJ, Hansen KC, et al. Interleukin 37 reverses the metabolic cost of inflammation, increases

- oxidative respiration, and improves exercise tolerance. *Proc Natl Acad Sci U S A* 2017;114:2313-2318.
54. Ross R, Grimm J, Goedicke S, Mobus AM, Bulau AM, Bufler P, Ali S, et al. Analysis of nuclear localization of interleukin-1 family cytokines by flow cytometry. *J Immunol Methods* 2013;387:219-227.
 55. Sharma S, Kulk N, Nold MF, Graf R, Kim SH, Reinhardt D, Dinarello CA, et al. The IL-1 family member 7b translocates to the nucleus and down-regulates proinflammatory cytokines. *J Immunol* 2008;180:5477-5482.
 56. Li S, Amo-Aparicio J, Neff CP, Tengesdal IW, Azam T, Palmer BE, Lopez-Vales R, et al. Role for nuclear interleukin-37 in the suppression of innate immunity. *Proc Natl Acad Sci U S A* 2019;116:4456-4461.
 57. Sakai N, Van Sweringen HL, Belizaire RM, Quillin RC, Schuster R, Blanchard J, Burns JM, et al. Interleukin-37 reduces liver inflammatory injury via effects on hepatocytes and non-parenchymal cells. *Journal of gastroenterology and hepatology* 2012;27:1609-1616.
 58. Bulau AM, Fink M, Maucksch C, Kappler R, Mayr D, Wagner K, Bufler P. In vivo expression of interleukin-37 reduces local and systemic inflammation in concanavalin A-induced hepatitis. *ScientificWorldJournal* 2011;11:2480-2490.
 59. Grabherr F, Grander C, Adolph TE, Wieser V, Mayr L, Enrich B, Macheiner S, et al. Ethanol-mediated suppression of IL-37 licenses alcoholic liver disease. *Liver Int* 2018;38:1095-1101.
 60. Moschen AR, Molnar C, Enrich B, Geiger S, Ebenbichler CF, Tilg H. Adipose and liver expression of interleukin (IL)-1 family members in morbid obesity and effects of weight loss. *Molecular medicine* 2011;17:840-845.
 61. Zhao JJ, Pan QZ, Pan K, Weng DS, Wang QJ, Li JJ, Lv L, et al. Interleukin-37 Mediates the Antitumor Activity in Hepatocellular Carcinoma: Role for CD57+ NK Cells. *Sci Rep* 2014;4:5177.
 62. Li TT, Zhu D, Mou T, Guo Z, Pu JL, Chen QS, Wei XF, et al. IL-37 induces autophagy in hepatocellular carcinoma cells by inhibiting the PI3K/AKT/mTOR pathway. *Mol Immunol* 2017;87:132-140.
 63. Liu R, Tang C, Shen A, Luo H, Wei X, Zheng D, Sun C, et al. IL-37 suppresses hepatocellular carcinoma growth by converting pSmad3 signaling from JNK/pSmad3L/c-Myc oncogenic signaling to pSmad3C/P21 tumor-suppressive signaling. *Oncotarget* 2016;7:85079-85096.
 64. Zimmermann HW, Seidler S, Nattermann J, Gassler N, Hellerbrand C, Zerneck A, Tischendorf JJ, et al. Functional contribution of elevated circulating and hepatic non-classical CD14CD16 monocytes to inflammation and human liver fibrosis. *PloS one* 2010;5:e11049.
 65. Xu L, Hui AY, Albanis E, Arthur MJ, O'Byrne SM, Blaner WS, Mukherjee P, et al. Human hepatic stellate cell lines, LX-1 and LX-2: new tools for analysis of hepatic fibrosis. *Gut* 2005;54:142-151.
 66. Gossard AA, Talwalkar JA. Cholestatic liver disease. *Med Clin North Am* 2014;98:73-85.
 67. Faubion WA, Guicciardi ME, Miyoshi H, Bronk SF, Roberts PJ, Svingen PA, Kaufmann SH, et al. Toxic bile salts induce rodent hepatocyte apoptosis via direct activation of Fas. *J Clin Invest* 1999;103:137-145.
 68. Minter RM, Fan MH, Sun J, Niederbichler A, Ipaktchi K, Arbabi S, Hemmila MR, et al. Altered Kupffer cell function in biliary obstruction. *Surgery* 2005;138:236-245.

69. Scott-Conner CE, Grogan JB. The pathophysiology of biliary obstruction and its effect on phagocytic and immune function. *J Surg Res* 1994;57:316-336.
70. Isayama F, Hines IN, Kremer M, Milton RJ, Byrd CL, Perry AW, McKim SE, et al. LPS signaling enhances hepatic fibrogenesis caused by experimental cholestasis in mice. *Am J Physiol Gastrointest Liver Physiol* 2006;290:G1318-1328.
71. Gehring S, Dickson EM, San Martin ME, van Rooijen N, Papa EF, Harty MW, Tracy TF, Jr., et al. Kupffer cells abrogate cholestatic liver injury in mice. *Gastroenterology* 2006;130:810-822.
72. Fujii T, Fuchs BC, Yamada S, Lauwers GY, Kulu Y, Goodwin JM, Lanuti M, et al. Mouse model of carbon tetrachloride induced liver fibrosis: Histopathological changes and expression of CD133 and epidermal growth factor. *BMC Gastroenterol* 2010;10:79.
73. Son G, Iimuro Y, Seki E, Hirano T, Kaneda Y, Fujimoto J. Selective inactivation of NF-kappaB in the liver using NF-kappaB decoy suppresses CCl4-induced liver injury and fibrosis. *Am J Physiol Gastrointest Liver Physiol* 2007;293:G631-639.
74. Mountford S, Ringleb A, Schwaiger R, Mayr D, Kobold S, Dinarello CA, Bufler P. Interleukin-37 Inhibits Colon Carcinogenesis During Chronic Colitis. *Front Immunol* 2019;10:2632.
75. Popov Y, Patsenker E, Fickert P, Trauner M, Schuppan D. Mdr2 (Abcb4)^{-/-} mice spontaneously develop severe biliary fibrosis via massive dysregulation of pro- and antifibrogenic genes. *J Hepatol* 2005;43:1045-1054.
76. Reiter FP, Wimmer R, Wottke L, Artmann R, Nagel JM, Carranza MO, Mayr D, et al. Role of interleukin-1 and its antagonism of hepatic stellate cell proliferation and liver fibrosis in the Abcb4^(-/-) mouse model. *World J Hepatol* 2016;8:401-410.
77. Smit JJ, Schinkel AH, Oude Elferink RP, Groen AK, Wagenaar E, van Deemter L, Mol CA, et al. Homozygous disruption of the murine mdr2 P-glycoprotein gene leads to a complete absence of phospholipid from bile and to liver disease. *Cell* 1993;75:451-462.
78. Tag CG, Sauer-Lehnen S, Weiskirchen S, Borkham-Kamphorst E, Tolba RH, Tacke F, Weiskirchen R. Bile duct ligation in mice: induction of inflammatory liver injury and fibrosis by obstructive cholestasis. *J Vis Exp* 2015.
79. Mendes FD, Levy C, Enders FB, Loftus EV, Jr., Angulo P, Lindor KD. Abnormal hepatic biochemistries in patients with inflammatory bowel disease. *Am J Gastroenterol* 2007;102:344-350.
80. Pusateri AJ, Kim SC, Dotson JL, Balint JP, Potter CJ, Boyle BM, Crandall WV. Incidence, pattern, and etiology of elevated liver enzymes in pediatric inflammatory bowel disease. *J Pediatr Gastroenterol Nutr* 2015;60:592-597.
81. Trepotec Z, Lichtenegger E, Plank C, Aneja MK, Rudolph C. Delivery of mRNA Therapeutics for the Treatment of Hepatic Diseases. *Mol Ther* 2019;27:794-802.
82. Dinarello CA, Nold-Petry C, Nold M, Fujita M, Li S, Kim S, Bufler P. Suppression of innate inflammation and immunity by interleukin-37. *Eur J Immunol* 2016;46:1067-1081.
83. Bulau AM, Nold MF, Li S, Nold-Petry CA, Fink M, Mansell A, Schwerd T, et al. Role of caspase-1 in nuclear translocation of IL-37, release of the cytokine, and IL-37 inhibition of innate immune responses. *Proc Natl Acad Sci U S A* 2014;111:2650-2655.
84. Grimsby S, Jaensson H, Dubrovskaja A, Lomnytska M, Hellman U, Souchelnytskyi S. Proteomics-based identification of proteins interacting with Smad3: SREBP-2

- forms a complex with Smad3 and inhibits its transcriptional activity. *FEBS Lett* 2004;577:93-100.
85. Neale G, Lewis B, Weaver V, Panveliwalla D. Serum bile acids in liver disease. *Gut* 1971;12:145-152.
 86. Rivera CA, Bradford BU, Hunt KJ, Adachi Y, Schrum LW, Koop DR, Burchardt ER, et al. Attenuation of CCl₄-induced hepatic fibrosis by GdCl₃ treatment or dietary glycine. *Am J Physiol Gastrointest Liver Physiol* 2001;281:G200-207.
 87. Cappello M, Randazzo C, Bravata I, Licata A, Peralta S, Craxi A, Almasio PL. Liver Function Test Abnormalities in Patients with Inflammatory Bowel Diseases: A Hospital-based Survey. *Clin Med Insights Gastroenterol* 2014;7:25-31.
 88. Maher JJ. Leukocytes as modulators of stellate cell activation. *Alcohol Clin Exp Res* 1999;23:917-921.
 89. Tsukamoto H. Cytokine regulation of hepatic stellate cells in liver fibrosis. *Alcohol Clin Exp Res* 1999;23:911-916.
 90. Prieve MG, Harvie P, Monahan SD, Roy D, Li AG, Blevins TL, Paschal AE, et al. Targeted mRNA Therapy for Ornithine Transcarbamylase Deficiency. *Mol Ther* 2018;26:801-813.
 91. Apgar JF, Tang JP, Singh P, Balasubramanian N, Burke J, Hodges MR, Lasaro MA, et al. Quantitative Systems Pharmacology Model of hUGT1A1-modRNA Encoding for the UGT1A1 Enzyme to Treat Crigler-Najjar Syndrome Type 1. *CPT Pharmacometrics Syst Pharmacol* 2018;7:404-412.
 92. Connolly B, Isaacs C, Cheng L, Asrani KH, Subramanian RR. SERPINA1 mRNA as a Treatment for Alpha-1 Antitrypsin Deficiency. *J Nucleic Acids* 2018;2018:8247935.
 93. Liu-Chen S, Connolly B, Cheng L, Subramanian RR, Han Z. mRNA treatment produces sustained expression of enzymatically active human ADAMTS13 in mice. *Sci Rep* 2018;8:7859.
 94. Roseman DS, Khan T, Rajas F, Jun LS, Asrani KH, Isaacs C, Farelli JD, et al. G6PC mRNA Therapy Positively Regulates Fasting Blood Glucose and Decreases Liver Abnormalities in a Mouse Model of Glycogen Storage Disease 1a. *Mol Ther* 2018;26:814-821.
 95. Jiang L, Berraondo P, Jerico D, Guey LT, Sampedro A, Frassetto A, Benenato KE, et al. Systemic messenger RNA as an etiological treatment for acute intermittent porphyria. *Nat Med* 2018;24:1899-1909.
 96. DeRosa F, Guild B, Karve S, Smith L, Love K, Dorkin JR, Kauffman KJ, et al. Therapeutic efficacy in a hemophilia B model using a biosynthetic mRNA liver depot system. *Gene Ther* 2016;23:699-707.
 97. Ramaswamy S, Tonnu N, Tachikawa K, Limphong P, Vega JB, Karmali PP, Chivukula P, et al. Systemic delivery of factor IX messenger RNA for protein replacement therapy. *Proc Natl Acad Sci U S A* 2017;114:E1941-E1950.
 98. Harvey CE, Post JJ, Palladinetti P, Freeman AJ, Ffrench RA, Kumar RK, Marinos G, et al. Expression of the chemokine IP-10 (CXCL10) by hepatocytes in chronic hepatitis C virus infection correlates with histological severity and lobular inflammation. *J Leukoc Biol* 2003;74:360-369.
 99. Hintermann E, Bayer M, Pfeilschifter JM, Luster AD, Christen U. CXCL10 promotes liver fibrosis by prevention of NK cell mediated hepatic stellate cell inactivation. *J Autoimmun* 2010;35:424-435.
 100. Sica A, Invernizzi P, Mantovani A. Macrophage plasticity and polarization in liver homeostasis and pathology. *Hepatology* 2014;59:2034-2042.

101. Mederacke I, Hsu CC, Troeger JS, Huebener P, Mu X, Dapito DH, Pradere JP, et al. Fate tracing reveals hepatic stellate cells as dominant contributors to liver fibrosis independent of its aetiology. *Nat Commun* 2013;4:2823.
102. Weiskirchen R, Tacke F. Cellular and molecular functions of hepatic stellate cells in inflammatory responses and liver immunology. *Hepatobiliary Surg Nutr* 2014;3:344-363.
103. Wang S, An W, Yao Y, Chen R, Zheng X, Yang W, Zhao Y, et al. Interleukin 37 Expression Inhibits STAT3 to Suppress the Proliferation and Invasion of Human Cervical Cancer Cells. *J Cancer* 2015;6:962-969.
104. Holt AP, Haughton EL, Lalor PF, Filer A, Buckley CD, Adams DH. Liver myofibroblasts regulate infiltration and positioning of lymphocytes in human liver. *Gastroenterology* 2009;136:705-714.
105. Matsuzaki K, Murata M, Yoshida K, Sekimoto G, Uemura Y, Sakaida N, Kaibori M, et al. Chronic inflammation associated with hepatitis C virus infection perturbs hepatic transforming growth factor beta signaling, promoting cirrhosis and hepatocellular carcinoma. *Hepatology* 2007;46:48-57.
106. Kawamata S, Matsuzaki K, Murata M, Seki T, Matsuoka K, Iwao Y, Hibi T, et al. Oncogenic Smad3 signaling induced by chronic inflammation is an early event in ulcerative colitis-associated carcinogenesis. *Inflamm Bowel Dis* 2011;17:683-695.
107. Murata M, Matsuzaki K, Yoshida K, Sekimoto G, Tahashi Y, Mori S, Uemura Y, et al. Hepatitis B virus X protein shifts human hepatic transforming growth factor (TGF)-beta signaling from tumor suppression to oncogenesis in early chronic hepatitis B. *Hepatology* 2009;49:1203-1217.
108. Tilg H, Vogel W, Wiedermann CJ, Shapiro L, Herold M, Judmaier G, Dinarello CA. Circulating interleukin-1 and tumor necrosis factor antagonists in liver disease. *Hepatology* 1993;18:1132-1138.

8. APPENDIX

8.1 List of abbreviations

%	per cent
°C	degrees Celsius
AP	alkaline phosphatase
BSA	Bovine serum albumin
BDL	Bile duct ligation
CAP	citrate acetate buffer
CCl ₄	Carbontetrachloride
cDNA	complementary deoxyribonucleic acid
cmRNA	chemically modified RNA
Dapi	4',6-diamidino-2-phenylindole
DMEM	Dulbecco's modified eagle's medium
DMSO	Dimethyl sulfoxide
DNA	Deoxyribonucleic acid
dNTPs	Deoxyribonucleotids
DTT	Dithiothreitol
ECM	extracellular matrix
EGTA	Ethylene glycol tetraacetic acid
FCS	Fetal calf serum
GOT	Aspartate Aminotransferase
GFP	Green fluorescent protein
GPT	Alanine Aminotransferase
HAI	Hepatic Activity Index
HBSS	Hank's Balanced Salt Sodium
HCC	Hepatocellular carcinoma
HCL	Hydrogen chloride
IBD	Inflammatory bowl disease
IFN	Interferon
IL-	Interleukin
IL-1F	Interleukin-1 family
i.p.	Intraperitoneal
KC	Kupffer cells

kD	kilo Dalton
KO	Knock-out
KRB	Krebs-Ringer-Buffer
LPS	Lipopolysaccharide
MDR2/Abcb4	ATP-binding cassette, subfamily B (MDR/TAP), member 4)
MgCl ₂	Magnesium chloride
mHSC	murine hepatic stellate cells
mRNA	messenger RNA
PBMCs	human peripheral blood monocytes
PBS	Phosphate buffered saline
PCR	Polymerase chain reaction
PFA	Paraformaldehyde
P/S	Penicillin/Streptomycin
PSC	Primary Sclerosing Cholangitis
qRT-PCR	quantitative real time polymerase chain reaction
s.c.	subcutaneous
Scr	scramble RNA
SIGIRR	Single Ig IL-1 related receptor
siRNA	small interfering ribonucleic acid
tg	transgene
TGF	Transforming Growth Factor
TLR	Toll like receptor
TNF	Tumour necrosis factor
rh	recombinant human
RT	room temperature
Wt	wild-type

All gene names are indicated in italics, human genes in capital letters, e.g. *CXCL1*, genes from other species in lowercase with capital first letters, e.g. *Cxcl1*. All proteins, regardless of species, are written in regular font. Chemical elements and compounds are abbreviated according to common chemical nomenclature. Amino acids are abbreviated according to the established three-letter system.

8.2 Affidavit

I hereby declare that the submitted thesis entitled '*Modulation of liver inflammation and fibrosis by the Interleukin-1 homologue IL-37*' is my own work. I have only used the sources indicated and have not made unauthorised use of services of a third party. Where the work of others has been quoted or reproduced, the source is always given.

I further declare that the submitted thesis of parts thereof have not been presented as part of an examination degree to any other university.

Munich, 07.01.2020

Place, Date

Steffeni Mountford

8.3 Confirmation of congruency between printed and electronic version of the doctoral thesis

I hereby declare that the electronic version of the submitted thesis, entitled '*Modulation of liver inflammation and fibrosis by the Interleukin-1 homologue IL-37*' is congruent with the printed version both in content and format

Munich, 07.01.2020

Place, Date

Steffeni Mountford

8.4 Acknowledgements

First, and foremost I would like to thank my supervisor Prof. Dr. Philip Bufler for giving me the opportunity to do my PhD in his research lab. I am grateful for the excellent mentorship, teaching and continuous support over the last years. He believed in my abilities and me at a time when I did not, and for that trust and confidence I will be forever grateful.

I would also like to thank my other TAC members Prof. Roland Kappler and Dr. Daniel Kotlarz (Ph.D) for the mentorship and valuable advice throughout the project.

Great thanks go to my lab colleagues Lucas Griessmair and Andrea Ringleb, who helped perform the experiments with me. I want to give special thanks to Heidi Noll-Puchta who supported me inside and outside the lab and continues to be a great friend. I also want to thank Gabi Heilig and Doris Bruer-Kleis for the uplifting and enjoyable conversations.

Further I would like to thank Prof. Stefan Endres and Prof. Sebastian Kobold for allowing me to be an associate i-Target member and participate in the network activities.

I would like to thank my friends Susanna Kinting and Tamara Krause for the coffee -, lunch -, ice-cream -, and hot chocolate breaks in which I gathered valuable advice for my experiments. I am especially grateful to have shared the tissue culture room with Susanna, which allowed me to make a new best friend for life.

Special thanks also go to my friends outside the lab, especially Birgit Stefan and Annika Volmari who always have an open ear and support for me.

Most importantly I want to thank my family: My parents Wendy and Kelvin Mountford and my brother Matthäus Mountford for their continuous support and belief in me. And lastly the loves of my life Nikolay, our daughter Jelena and our baby boy, who supported me immensely during this time and always put a smile on my face. Without their support and help I wouldn't have been able to complete the project.

8.5 List of all scientific publications to date

- 1) **Mountford S**, Effenberger M, Noll-Puchta H, Griessmair L, Ringleb A, Denk G, Reiter FP, Mayr D, Dinarello CA, Tilg H, Bufler P. Modulation of liver inflammation and fibrosis by Interleukin-37. *Submitted to Hepatology*, 2020
- 2) **Mountford S**, Ringleb A, Schwaiger R, et al. Interleukin-37 Inhibits Colon Carcinogenesis During Chronic Colitis. *Front Immunol.* 2019;10:2632
- 3) Marinoni I, Lee M, **Mountford S**, et al. Characterization of MENX-associated pituitary tumours. *Neuropathol Appl Neurobiol.* 2013;39(3):256-269.